TECHNICAL NOTE

D-1387

THE ATMOSPHERE AS A PART OF THE SPACE ENVIRONMENT

By Richard A. Hord, Wilber B. Huston,
and Harold B. Tolefson

Langley Research Center
Langley Station, Hampton, Va.

NATIONAL AERONAUTICS AND SPACE ADMINISTRATION

WASHINGTON

January 1963

CONTENTS

NATIONAL AERONAUTICS AND SPACE ADMINISTRATION

TECHNICAL NOTE D-1387

THE ATMOSPHERE AS A PART OF THE SPACE ENVIRONMENT

By Richard A. Hord, Wilber B. Huston,
and Harold B. Tolefson

GENERAL SUMMARY

A survey of the main features of the earth's atmosphere which define a substantial portion of the near-earth space environment is presented in three parts. Part I deals with atmospheric composition, temperature, density, pressure, and the variations of these properties with altitude and other parameters. Part II describes the energy balance of the atmosphere with emphasis on the principal processes for the absorption and emission of radiation. Part III treats the large- and small-scale motions of the atmosphere, the methods of measurement, and the existing data on winds, wind shear, and turbulence.

GENERAL INTRODUCTION

The development of rockets and satellites has resulted in vast increases in the technological requirements for knowledge of the properties of the earth's atmosphere. Intermeshed with this development has been the comparable extension of direct atmospheric measurements to great altitudes. The primary requirement of the vehicle dynamicist, in many cases, is the atmospheric density distribution. Closely following this in general importance is the wind distribution. As vehicle systems and missions become more refined, however, the list of requirements quickly reaches proportions not entirely unrepresentative of the range of interests of the atmospheric scientists.

This paper is one of a series of NASA Technical Notes aimed at surveying the field of satellite environment. It is designed to provide a summary of the main features of the earth's atmosphere and a guide to the extensive literature on this subject. With this broad objective, it was deemed advisable to restrict somewhat severely the discussions of individual topics and to list only an appropriate number of key references. Consequently, the paper should prove to be of most use to the reader who requires a concise introduction to those aspects of the earth's atmosphere which are pertinent to the field of space environment.

The paper contains three parts: the first on composition, temperature, density, and pressure is the contribution of Wilber B. Huston; the second on the radiation balance is the contribution of Richard A. Hord who has also coordinated the entire volume; and the third on the winds and motions in the atmosphere is the contribution of Harold B. Tolefson. Most of the preparation of this volume was completed late in 1960. Parts of the paper, however, are concerned with more recent work.

I. COMPOSITION, TEMPERATURE, DENSITY, AND PRESSURE OF THE ATMOSPHERE

By Wilber B. Huston

INTRODUCTION

Prior to the advent of the sounding rocket, direct measurement of many properties of the earth's atmosphere on a broad scale was limited to the operating altitudes of aircraft and sounding balloons. Properties above about 50 kilometers were inferred from theory and indirect measurements. The sounding rocket raised the altitude limit for direct measurement. Out of the research rocket efforts of the International Geophysical Year (IGY) have come increased knowledge of conditions up to about 300 kilometers and a better basis for understanding atmospheric properties above this altitude. As a research tool the artificial earth satellite has provided an opportunity for direct measurement in the high atmosphere and in essence removes any limit above which properties must be inferred.

Because of the rapid decrease in density with altitude above the surface of the earth, the demands of research in the upper atmosphere on instrumentation techniques are very severe. As compared with airplane and balloon studies, the quantity of rocket and satellite data is small; these data are more in the nature of samples in space and time with a coverage that is, as yet, by no means worldwide. While for many purposes it is convenient to interpret these data in terms of a "standard atmosphere," the picture that emerges is one of a dynamic atmosphere with many important properties which vary with latitude, time of day, and season of the year, and with properties which reflect complex interactions between the earth and the sun. In the subsequent sections of this part of the survey, the composition of the atmosphere will be discussed first, then the data on temperature, density, and pressure.

COMPOSITION

To simplify the discussion of atmospheric properties, the commonly accepted nomenclature for the various regions is illustrated in figure 1. Two schemes of nomenclature adopted from reference 1 are shown, one based on composition (homosphere and heterosphere), the other based on temperature distribution. The altitude scale represents the approximate heights of the regions referred to.

Two physical processes, convective mixing and diffusive separation, are largely responsible for characteristic differences between the composition at low altitudes (homosphere) and the composition at higher altitudes (heterosphere). Convective mixing, associated with the general circulation, local turbulence, and tidal winds, successfully maintains a general constancy of the proportion of the major atmospheric constituents in samples taken throughout at least 95 percent of the atmosphere (below altitudes of 20 kilometers). In the more tenuous regions convective mixing becomes less effective. The processes of diffusive separation and dissociation produce changes of composition and a general lowering of the average molecular weight of the constituents. At heights of the order of 1,000 kilometers to several earth radii, the escape of molecules and atoms from the atmosphere and the influx of particles from the solar corona produce a transition region with composition of special interest to theoreticians and to studies with earth satellites. Mitra (ref. 2) has summarized the state of knowledge of atmospheric properties, including the composition as of 1952. More recent summary papers on composition have been given by Townsend (ref. 3), by Meadows and Townsend (ref. 4), and by Nicolet (ref. 1). Chapman (ref. 5) has discussed the thermosphere in the light of current astronomical knowledge.

Region of Convective Mixing

Sea-level composition.- The constituents of the atmosphere, as determined by measurements at or near sea level, are given in table I, adapted from reference 3. On a worldwide basis the constancy of the principal constituents is comparatively well established, although small local geographical variations of oxygen content have been suspected. The constancy of the noble gases is also well established. An entry in the column headed molecular weight in table I indicates the 11 constituents which are considered as composing the "standard dry air" upon which the standard value of the molecular weight of air, 28.966 grams per molecular weight (ref. 6), is based.

Of the seven constituents listed in table I which are not included in the standard atmosphere, most are of biological or industrial origin. Constancy of atmospheric composition with time, therefore, implies an equilibrium. Methane and nitrous oxide are believed to be of biological origin, but the processes which maintain the apparent equilibrium are not well understood. Carbon monoxide, sulfur dioxide, nitrogen dioxide, and nitric oxide are gases which are believed to be associated with industrial activity, and variations with geographical location and time are to be expected. Lightning may also be a factor in the creation of the two nitrogen compounds. Carbon dioxide, a factor in both biological and industrial processes, has apparently increased with time during the past 60 years. Like water vapor and ozone, it plays an

important part in the energy balance of the atmosphere. Water is subject to vapor-pressure equilibrium and ozone is subject to radiation equilibrium; both consequently show large variation with time, geographical location, and meteorological condition. The solubility of carbon dioxide in sea water makes feasible a sort of equilibrium condition which is quite sensitive to temperature, since the solubility is reduced with water temperature; this phenomenon has been used to identify air masses, but the range of the variability is small, of the order of 5 percent of the average carbon dioxide content.

Altitude variation of major constituents.- Because of the importance of the value of the molecular weight in relating temperature, density, and pressure, one of the major directions of atmospheric research has been to detect altitude variations of atmospheric constituents and thus to establish the altitude at which changes in composition are sufficiently great that the standard value of molecular weight is no longer applicable. Insofar as the principal components are concerned, balloon measurements and rocket flights at altitudes up to at least 60 kilometers have shown that the composition remains unchanged and thus that mixing processes counteract the tendency toward diffusive separation. Both experiment and theory for establishing an upper limit to the homosphere (or a lower limit to the heterosphere) depend in general upon the ratio of atomic to molecular oxygen and of argon to molecular nitrogen. Townsend (ref. 3) has summarized theoretical studies of the time required to establish diffusive equilibrium, the results of chemical analysis from rocket-flown vacuum bottles and mass spectrometers, and measurements of the oxygen green line in the Aurora. The evidence indicates a transition region of about 20 kilometers in which both diffusion and mixing processes are in operation. This region has been identified with the mesopause, but the identification is not certain (ref. 1). There is some evidence that at low latitudes the transition may begin at higher altitudes than is the case at higher latitudes. If, as in reference 3, an average value for the end of the homosphere is 110 kilometers, the molecular weight of air may be regarded as essentially constant at the adopted standard value to an altitude of 110 ± 10 kilometers.

Altitude variation of minor constituents.- Despite the general constancy of the proportions of the major constituents in the homosphere, photochemical and collision mechanisms affecting minor constituents result in changes of considerable aeronomic importance. Principal interest has focused on the action of ultraviolet on oxygen to produce ozone and atomic oxygen, but other minor constituents are also involved.

Ozone: Ground measurements by means of optical spectrographs and photon counters have shown an altitude variation of ozone concentration in the region between 15 and 40 kilometers. Measurements obtained

with rocket-borne instrumentation summarized in reference 7 confirm concentrations based on ground measurements summarized in chapter IV of reference 2. When expressed as percentage concentrations, peak values in the ozonosphere have generally been reported between 25 and 35 kilometers. The maximum absolute concentration, about 10^{13} molecules cm^3, occurs at a somewhat lower altitude; the peak values reported in reference 7 varied between about 22 and 28 kilometers. The mechanisms responsible for the ozone region and the relative rates of these processes have been extensively studied. Since these processes are photochemical, variations in ozone concentration associated with diurnal, seasonal, latitudinal, and solar indices may be expected.

Atomic oxygen: Atomic oxygen is present as a minor constituent of the mesosphere, as a result of a photodissociation. Because of its role in the formation and destruction of ozone, the vertical distribution of atomic oxygen in the mesosphere is of considerable interest. Diurnal and seasonal effects can be inferred because of the chemical and photochemical reactions. Direct measurements, however, are lacking.

Other minor constituents: The presence of water vapor in the stratosphere and mesosphere is inferred from the detection of the hydroxyl OH radical in the night airglow. The maximum intensity of these emissions is believed to occur at about 85 kilometers. The photodissociation of water vapor has been investigated by Bates and Nicolet (ref. 8) who have discussed the possibility of a layer of H_2 molecules at the height of the temperature minimum at the top of the mesosphere, where the hydrogen concentration could be of the order of 10^{10} molecules cm^3. From 20 kilometers above this maximum, it is believed that hydrogen compounds no longer exist, and there is a continued escape of hydrogen atoms into outer space.

Detection of the sodium D lines in the night airglow and twilight flash demonstrates the presence of sodium. Rocket measurements (ref. 9) show that the emission lies in the region from 75 to 110 kilometers, confirming earlier ground studies of the twilight flash (ref. 2, ch. X). Few details of the distribution, however, are known. Conjectures as to the source of sodium include the sea, volcanic action, the sun, and interplanetary space.

Carbon dioxide and the oxides of nitrogen are detected in the mass spectrometers of rocket flights. Little information on the distribution of these gases in the mesosphere is available, however.

Region of Diffusive Separation

In constrast to the uniform molecular weight of the homosphere, the heterosphere is a region where the composition and average molecular

weight vary with altitude. In the absence of convective mixing and gross transport mechanisms, the vertical distribution of each constituent is determined by gravitational separation, as modified by diffusion and a number of photochemical and photoionic processes discussed in part II.

The lower regions of the heterosphere are marked by a major change in composition, the increase in the proportion of atomic oxygen. Based on estimates that the equivalent temperature of the sun in the ultraviolet region could be taken in the range of 5,000° to 6,000° K, the dissociation of molecular oxygen was calculated (prior to the IGY) to be negligible up to altitudes of 90 kilometers, but nearly complete at 130 kilometers. (See ref. 2, ch. V.) Rocket evidence (ref. 10) that the radiation temperature was lower than expected, about 4,500° K, reduces the gradient of this dissociation, and thus increases the vertical extent of the region of dissociation. Rocket- and satellite-borne mass spectrometers have been used in an attempt to define the vertical distribution of the ratio of atomic to molecular oxygen. The results, as reviewed in reference 11, agree in showing an increase above 100 kilometers but differ markedly in the rate of increase. A complicating factor in the measurements is the possible recombination of atomic oxygen within the spectrometer. No molecular oxygen was found above 230 kilometers (ref. 3), and above this altitude atomic oxygen apparently is a major constituent.

In the region of oxygen dissociation, no evidence has been found (ref. 11) for appreciable nitrogen dissociation up to altitudes of about 185 kilometers, although there is evidence (ref. 1) that the photochemical processes associated with nitrogen dissociation are activated at lower levels. From the standpoint of determining molecular weight, nitrogen and atomic oxygen would be the principal constituents above 200 to 300 kilometers to the altitude where helium and neutral hydrogen become the most abundant components. In such an atmosphere the oxides of nitrogen play an important part in photochemical processes and atmospheric energy balance. Miller (ref. 12) has summarized the available information on nitrogen distribution.

A major effect of solar ultraviolet and higher energy radiation is the ionization of the gases of the upper atmosphere. Ionization, which commences in the D region at a height of about 60 kilometers increases rapidly with altitude to about 300 kilometers. A review of the data obtained by radio sounding from the ground is given in reference 13. Other current summaries may be found in references 14 and 15. Jackson, of the Naval Research Laboratories, has summarized the results of a number of direct and indirect measurements of determinations of electron distribution in the ionosphere to arrive at an average for summer noon in middle latitudes at a time of sunspot maximum. (See ref. 3.)

In view of the dependence of electron density on ultraviolet insolation, large departures from nominal values are associated with solar activity, season, and day and night. In particular, at altitudes from 60 to 80 kilometers (the D region), the ionization increases during the day and decreases at night. Sporadic pockets of added ionization in the E region have been ascribed to the effects of meteors, thunderstorms, and (especially near auroral zones) to bombardment by solar corpuscles. These ion clouds may be of long duration (hours to days) or they may be of a transient or burst type. In the auroral zones, where solar illumination of the upper atmosphere may be absent for months at a time or occur only by oblique rays, ionospheric conditions may vary markedly from conditions at low latitudes, and "abnormal" conditions may be regarded as "normal." During periods of magnetic disturbance, the electron concentrations in the D and E regions in the auroral zone are increased by factors of 10 or more and if the great-circle path joining a radio transmitter and the receiving station passes through the northern or southern auroral zones (a circle of about 23° from the magnetic poles) transmission is ordinarily unreliable.

In addition to atomic oxygen, atomic nitrogen, and neutral molecular nitrogen, the presence of positive ions of both molecular oxygen and molecular nitrogen in the upper atmosphere is shown by the spectra of auroras. Sodium, atomic hydrogen, and normal and ionized helium have also been reported. The relative intensities of the spectral lines characteristic of these substances have been utilized to estimate the variations with altitude of the composition and physical state of the upper atmosphere, but the analysis is complicated by variations in both altitude and intensity. Satellite measurements of the ratio N^+/O^+ between 230 kilometers and 820 kilometers (reported in ref. 3) showed an increase from 0.03 at 250 kilometers to 0.07 at about 700 kilometers, with evidence of a reduction in the ratio above about 700 kilometers.

The Protonosphere

Nicolet (refs. 1 and 16), Chapman (ref. 5), and Johnson (ref. 17) have discussed the composition of the atmosphere at altitudes above the 500- to 700-kilometer region until it merges with the outward extension of the solar corona. The names "protosphere" (refs. 1 and 5) and more recently "protonosphere" (ref. 18) have been applied to this region. In the general view, at about 500 kilometers, the principal constituents are believed to be atomic oxygen and atomic nitrogen with small amounts of atomic hydrogen. Nicolet (ref. 16) has proposed that neutral helium should also be an important constituent. In this helium model the details of the relative proportions of the various constituents depend upon the temperature assumed for the thermosphere above 500 kilometers. The lower the temperature assumed for the region above 500 kilometers the greater the abundance of helium as compared with the other heavier

constituents. Johnson (ref. 18) estimates a predominantly hydrogen atmosphere above 1,300 kilometers, Nicolet (ref. 16) finds the possibility of helium still predominant at 2,000 kilometers. At a distance of 1 earth radius, the concentration of hydrogen might be of the order of 4×10^3 atoms/cm^3, falling to 30 to 60 atoms/cm^3 at 10 earth radii. With increasing altitude, the relative proportions of ionized hydrogen atoms (protons) would increase, their distribution would be affected by the rotation of the earth in the presence of the geomagnetic field and because of the interaction with the solar wind would differ on the day and night sides of the earth (ref. 9).

Molecular Weight

The molecular weight of air may be regarded as constant at its standard sea-level value up to the region of diffusive separation. Because of the interdependence of temperature and molecular weight in defining the structure of the atmosphere, special interest is attached to the determination of the variation of molecular weight with altitude in the heterosphere. Rocket measurements (ref. 4) have shown values of molecular weight from about 28 at 130 kilometers to about 20 at 235 kilometers. The measured variation is shown in figure 2. Beyond these levels, as the proportions of atomic oxygen (molecular weight 16) and atomic nitrogen (molecular weight 14) increase, the molecular weight would continue to decrease. Several possible altitude variations are shown in figure 2. For the helium models considered by Nicolet (ref. 16) the altitude variation depends critically on the temperature assumed for the thermosphere. The variations shown in figure 2 correspond to temperatures of 2,133° K and 903° K in an isothermal region extending from heights of 1,000 to 2,000 kilometers, temperatures which can be identified with the maximums and minimums of the solar cycle (ref. 18). In such models the molecular weight decreases from about 26 at 150 kilometers to about 4 at 2,000 kilometers. If, however, the supposition of the predominance of atomic hydrogen is correct, the molecular weight would have decreased to 1 at altitudes between 1,500 kilometers and 2,500 kilometers (refs. 17 and 18). For an ionized hydrogen (proton) atmosphere, the molecular weight would be 1/2. Other authors (for example, ref. 19) have considered the decrease of molecular weight with altitude to be more gradual, reaching 1 at about 10^5 kilometers. A definitive variation of molecular weight in the high atmosphere does not appear possible at this time.

TEMPERATURE, DENSITY, AND PRESSURE

Any description of the atmosphere and its variations above the surface of the earth must deal with a total of six variables, density ρ, pressure P, temperature T, molecular weight M, acceleration due to

gravity g, and height Z. There are two equations which relate these quantities. The ideal gas law

$$P = \frac{\rho RT}{M} \tag{1}$$

relates P, ρ, T, and M to the universal gas constant R. The hydrostatic equation

$$\frac{dP}{dZ} = -\rho g \tag{2}$$

relates the pressure gradient to the density and local value of gravity. Although these relations are not applicable to small regions of extremely rarefied gases, or to gases under the influence of electromagnetic fields, they may be used through that portion of the atmosphere extending upward for a distance of about 1,000 kilometers. If conditions at some reference level are specified, for example, sea level ($Z = 0$), then it is possible to calculate the conditions at some other height z. In order to accomplish this, the variation with height of either ρ, P, or T must be specified, and T is the commonly selected parameter. Since both the acceleration due to gravity and the molecular mass vary with altitude, some provision must be made for these quantities. Many model atmospheres, references 20 to 25, have been constructed in this way. In early ones, applicable only over a limited altitude range (ref. 20) g and M were regarded as constant. To provide for a wider range of attitudes as in reference 21, g has been varied in accordance with the inverse square law, or the concept of geopotential has been introduced as in references 24 and 25. Since, as in equation (1), temperature frequently enters the problem, not independently but in the ratio T/M, it is convenient for many purposes to specify a quantity T_M, the molecular scale temperature, defined as

$$T_M = \frac{T}{M} M_o \tag{3}$$

which is equal to the real kinetic temperature T when the molecular mass is equal to the standard sea-level value M_o, but accounts for changes in molecular weight without specifying its functional variation with altitude. Although the variation with altitude of either the kinetic or the molecular scale temperature is generally used as the defining relation for atmospheric properties, temperatures are not ordinarily measured directly above balloon altitudes. They may be inferred from acoustic experiments which determine the velocity of sound a since

$$a = \sqrt{\frac{\gamma RT}{M}}$$

$$= \sqrt{\frac{\gamma RT_M}{M_o}} \tag{4}$$

where γ is the ratio of the specific heats. Above about 90 kilometers, temperatures are inferred from the altitude gradient of density or pressure. The ideal gas law, and the hydrostatic equation combined yield the relations

$$\frac{dP}{P} = - \frac{dZ}{RT/gM} \tag{5}$$

$$\frac{d\rho}{\rho} = - \frac{dZ}{RT/gM} - \frac{dT}{T} \tag{6}$$

The group of quantities RT/gM which has the dimension length is termed the scale height H' where

$$H' = \frac{R}{gM_o} T_M \tag{7}$$

From the solution of equation (5)

$$d \log_e P = - \frac{dZ}{H'} \tag{8}$$

or of equation (6)

$$\frac{d \log_e \rho}{dZ} = - \frac{1}{H'} - \frac{dT_M}{T_M \, dZ} \tag{9}$$

it follows that the scale height for an isothermal atmosphere (ignoring the change of gravity) is the distance over which the pressure would decrease by a factor e^{-1}. At sea level H' is approximately 8.4 kilometers. It also follows that from the slope of a plot of $\log P$ or $\log \rho$ against altitude the scale height can be determined, at least by approximate methods, and, in turn, the molecular scale temperature T_M can be obtained. (See ref. 25.)

Temperature as a Defining Property

For defining purposes it is convenient to specify the altitude variation of T or T_M; for calculations, linear segments are convenient but not required. Two such segments were the basis of the NACA standard atmosphere (ref. 20). On the basis of sound propagation, ozone measurements, and (between 60 and 110 kilometers) densities inferred from meteor visibility data, seven segments were required for a tentative extension (ref. 21). Above 110 kilometers, the sounding rocket has provided the first source of direct information on the atmosphere. Such data have been used in the preparation of the ARDC atmospheres of 1956 and 1959 (refs. 24 and 25). Densities inferred from changes in the orbital period of satellites also contributed to the preparation of the 1959 atmospheric table, for the altitude range from 170 to 650 kilometers. The two tables differ in the assumption made for temperatures at high altitudes in the thermosphere above 300 to 400 kilometers. The essentially isothermal assumption in reference 24 was replaced by an increasing temperature in 1959, in line with Chapman's view of the interaction between the high atmosphere and the solar corona. More recently Johnson (ref. 18) and others have returned to the view of an isothermal region extending from about 400 kilometers to several thousand kilometers and characterized by temperatures which vary from 1,000° K at periods of sunspot minimum to 1,500° K at periods of sunspot maximum. Because they are readily available and widely used, and because they are based on the rocket and satellite data, it is convenient to discuss the properties of the high atmosphere in terms of references 24 and 25.

Atmospheric Measurements

Shown in table II are the defining temperatures used to specify the ARDC 1956 and 1959 atmospheres. The defining relations shown on the left portion of the table are expressed in terms of molecular scale temperature T_M, at various geopotential altitudes H expressed in terms of standard geopotential kilometers km'. On the right are the real kinetic temperatures T based on the assumed variation of molecular weight M and the altitudes Z corresponding to the specifying values of geopotential. These altitudes, strictly applicable only to a reference latitude of 45°32'33", can be converted to altitudes for other latitudes by the methods given in reference 25. The defining temperatures of table II result in the two temperature distributions plotted in figure 3. The marked changes in molecular scale temperature introduced by the satellite density data above 100 kilometers are evident.

Rocket data.- The rocket studies of air density, pressure, and temperature have been reported by LaGow and coworkers (refs. 26 to 30) and summarized by Newell (ref. 7). The instrumentation and data-reduction

technique described in reference 27 are the result of a long evolution which has shown a steady improvement in precision to the point that measurements based on diaphragm-type pressure gages are believed accurate to 3 to 5 percent, while ionization-gage data are accurate to ±30 percent. Shown in table III are the air-density determinations above 100 kilometers, reported in references 7 and 26 to 30, based on six rocket flights extending over the period 1947 to 1958: two at White Sands, New Mexico, a winter day and a summer day; four at Fort Churchill, Canada, two representative of winter days, one of a summer day, and one of a winter night. These data are plotted in figure 4 in comparison with the ARDC density values at the corresponding altitudes. These data have been interpreted (ref. 30) as showing:

1. A latitude effect, density larger at the higher latitude

2. A seasonal effect, summer density larger than winter

3. A diurnal effect, daytime density larger than nighttime

At 200 kilometers these effects appear to be of the order of about 5 to 1. The marked change in slope of the density curve at about 160 kilometers is associated with the change in temperature gradient in the same altitude range indicated in figure 3.

As compared with the 1956 atmosphere, the decreased density in the range for 80 to 150 kilometers in the 1959 atmosphere appears to be a better average of the available data. The increased densities which have been interpreted as a latitude effect may be the result of increased ionospheric activity in the auroral zone.

As an average of latitude, seasonal, and diurnal effects, the 1959 atmosphere appears to be a reasonably successful representation of rocket data. In the region of 90 to 120 kilometers the shape of the temperature distribution is rather complex, a reflection of the complex photochemical processes characteristic of the lower regions of the heterosphere. Since these processes are sensitive to the level of solar activity, it seems reasonable to expect considerable diurnal, seasonal, latitudinal, and random fluctuation in the details of the temperature, density, and pressure levels at those altitudes and further study on a global basis appears to be indicated.

Satellite data.- From the observed changes in the period of a number of satellites placed in orbit since 1957, densities at various altitudes from 180 to 656 kilometers have been inferred. The relationship between changes in orbital elements and a drag force D is ordinarily represented in conventional aerodynamic form as

$$D = \frac{1}{2} \rho V^2 C_D A$$

where V is the orbital velocity (sometimes corrected for the motion of the atmosphere), A is the effective cross-sectional area, and C_D the drag coefficient. This equation has been discussed by Sterne, Harris, Jastrow, King-Hele, Cook, Walker, El'yasberg, and Groves (refs. 31 to 36). The appropriate value of neutral-particle drag coefficient C_D for free molecule flow has been discussed by Baker and Charwat (ref. 37) and by Stirton (ref. 19). For spheres, a comprehensive study made in connection with the falling-sphere method of density determination is given in reference 38. Although drag effects may be present at all parts of the orbit, the principal effects are associated with the part of the orbit near perigee, and the principal result is a decrease in the radius of apogee. Integration of the drag over the entire orbit results in obtaining an average density which is either related to an effective altitude increment above perigee as in reference 33, or corrected to the altitude of perigee as in references 31, 34, 35, and 36.

The available data, adapted from reference 39 and extended by use of references 31, 33, 36, and 40 to 48, are given in table IV. In the preparation of table IV, it was found that some authors have given altitudes of perigee in terms of geopotential H, others in terms of geometric height Z. To present the data on a comparable basis, reference 25 has been used to establish a relationship between H and Z. As in table II, values of both Z and H are given in table IV. Because of rotation of the argument of perigee, it has been possible in some instances to relate deduced values of density to particular latitudes or bands of latitude. These data are given in table IV when available, as is the column labeled "epoch" which relates to the calendar period to which the calculation is applicable. The references from which the data of table IV were obtained are also shown.

The density data of table IV are plotted against geometric altitudes in figure 5. For comparison the density values of the ARDC 1956 and 1959 atmospheres are also shown. Also shown in figure 5 by the diamond-shaped symbols are independent determinations of density by the dispersion of a sodium vapor cloud and by a densitometer flown in Sputnik III. These Russian data given in table V (from refs. 41 and 49) are in remarkable agreement with the satellite drag determinations.

Because of the averaging process involved in determining changes in orbital period, most studies of density have tended to obscure any evidence of seasonal, latitudinal, or diurnal effects. The observed changes in period are small, 2.7 sec/day for 1957 $\alpha 2$ (Sputnik I), 0.018 sec/day for 1958 $\beta 2$ (Vanguard I). The difficulties in detecting changes in these periods have been discussed by Jacchia and Briggs (ref. 46); tabulations

of rate of change of period for 1958 β2 at 2-day intervals represent departures from smoothing functions which average over several days, and thus over 30 to 50 orbital passes. Fluctuations have been observed which correlate well with various indices of solar activity. From 1958 β2 (Vanguard I), 1958 α (Explorer I), and 1958 δ (Sputnik III), Martin and Preister (ref. 45) have been able to detect both a diurnal change in density and a correlation with solar activity as indicated by the 20-centimeter radiation from the sun. Both effects increase with altitude, and at 650 kilometers the diurnal effect is such that the density peak which occurs 1 hour 40 minutes after local noon, is greater by a factor of 6.5 than the minimum 12 hours later. The association with solar activity is present both day and night, suggesting a global basis. The values plotted in figure 5 are for the moderately active sun of reference 45; the solid symbols, indicating nighttime values, are connected to the open daytime symbols by braces.

King-Hele and Walker (ref. 50) have studied the densities derived from drag data on 21 satellites. (See fig. 6.) They found that at heights of 200 to 300 kilometers the density probably does not depart from its average value by more than 10 percent as a result of day-to-night variation, but at heights above 400 kilometers this day-to-night variation becomes more important, and is of the order of 11 to 1 at 700 kilometers. They also found that at heights of 180 to 250 kilometers, there is evidence of a slow variation with time, the density for the end of 1959 being about 20 percent less than the density for mid-1958. They suggest that just as solar disturbances largely control day-to-day variation in air density at heights of 200 to 300 kilometers, with density tending to be high when sunspots are more numerous, the average air density is likely to vary in the course of the 11-year sunspot cycle. Average air density may, therefore, be expected to be high during the sunspot maximum of 1957 and 1958 and to decrease slowly thereafter for several years.

The marked diurnal effect of incident solar radiation found in references 40 and 45, and also reference 51, seems to depend primarily on the zenith distance of the sun, being highest when the sun is nearly overhead. Thus daytime equatorial densities would be high in summer, density would be low over the poles during the polar winter. Although such variations would appear as a "latitude effect," it would perhaps be well to avoid the use of such a term in view of their solar origin.

No critical evaluation of the satellite data will be attempted. Some early determinations of density might be improved by a better choice of drag coefficient, and there remains a need for more exact data on mass, shape, and effective area for some configurations, especially those with marked departures from spherical shape. Chopra (ref. 52) has outlined a number of possible electrostatic and electromagnetic processes which can, for some configurations, produce forces

which could be confused with aerodynamic drag. In general, these considerations appear to apply to satellites with perigees in excess of 1,000 kilometers and to satellites of low mass in proportion to their size. It does appear that the ARDC 1959 density distribution provides a reasonable fit to the data and that satellite drag estimates based upon it should give reasonable results. In view of the interdependence of temperature, density, and pressure, the other portions of the ARDC standard are probably a valid representation of average conditions in the atmosphere. In view, however, of the uncertainties in molecular weight, estimates of true or kinetic temperature obtained from molecular scale temperatures at altitudes above about 200 kilometers must be viewed with reservation.

Above 700 Kilometers

Early concepts of the high atmosphere generally revolved around an exosphere, a region in which the decreasing density and increasing mean free path served to permit the escape of a portion of the air molecules which between infrequent collisions were in orbital paths about the center of the earth. Some of these molecules would acquire escape velocity and be lost to the atmosphere. Due to the process of diffusive separation, the uppermost constituents of the atmosphere were the lighter components, molecular and atomic hydrogen.

The modern view, summarized by Chamberlain (ref. 53), conceives of a region of interchange between the atmosphere and the outer reaches of the solar corona. This region, the protonosphere, consists mainly of hydrogen atoms (protons) - some from the sun, some arriving from below from the levels where water vapor and molecular hydrogen are dissociated by sunlight. In this region the probable temperature lies between 5,000° K and 20,000° K. The number of protons or electrons is uncertain, estimates based on a peak coronal temperature of 1,000,000° K came to 340 per cm^3, estimates based on the zodiacal light have given upper limits between 100 per cm^3 and 1,000 per cm^3. Estimates by Cole (ref. 54) are much lower, 0.1 per cm^3. In any event, the number is not constant, being subject to sporadic streaming from active areas on the sun, disturbances which travel at speeds of about 1,000 km/sec or one-thirtieth of the speed of light. In such an environment, which must be strongly affected by the earth's magnetic field, it is no longer clear that such concepts as density or pressure have their ordinary meanings. Pressure, in particular, may be the result of collisions with streaming particles as well as the effect of random collisions, in which case pressure would depend on orientation, perhaps relative to the geomagnetic lines of force. An interrelation between such a gas and the Van Allen radiation belts can be supposed but the consequences have not yet been thoroughly investigated.

REFERENCES

1. Nicolet, M.: The Properties and Constitution of the Upper Atmosphere. Physics of the Upper Atmosphere, J. A. Ratcliffe, ed., Academic Press, Inc. (New York), 1960, pp. 17-71.

2. Mitra, S. K.: The Upper Atmosphere. Second ed., The Asiatic Society (Calcutta, India), 1952. (Available from Hafner Pub. Co., New York.)

3. Townsend, John W., Jr.: Composition of the Upper Atmosphere. Physics and Medicine of the Atmosphere and Space. Otis J. Benson, Jr., and Hubertus Strughold, eds., John Wiley & Sons, Inc., c.1960, pp. 112-133.

4. Meadows, E. B., and Townsend, J. W., Jr.: IGY Rocket Measurements of Arctic Atmospheric Composition Above 100 km. Space Research, Hilde Kallmann Bijl, ed., Interscience Publ., Inc. (New York), 1960, pp. 175-198.

5. Chapman, Sydney: The Thermosphere - The Earth's Outermost Atmosphere. Physics of the Upper Atmosphere, J. A. Ratcliffe, ed., Academic Press, Inc. (New York), 1960, pp. 1-16.

6. Anon.: Standard Atmosphere - Tables and Data for Altitudes to 65,800 Feet. NACA Rep. 1235, 1955. (Supersedes NACA TN 3182.)

7. Newell, Homer E., Jr.: The Upper Atmosphere Studied by Rockets and Satellites. Physics of the Upper Atmosphere, J. A. Ratcliffe, ed., Academic Press, Inc. (New York), 1960, pp. 73-132.

8. Bates, D. R., and Nicolet, M.: Atmospheric Hydrogen. Pub. Astronomical Soc. Pacific, vol. 62, no. 366, June 1950, pp. 106-110.

9. Heppner, J. P., and Meredith, L. H.: Nightglow Emission Altitudes From Rocket Measurements. Jour. Geophys. Res., vol. 63, no. 1, Mar. 1958, pp. 51-65.

10. Byram, E. T., Chubb, T. A., and Friedman, H.: Dissociation of Oxygen in the Upper Atmosphere. Phys. Rev., vol. 98, no. 6, Second ser., June 15, 1955, pp. 1594-1597.

11. Johnson, C. Y., Hoffman, J. H., Young, J. M., and Holmes, J. C.: A Method for Measuring Temperature Directly in the Upper Atmosphere With a Rocket-Borne Magnetic Mass Spectrometer. Jour. Geophys. Res., vol. 65, no. 9, Sept. 1960, pp. 2996-2997.

12. Miller, Lewis E.: The Chemistry and Vertical Distribution of Atomic Nitrogen in the Upper Atmosphere. Geophys. Res. Papers No. 71 (AFCRL-TR-60-280), Air Force Res. Div., Dec. 1960.

13. Ratcliffe, J. A., and Weekes, K.: The Ionosphere. Physics of the Upper Atmosphere, J. A. Ratcliffe, ed., Academic Press, Inc. (New York), 1960, pp. 377-470.

14. Seddon, J. Carl: Summary of Rocket and Satellite Observations Related to the Ionosphere. NASA TN D-667, 1961.

15. Poeverlein, H., ed.: The Upper Atmosphere Above F2-Maximum. AGARDograph 42, North Atlantic Treaty Organization (Paris), May 1959.

16. Nicolet, Marcel: Density of the Heterosphere Related to Temperature. Special Rep. No. 75, Smithsonian Institution Astrophysical Observatory, Sept. 19, 1961.

17. Johnson, Francis S.: The Composition of Outer Space. Astronautics, vol. 5, no. 4, Apr. 1960, pp. 30-31, 92, 94.

18. Johnson, Francis S., ed.: Satellite Environment Handbook. Stanford Univ. Press, 1961.

19. Stirton, R. J.: The Upper Atmosphere and Satellite Drag. Smithsonian Contributions to Astrophysics, vol. 5, no. 2, 1960, pp. 9-15.

20. Diehl, Walter S.: Standard Atmosphere - Tables and Data. NACA Rep. 218, 1925. (Reprinted 1940.)

21. Warfield, Calvin N.: Tentative Tables for the Properties of the Upper Atmosphere. NACA TN 1200, 1947.

22. Grimminger, G.: Analysis of Temperature, Pressure, and Density of the Atmosphere Extending to Extreme Altitudes. U.S. Air Force Project RAND Rep. R-105, The RAND Corp., Nov. 1948.

23. The Rocket Panel: Pressures, Densities, and Temperatures in the Upper Atmosphere. Phys. Rev., vol. 88, no. 5, Second ser., Dec. 1, 1952, pp. 1027-1032.

24. Minzner, R. A., and Ripley, W. S.: The ARDC Model Atmosphere, 1956. Air Force Surveys in Geophysics No. 86 (AFCRC-TN-56-204), Air Force Cambridge Res. Center, Dec. 1956.

25. Minzner, R. A., Champion, K. S. W., and Pond, H. L.: The ARDC Model Atmosphere, 1959. Air Force Surveys in Geophysics No. 115 (AFCRC-TR-59-267), Air Force Cambridge Res. Center, Aug. 1959.

26. LaGow, H. E., and Ainsworth, J.: Arctic Upper-Atmosphere Pressure and Density Measurements With Rockets. Jour. Geophys. Res., vol. 61, no. 1, Mar. 1956, pp. 77-92.

27. Horowitz, R., and LaGow, H. E.: Upper Air Pressure and Density Measurements From 90 to 220 Kilometers With the Viking 7 Rocket. Jour. Geophys. Res., vol. 62, no. 1, Mar. 1957, pp. 57-78.

28. Horowitz, R., and LaGow, H. E.: Summer-Day Auroral-Zone Atmospheric-Structure Measurements From 100 to 210 Kilometers. Jour. Geophys. Res., vol. 63, no. 4, Dec. 1958, pp. 757-773.

29. Horowitz, R., LaGow, H. E., and Giuliani, J. F.: Fall-Day Auroral-Zone Atmospheric Structure Measurements From 100 to 188 km. Jour. Geophys. Res., vol. 64, no. 12, Dec. 1959, pp. 2287-2295.

30. LaGow, H. E., Horowitz, R., and Ainsworth, J.: Arctic Atmospheric Structure to 250 km. Planetary and Space Sci., vol. 2, no. 1, Oct. 1959, pp. 33-38.

31. Sterne, Theodore E.: High-Altitude Atmospheric Density. The Physics of Fluids, vol. 1, no. 3, May-June 1958, pp. 165-170.

32. Sterne, Theodore E.: An Atmospheric Model, and Some Remarks on the Influence of Density From the Orbit of a Close Earth Satellite. The Astronomical Jour., vol. 63, no. 3, Mar. 1958, pp. 81-87.

33. Harris, I., and Jastrow, R.: An Interim Atmosphere Derived From Rocket and Satellite Data. Planetary and Space Sci., vol. 1, no. 1, Jan. 1959, pp. 20-26.

34. King-Hele, D. G., Cook, G. E., and Walker, D. M. C.: The Contraction of Satellite Orbits Under the Influence of Air Drag. Part I: With Spherically Symmetrical Atmosphere. Tech. Note No. G.W. 533, British R.A.E., Nov. 1959.

35. El'yasberg, P. E. (J. W. Palmer, trans.): The Relationship of Secular Variations of Orbital Elements to Air Drag. Lib. Translation No. 893, British R.A.E., Apr. 1960.

36. Groves, G. V.: Effect of the Earth's Equatorial Bulge on the Life-Time of Artificial Satellites and Its Use in Determining Atmospheric Scale-Heights. Nature (Letters to the Editor), vol. 181, no. 4615, Apr. 12, 1958, p. 1055.

37. Baker, R. M. L., Jr., and Charwat, A. F.: Transitional Correction to the Drag of a Sphere in Free Molecule Flow. The Physics of Fluids, vol. 1, no. 2, Mar.-Apr. 1958, pp. 73-81.

38. Peterson, J. W., Schulte, H. F., and Schaefer, E. J.: A Simplified Falling-Sphere Method for Upper-Air Density. Part II. Density and Temperature Results From Eight Flights. Tech. Rep. No. 2215-19-F (AFCRC-TR-59-263), Res. Inst., Univ. of Michigan, May 1959.

39. Kallmann, H. K., and Juncosa, M. L.: A Preliminary Model Atmosphere Based on Rocket and Satellite Data. U.S. Air Force Project RAND Res. Memo. RM-2286 (ASTIA Doc. No. AD 207752), The RAND Corp., Oct. 30, 1958.

40. Whitney, Charles A.: The Structure of the High Atmosphere - I. Linear Models. Ephemeris of Satellite 1957 Alpha 2 and Collected Reports on Satellite Observations. IGY Satellite Rep. Ser., No. 8, Nat. Acad. Sci., June 15, 1959, pp. 103-114.

41. Mikhnevich, V. V., Danilin, B. S., Repnev, A. I., and Sokolov, V. A.: Some Results of the Determination of the Structural Parameters of the Atmosphere Using the Third Soviet Artificial Earth Satellite. NASA TT F-13, 1960.

42. Schilling, G. F., Whitney, C. A., and Folkart, B. M.: Preliminary Note on the Mass-Area Ratio of Satellites 1958 δ1 and δ2. Reports and Analyses of Satellite Observations. IGY Satellite Rep. Ser. No. 6, Nat. Acad. Sci., Aug. 15, 1958, pp. 22-24.

43. Sterne, Theodore E.: The Density of the Upper Atmosphere. Status Reports on Optical Observations of Satellites 1958 Alpha and 1958 Beta. IGY Satellite Rep. Ser. No. 2, Nat. Acad. Sci., Apr. 30, 1958, pp. 18-22.

44. Sterne, T. E., Folkart, B. M., and Schilling, G. F.: An Interim Model Atmosphere Fitted To Preliminary Densities Inferred From U. S. S. R. Satellites. Smithsonian Contributions to Astrophysics, vol. 2, no. 10, 1958, pp. 275-280.

45. Martin, H. A., and Priester, W.: Measurement of Solar and Diurnal Effects in the High Atmosphere by Artificial Satellites. Nature (Letters to the Editors), vol. 185, no. 4713, Feb. 27, 1960, pp. 600-601.

46. Jacchia, L. G., and Briggs, R. E.: Orbital Acceleration of Satellite 1958 Beta Two. Ephemesis of Satellite 1957 Alpha 2 and Collected Reports on Satellite Observations. IGY Satellite Rep. Ser. No. 8, Nat. Acad. Sci., June 15, 1959, pp. 67-70.

47. Lidov, M. L.: Determination of Atmospheric Density From Observations of the First Sputniks' Drag. B4, Nat. Acad. Sci., 1958.

48. Schilling, G. F., and Whitney, C. A.: Atmospheric Densities From Explorer IV. Ephemeris of Satellite 1957 Alpha 2 and Collected Reports on Satellite Observations. IGY Satellite Rep. Ser. No. 8, Nat. Acad. Sci., June 15, 1959, pp. 93-102.

49. Shklovskiy, I. S., and Kurt, V. G.: The Determination of the Density of the Atmosphere at an Altitude of 430 Kilometers by the Sodium Vapor Diffusion Method. NASA TT F-15, 1960.

50. King-Hele, D. G., and Walker, D. M. C.: Density of the Upper Atmosphere and Its Dependence on the Sun, as Revealed by Satellite Orbits. Nature, vol. 186, no. 4729, June 18, 1960, pp. 928-931.

51. Jacchia, Luigi G.: A Variable Atmospheric-Density Model From Satellite Accelerations. Special Rep. No. 39, Smithsonian Institution Astrophysical Observatory, Mar. 30, 1960.

52. Chopra, K. P.: Interactions of Rapidly Moving Bodies in Terrestrial Atmosphere. Rep. 56-212 (Contract AF 18(603)-95), Eng. Center, Univ. of Southern California, Mar. 31, 1960.

53. Chamberlain, Joseph W.: Physics of the Aurora and Airglow. Academic Press, Inc. (New York), 1961.

54. Cole, K. D.: Solar Terrestrial Relationships. Nature (Letters to the Editors), vol. 186, no. 4728, June 11, 1960, p. 874.

TABLE I.- COMPOSITION OF THE ATMOSPHERE AT SEA LEVEL

Gas	Molecular weight	Percent by volume	Notes
Nitrogen (N_2)	28.016	78.084 ± 0.004	
Oxygen (O_2)	32.0000	20.946 ± 0.002	
Water (H_2O)	--------	0.1 to 2.8	Variable
Argon (A)	39.944	0.934 ± 0.001	
Carbon dioxide (CO_2)	44.010	0.033 ± 0.001	Increasing with time
Neon (Ne)	20.183	$1.818 \pm 0.004 \times 10^{-3}$	
Helium (He)	4.003	$5.24 \pm 0.004 \times 10^{-4}$	
Methane (CH_4)	--------	1.5×10^{-4}	Invariant - biological
Krypton (Kr)	83.7	$1.14 \pm 0.01 \times 10^{-4}$	
Carbon monoxide (CO)	--------	6×10^{-6} to 1×10^{-4}	Variable - industrial
Sulfur dioxide (SO_2)	--------	1×10^{-4}	Variable - industrial
Hydrogen (H_2)	2.0160	5×10^{-5}	
Nitrous oxide (N_2O)	--------	5×10^{-5}	Invariant - biological
Ozone (O_3)	48.0000	1×10^{-6} to 1×10^{-5}	Variable
Xenon (Xe)	131.3	$8.7 \pm 0.1 \times 10^{-6}$	
Nitrogen dioxide (NO_2)	--------	5×10^{-8} to 2×10^{-6}	Variable - industrial
Radon (Rn)	222	6×10^{-18}	Variable
Nitric oxide (NO)	--------	Trace	Variable - industrial

TABLE II.- DEFINING TEMPERATURES FOR ARDC ATMOSPHERES

Geopotential altitude, H, km'	Molecular scale temperature, T_M, °K		Real kinetic temperature, T, °K		Geometric altitude, Z, km
	1956	1959	1956	1959	
0	288.16	288.16	288.16	288.16	0
11	216.66	216.66	216.66	216.66	11.019
25	216.66	216.66	216.66	216.66	25.099
47	282.66	282.66	282.66	282.66	47.350
53	282.66	282.66	282.66	282.66	53.446
75	196.86		196.86		75.895
79		165.66		165.7	79.994
90	196.86	165.66	196.86	165.7	91.293
105		225.66		224.7	106.764
126	322.86		273.6		128.548
160		1325.66		1277	164.131
170		1425.66		1356	174.671
175	812.86		669.0		179.954
200		1575.66		1413	206.497
500	2697.9		1489		542.686
700		3325.66		1930	

TABLE III.- ATMOSPHERIC DENSITY, ROCKET DATA

Geometric altitude, Z, km	Density, ρ, g/cm^3 for -					
	Latitude 32° N.		Latitude 59° N.			
	Mar. 7, 1947 1123 m.s.t.	Aug. 7, 1951 1100 m.s.t.	Nov. 17, 1956 1100 c.s.t.	July 29, 1957 1600 c.s.t.	Feb. 24, 1958 0100 c.s.t.	Oct. 31, 1958 1400 c.s.t.
100		2.5×10^{-10}		7.2×10^{-10}		4.9×10^{-10}
110		5.0×10^{-11}		1.3		1.1
120		1.2		2.6×10^{-11}		2.5×10^{-11}
130		3.3×10^{-12}		6.4×10^{-12}		6.7×10^{-12}
140		1.2		3.0		3.0
150		6.6×10^{-13}		1.9		1.8
156	$(2.0 \pm 0.5) \times 10^{-12}$					
160		4.3		1.4		1.2
170		3.0		1.1		8.6×10^{-13}
180		2.3		8.9×10^{-13}		6.4
188						5.2
190		1.8		7.9		
200		1.4	$\left(3.6 \pm \frac{3.0}{1.5}\right) \times 10^{-13}$	7.0		
202					$(1.3 \pm 0.6) \times 10^{-13}$	
210		1.1		6.2		
220		9.0×10^{-14}				

TABLE IV.- ATMOSPHERIC DENSITIES, SATELLITE DRAG METHOD

Vehicle		Altitude		Density, ρ, g/cm^3	Epoch	Latitude	Reference
		Geometric, Z, km	Geopotential, H, km'				
1957 α2	Sputnik I	282	270	8.5×10^{-14}	Oct. 13 to 25, 1957	39° ± 6° N.	33
		220	213	4.1×10^{-13}	Spring and summer 1957		40
		206	200	5.4	Oct. 15, 1957	37° N.	36
		201	195	6.7	Nov. 9, 1957	26° N.	36
		225	217	3.5	Prior to Aug. 1958		41
		228	220	2.8			42
		220	213	4			43
		220	213	4.5			44
1958 α	Explorer I	405	381	9×10^{-15}	Feb. 5 to May 17, 1958	33° N. to 33° S.	33
		368	348	1.4×10^{-14}	Feb. 1, 1958		43
		347	341	1.8			40
		350	332	3	Day		45
		350	332	1.4	Night		45
1958 β2	Vanguard I	720	648	1.2×10^{-16}	May 1 to June 25, 1958	33° N. to 33° S.	33
		654	594	3.5	Spring and summer 1958		40
		656	596	4.5	Mar. to Aug. 1958		46
		660	600	1.2	Night		45
		660	600	8	Day		45
1958 γ	Explorer III	185	180	7.6×10^{-12}	Spring and summer 1958		40
		186	181	6.7×10^{-13}			31
1958 δ2	Sputnik III	190	185	3.3	Day		47
		190	185	2	Night		47
		190	185	5.3		40° N.	42
		210	203	4.5	Day		45
		210	203	3.5	Night		45
1958 ϵ	Explorer IV	258	247	1	Spring and summer 1958		40
		263	252	1.3	Aug. and Sept. 1958	50° N. to 31° S.	48

TABLE V.- ATMOSPHERIC DENSITIES, OTHER METHODS

Method	Altitude		Density, ρ, g/cm^3	Epoch	Latitude	Reference
	Geometric, Z, km	Geopotential, H, km'				
Sodium vapor diffusion	430	403	6.7×10^{-15}	Early morning		49
	430	403	4.7	Early morning		49
Manometer	225	218	2.12×10^{-13}	May 16, 1958, daytime	57° to 65° N.	41
	250	240	1.1	May 16, 1958, daytime	57° to 65° N.	41
	300	287	3.53×10^{-14}	May 16, 1958, daytime	57° to 65° N.	41
	400	377	6.6×10^{-15}	May 16, 1958, daytime	57° to 65° N.	41
	500	464	2.21	May 16, 1958, daytime	57° to 65° N.	41

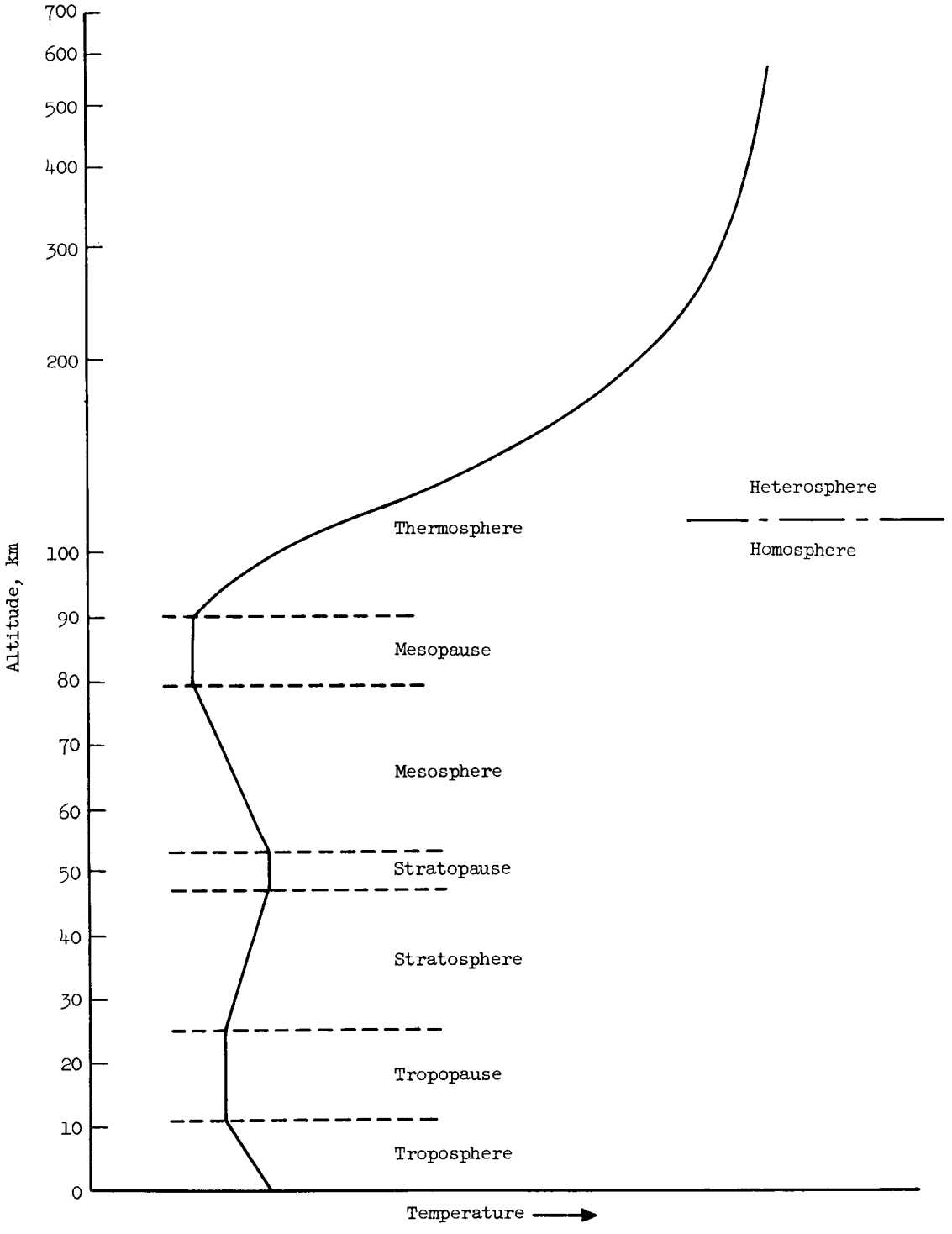

Figure 1.- Atmospheric nomenclature for discussion of composition or thermal properties.

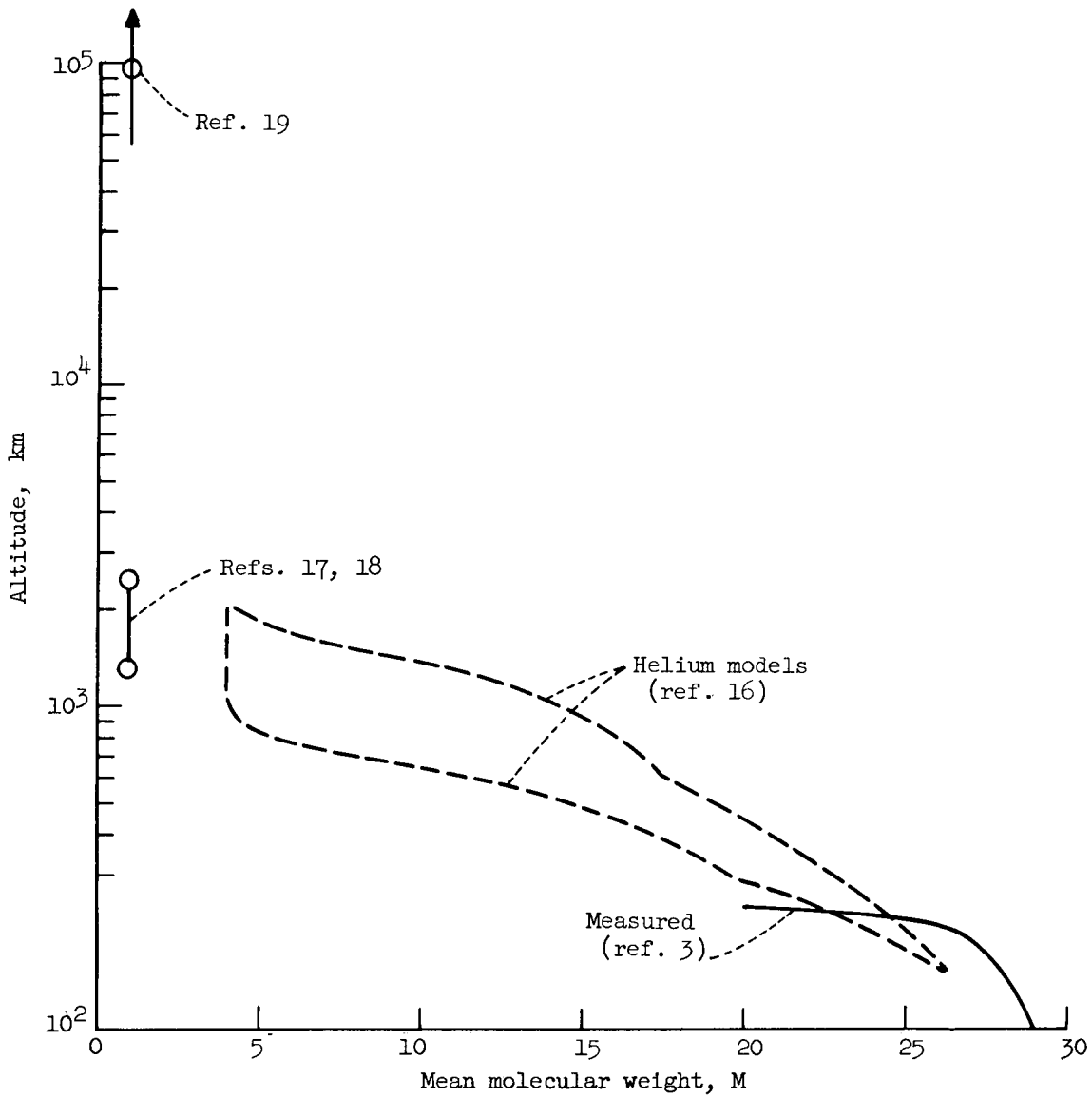

Figure 2.- Summary of molecular-weight data.

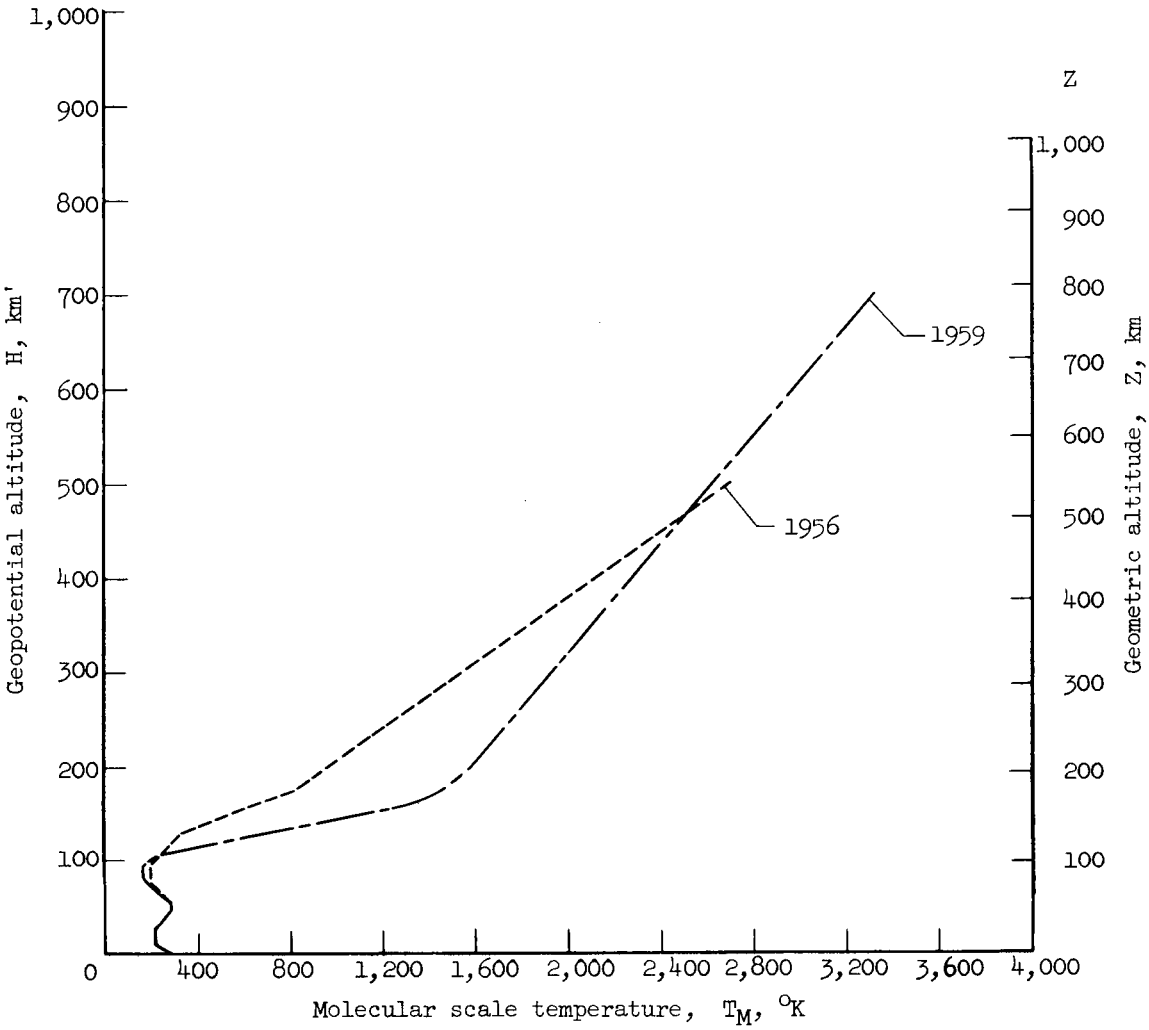

Figure 3.- Molecular scale temperatures used in defining ARDC atmospheres.

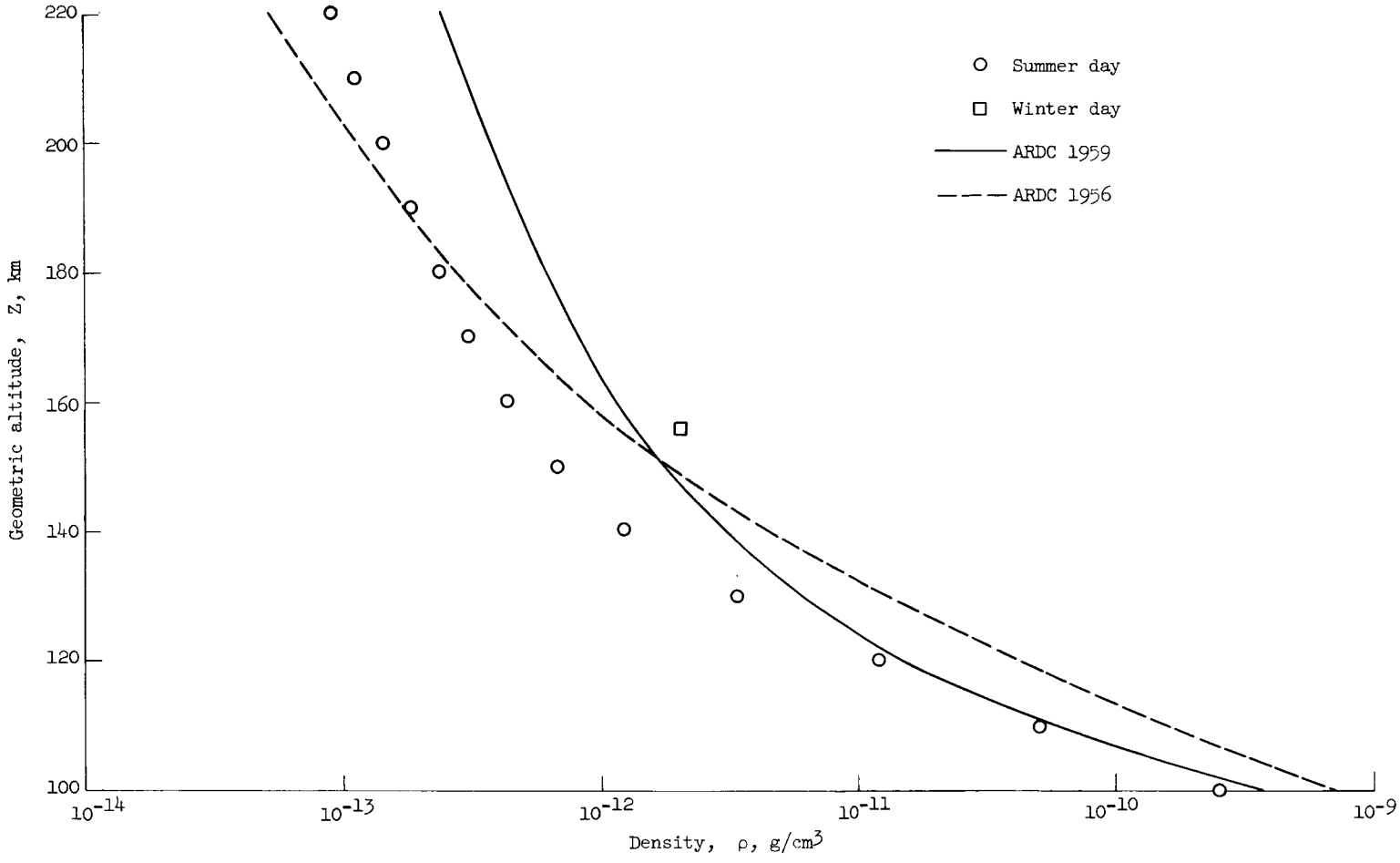

(a) Latitude 32° N.

Figure 4.- Atmospheric density above 100 kilometers, obtained from rocket measurements.

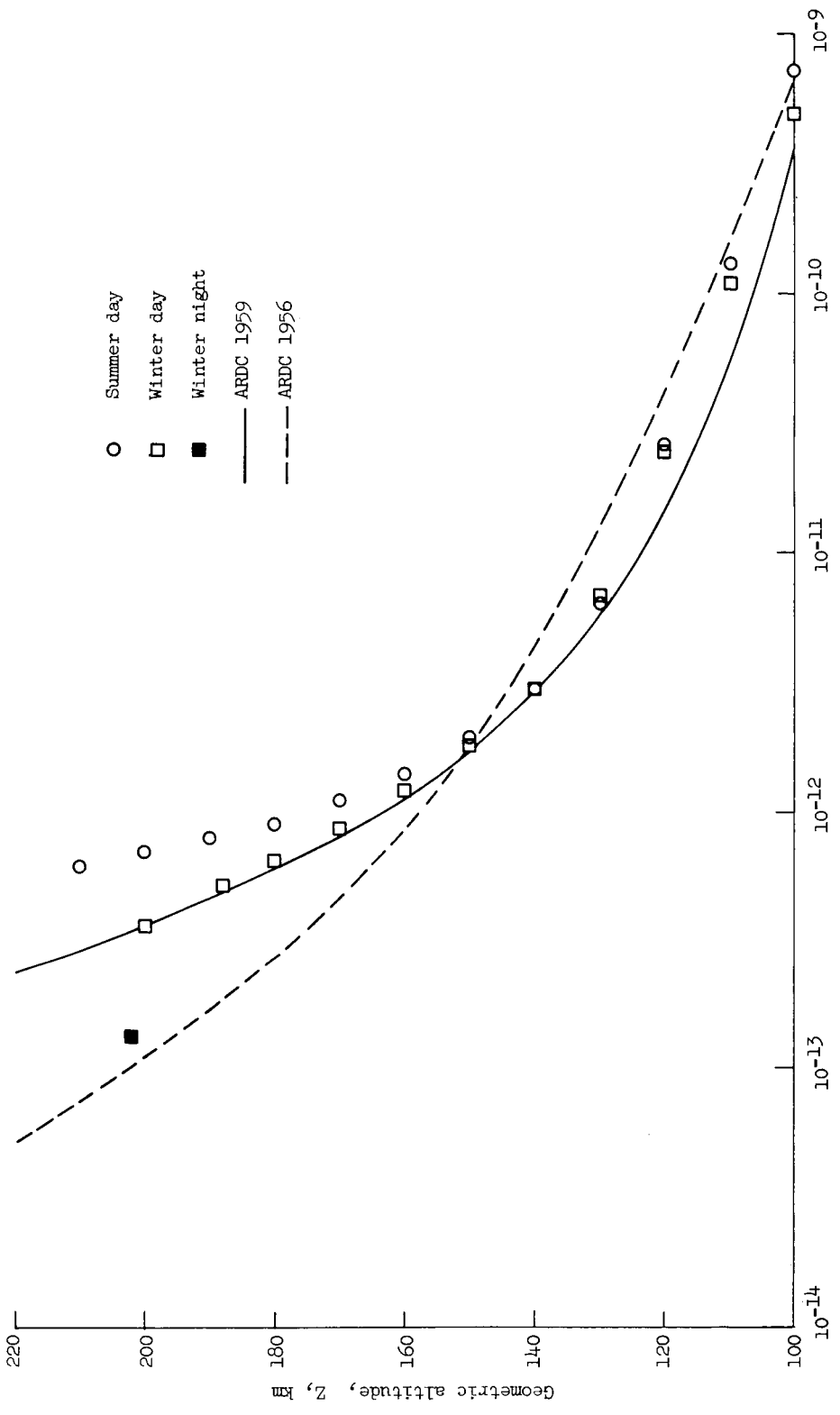

(b) Latitude 59° N.

Figure 4.- Concluded.

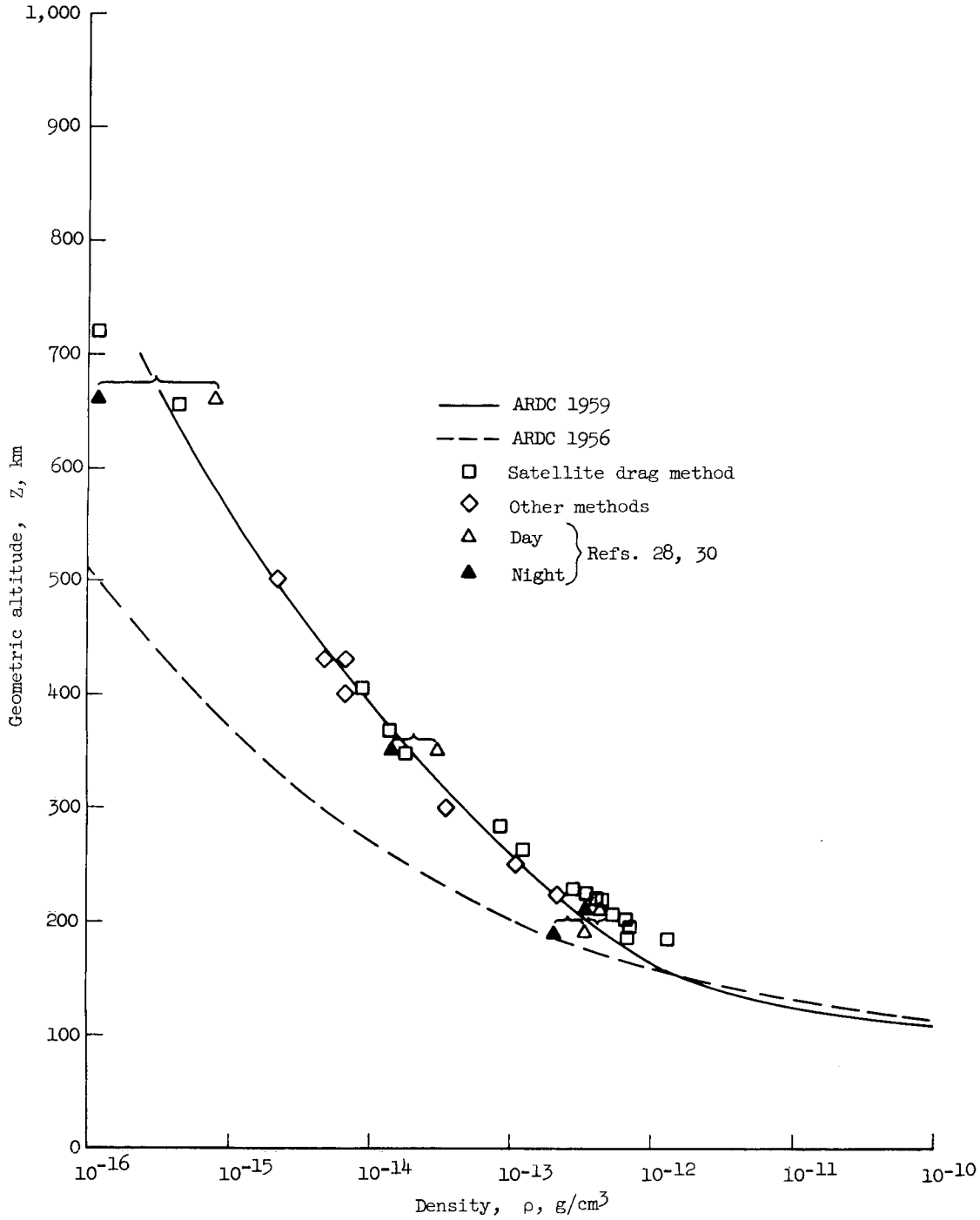

Figure 5.- Atmospheric density above 150 kilometers, obtained by satellite drag method.

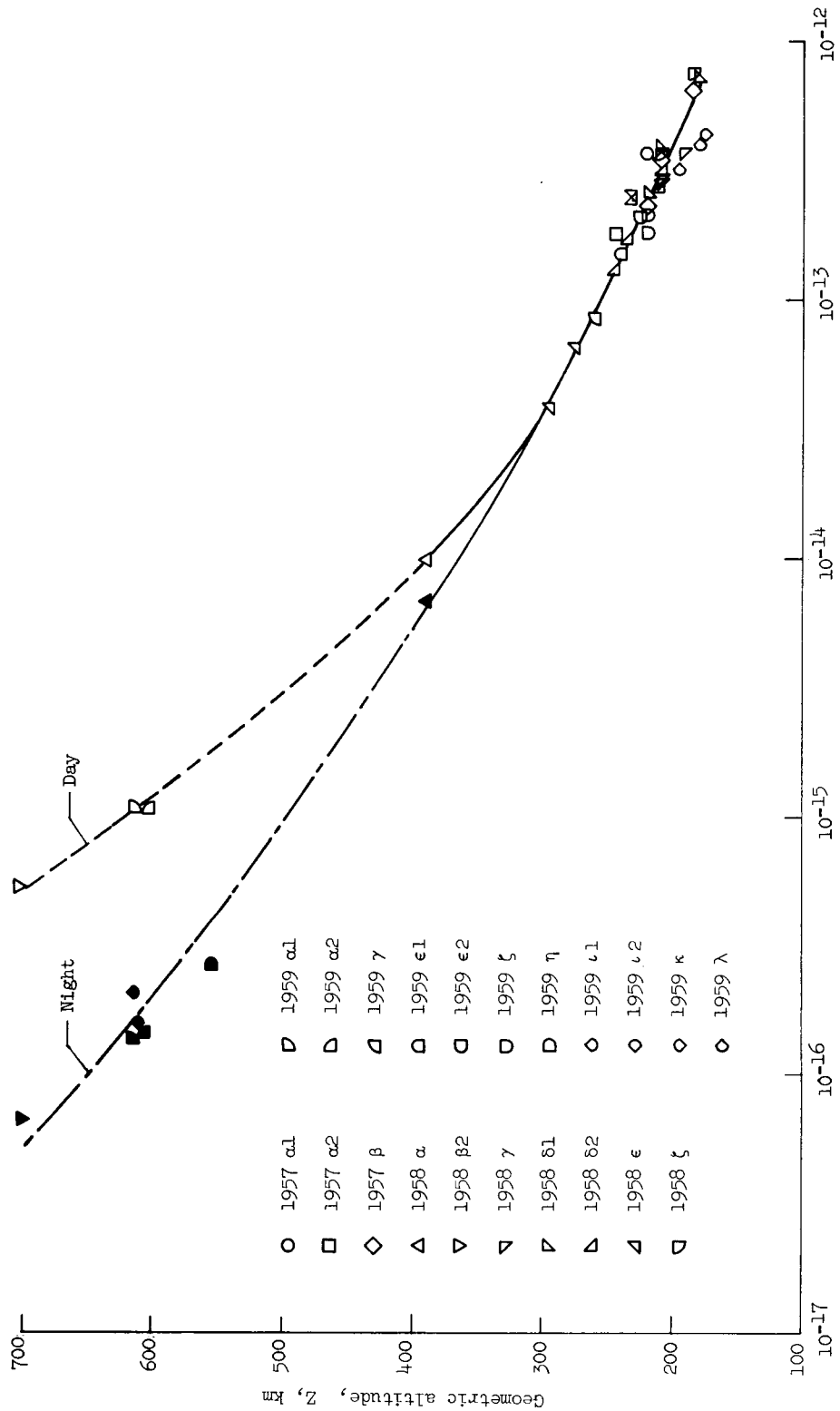

Figure 6.- Upper air densities obtained from orbits of 21 satellites (adapted from ref. 50).

II. RADIATION BALANCE OF THE EARTH'S ATMOSPHERE

By Richard A. Hord

INTRODUCTION

The earth's atmosphere, comprising less than one-millionth of the earth's total mass, serves to modify, retain, and distribute energy and matter, especially that incident upon the earth from the sun. The radiation energy balance of the earth's atmosphere is closely related to a number of features of the near-earth space environment and is discussed in this part of the survey.

Of the total solar electromagnetic radiation falling upon the earth and the bulk of its atmosphere, approximately 35 percent (the earth's albedo) is returned directly to space by reflection and scattering. Of the total albedo, 24 percent is due to reflection from clouds, 7 percent to scattering by molecules (dry air and water vapor) and dust, and 4 percent to ground reflection. (See ref. 1, pp. 32-38.)

The remaining 65 percent of the incident solar radiation is absorbed, 47 percent by the ground, 13 percent by water vapor and dust, 3 percent by ozone, and 2 percent by clouds. (See ref. 1, pp. 27-32.) Moreover, a small fraction of 1 percent of the incident radiation is absorbed in the upper atmosphere above the ozonosphere; the extinction of radiation of all wavelengths less than about 2,000 A (angstrom units) occurs there. (See ref. 2, pp. 122-126.)

By a variety of physical and chemical processes the absorbed energy is distributed through the atmosphere and the earth's surface layers. Along with the familiar processes of convection, conduction, and radiation, phase changes of water substance play a fundamental role in the transfer of heat in the lower atmosphere while dissociation or ionization, followed by diffusion and recombination, lead to important transfers of energy in the upper atmosphere. The redistribution of energy from the sun leads to a much more uniform temperature pattern at the earth's surface and in the bulk of the atmosphere than would exist in the absence of these energy transport processes.

The net result of these processes is a large increase in entropy. Thus, while the incoming solar radiation is mostly in or near the visible range of wavelengths and approximately equivalent to that from a black body at 6,000° K, the earth and its atmosphere radiate mostly in the infrared range approximately as a black body at a temperature not very different from the average temperature in the troposphere. The rate at which energy is returned to space is, on the average, the same as the

rate at which energy is received from the sun (ref. 3, p. 74). From the standpoint of the energies involved, the effective wavelength ranges of solar and terrestrial radiation do not overlap and a practical boundary between these ranges may be taken at about 40,000 A (4 microns).

Infrared absorption by such minor atmospheric species as water vapor, carbon dioxide, and ozone exerts the "greenhouse effect" which impedes terrestrial radiation and maintains temperatures at the earth's surface and in the lower troposphere at relatively high levels. As a result, terrestrial radiation proceeds mainly from the troposphere (87 percent), with smaller contributions from the earth's surface (8 percent), the stratosphere (4 percent), and so forth. (See ref. 1, p. 71.) Although the earth's surface, including snow, and the tops of sufficiently thick clouds radiate nearly as black bodies, the spectrum of the net outward radiation into space is complicated by the absorption and reemission by the minor gaseous species mentioned previously. (See, for example, ref. 4.) Measurements from satellites are expected to provide much valuable information on the nature of terrestrial radiation. The overall radiation balance of the earth and its atmosphere is shown schematically in figure 1.

The amount of energy involved in the numerous processes of the upper atmosphere is much smaller than the amount concerned with the lower atmospheric processes previously mentioned. However, many upper atmospheric phenomena have direct bearing on space flight near the earth. The flow of high-energy photons and particles from the sun is drastically altered in the upper part of the earth's atmosphere to such an extent that it for the most part never penetrates the lower atmosphere. For the stream of high-energy photons (wavelengths $< 2,000$ A), the transition region is mainly confined to a layer in the altitude range from 50 to 500 kilometers. For the corpuscular stream, which probably consists principally of protons and electrons, the transition region is mainly determined by the earth's magnetic field and extends outward to several earth radii, at least. General discussions of the upper atmosphere will be found in references 2, 5, and 6, and the sources mentioned therein.

Valuable reviews of research in meteorology, atmospheric physics, geomagnetism, and aeronomy are published regularly by the American Geophysical Union of the National Academy of Sciences, National Research Council. (See, for example, ref. 7.)

SOLAR RADIATION

Solar Spectrum

The flux of solar electromagnetic radiation threading the unit area situated normal to a ray from the sun at the earth's mean distance is

called the solar constant. A U.S. Naval Research Laboratory study in the visible and ultraviolet ranges has led to an improved estimate of 2.00 ± 0.04 langleys min^{-1} (1 langley = 1 gram calorie per square centimeter) for the solar constant (ref. 8). The slight variations of the solar constant which probably follow disturbed conditions on the sun are not yet accurately known, but they are likely to be within the limits of accuracy quoted. (See, for example, ref. 9, p. 1651.)

Most of the sun's radiation comes from the photosphere, a gaseous layer whose thickness is about 400 kilometers. The temperature decreases from about $8,000^{\circ}$ K at the inner boundary to about $4,200^{\circ}$ K at the outer boundary. Absorption by the cooler gases in the upper levels introduces the dark Fraunhofer lines in the observed spectrum. Radiation from levels below the photosphere is absorbed and reemitted and is not observed directly. The gas density falls rapidly near the top of the photosphere and the emitted light correspondingly decreases. With respect to the emitted near-continuum of visible wavelengths and more, the photosphere is the apparent solar "surface."

Above the photosphere lies a complex transition region about 12,000 kilometers deep known as the chromosphere, which has a profound effect on the ultraviolet portion of the solar spectrum. Although the distribution of temperatures in the chromosphere is closely related to its spicular structure and is therefore not simple, it appears that temperatures increase slowly at first and then very rapidly with increasing height. Chromospheric radiation includes an ultraviolet continuum from its lower levels together with a number of bright lines.

The corona, the sun's tenuous "atmosphere," begins at the top of the chromosphere and, with decreasing density, extends perhaps 10 astronomical units from the sun, where it probably merges with the interstellar medium. The temperatures near the base of the corona are strongly dependent on local solar disturbances and are of the order of $1,000,000^{\circ}$ to $5,000,000^{\circ}$ K. Unlike the photosphere, where the degree of ionization is small, the coronal gas is almost completely composed of electrons and protons, together with an appreciable percentage of heavier positive ions. The positive ions contribute bright lines to the solar spectrum. Moreover, the high-temperature gas yields X-rays over a continuous range of wavelengths. Both the chromosphere and the corona scatter considerable portions of the total solar radiation.

In summary, most of the solar radiation comes from the photosphere, which emits approximately as a black body at a temperature of $6,000^{\circ}$ K. In the ultraviolet the Fraunhofer lines increase in number and the effective temperature is reduced to about $4,200^{\circ}$ K. Beyond this minimum (i.e., toward shorter wavelengths) the contributions of the chromosphere and the corona, although relatively small in total energy, cause the

radiation distribution with respect to wavelength to rise, in places, far above that of a black body at 6,000° K in the wavelength range concerned.

The preceding discussion is intended as a very brief introduction to the detailed accounts of the origin of the solar spectrum to be found, for example, in references 5 and 10.

The energy balance of the earth's atmosphere is primarily influenced by the near-continuum radiation of the photosphere. On the other hand, the high-energy radiations of the chromosphere and the corona are of first importance to the phenomena associated with ionization and dissociation in the earth's upper atmosphere.

Solar Radiation Returned to Space - The Earth's Albedo

As indicated in the introduction, the earth's albedo (35 percent) is principally due to the reflection of insolation by clouds (24 percent). The 24 percent represents the product of an average cloud reflectivity of 47 percent and an average cloudiness of 51 percent. (See ref. 1, pp. 36-37.) The 47-percent value for cloud reflectivity, in turn, results from averaging over cloud distributions and types for which reflectivities vary over a wide range. (Cf. ref. 1, p. 36, and ref. 11, p. 7.) Similarly, it is necessary to average a wide range of values in order to obtain the contribution of ground reflection to the albedo. For example, with respect to visible wavelengths, the reflectivity of fresh snow may exceed 0.8, whereas the reflectivity of smooth water, even in the presence of a swell, is very small (<0.02) when the sun is high. The effect of scattering in the atmosphere on the earth's albedo is also difficult to evaluate. Besides the Rayleigh scattering, which accounts for the blueness of the sky through strong dependence on wavelength, nonisotropic scattering processes also occur in the cases of haze and dust. Discussions of these questions will be found in references 1, 11, 12, and 13, and in the papers mentioned therein.

The complexity of the processes and their interactions involved in the depletion of the incoming solar radiation raises considerable doubt as to the separability and simple additivity of the effects of clouds, atmosphere, and ground. To the extent that the concept of a local albedo is valid and can be evaluated, the earth's albedo can be calculated by averaging the local albedo, suitably weighted with respect to the local insolation, over the earth's surface and over the desired time interval. Specifically, the expression for the earth's albedo a becomes

$$a = \frac{\int_0^t \int_{-\pi/2}^{\pi/2} \int_0^{2\pi} a_l \gamma \cos \varphi \, d\theta \, d\varphi \, dt}{\int_0^t \int_{-\pi/2}^{\pi/2} \int_0^{2\pi} \gamma \cos \varphi \, d\theta \, d\varphi \, dt}$$

where

t	time
φ	latitude, radians
θ	longitude, radians
a_l	local albedo (function of φ, θ, t)
γ	cos α, during day; 0, during night
α	solar zenith angle

The relation of the solar zenith angle to latitude, longitude, and time is discussed in reference 12, pages 87-89.

Solar Radiation Absorbed

The insolation reaching the ground at a point is clearly dependent on the zenith angle of the sun, and the distribution of clouds. It is further dependent on the distribution of water substance in the forms of vapor and hydrometeors (fog, rain, snow, etc.), the distribution of dry particles such as dust, the distribution of ozone, and a number of other characteristics of the atmosphere. The fraction of the insolation reaching the ground which is absorbed there depends upon the nature of the surface and the structure of the incident radiation. The principal parts of this radiation are the diffuse component and the direct solar beam. Since scattering and absorption are selective, the spectrum is also a variable. The distribution of effective insolation at the earth's surface is discussed in reference 1. Averaged over the earth and the seasons, 47 percent of the solar radiation incident on the atmosphere is absorbed at the ground. With the presently accepted value of the earth's albedo (35 percent), then, the atmosphere absorbs 18 percent of the sun's radiation falling upon it.

Most of the atmospheric absorption of the incoming radiation is by water vapor in the troposphere and occurs in the infrared wavelengths.

The absorptivity of water vapor is a complicated function of the wavelength. The literature in the field of longwave radiation in the atmosphere, both with regard to absorption and emission, is reviewed in reference 13, pages 34-49. Some sources of more recent origin are mentioned in reference 11. Since the distribution of water vapor is extremely variable, the absorption of radiation in the atmosphere is far from constant. However, the incoming infrared radiation which escapes absorption in the atmosphere is almost completely absorbed at the surface. With respect to this range of wavelengths, for example, snow is practically a black body.

The absorption of insolation by dust and clouds is not well understood, particularly for the earth's atmosphere as a whole. Some discussion, however, of this problem is contained in references 1, 11, 13, and 14. Reference 1 states that, of the solar radiation incident on the atmosphere, 13 percent is absorbed by water vapor and dust, 2 percent by clouds, and 3 percent by ozone.

Beginning with the atmospheric layer (altitude range 10 to 40 kilometers) which contains most of the ozone, a number of chemical and ionic processes are initiated in the upper atmosphere by the absorption of insolation of wavelengths shorter than about 2,900 A. These processes are largely responsible for the composition and properties of the upper atmosphere.

The total quantity of ozone in the atmosphere varies approximately from 0.2 to 0.4 centimeter reduced to normal temperature and pressure. (See ref. 15, p. 438.) Its variation with latitude and season are shown in reference 15, page 582. The absorption of insolation by ozone, also with respect to latitude and season, is discussed in reference 1, pages 27-28, and in reference 11, pages 15-19; in reference 11, the variation with altitude is also discussed. Ozone absorbs ultraviolet light strongly in the range from 2,200 to 2,900 A; the absorption coefficient as a function of wavelength is given in reference 15, page 440.

The formation of ozone results from the dissociation of diatomic oxygen by the weak absorption of light in the Herzberg continuum (wavelengths $< 2{,}420$ A), yielding two oxygen atoms in the ground state, followed by the chemical reaction

$$O_2 + O + M \rightarrow O_3 + M$$

where M denotes a third body. Ozone is destroyed by the absorption of ultraviolet light (2,200 to 2,900 A); the photodissociation yields a diatomic oxygen molecule plus an oxygen atom in an excited electronic state. In addition, some ozone is destroyed by reaction with atomic oxygen, yielding diatomic oxygen, and by photodissociation resulting from the weak absorption of visible light near 6,100 A (ref. 15, p. 577).

The atmospheric absorption is somewhat weaker in the range from 2,100 to 2,200 A and a substantial portion of the ultraviolet light in this range reaches the middle of the ozonosphere (at approximately 25 kilometers). For shorter wavelengths, diatomic oxygen becomes increasingly prominent as an absorber through its Schumann-Runge band system, which converges to the Schumann dissociation continuum at 1,750 A. Absorption in the Schumann continuum, which produces one ground-state and one excited-state oxygen atom, is very strong, has a broad maximum around 1,425 A, and extends below 1,300 A. At shorter wavelengths, down to the ionization threshold for diatomic oxygen at 1,027 A, the absorption coefficient is highly variable due to a number of molecular bands. In particular, one "window" (low absorption coefficient) coincides with the wavelength (1,214.7 A) of the Lyman-alpha line of hydrogen, which is strong in the solar spectrum. Below 1,027 A the ionization continuum and a number of bands yield a somewhat smoother variation of absorption coefficient with wavelength. (See refs. 5 and 16.)

By lower atmosphere standards the latent energy of atomic oxygen associated with dissociation is large. For example, the latent energy of 1 mole of oxygen atoms is more than ten times the latent heat of vaporization of 1 mole of water. Most of the photodissociation of oxygen occurs, however, in the tenuous air above 100 kilometers. The convective and diffusive transport of atomic oxygen to lower altitudes, where the recombination reaction

$$2\ O + M \rightarrow O_2 + M + \text{Thermal energy}$$

is more likely because of the greater air density, results in a considerable downward flow of the energy absorbed in the Schumann continuum. The upward transport of O_2, followed by photodissociation, completes the cycle. The effect of diffusion in maintaining an appreciable mole fraction of O_2, even above 200 kilometers, is a comparatively recent result of upper atmosphere research. (See ref. 5, p. 127.)

Unlike diatomic oxygen, the photodissociation of diatomic nitrogen has a very low probability of occurrence. The sequence of reactions

$$N_2 + \text{Photon} \rightarrow N_2^+ + e^-$$

$$N_2^+ + e^- \rightarrow 2\ N$$

may account for the production of some atomic nitrogen above 150 kilometers. (See, for example, ref. 16, p. 201.)

A number of other absorption processes are important in the upper atmosphere. Detailed accounts of these may be found in references 2,

5, 6, 13, 15, 16, 17, and 18. In particular, the various theories of formation of the ionosphere are discussed in these references. Rocket and satellite measurements of electron densities and other ionospheric parameters during the years 1958-60 have been summarized by Seddon (ref. 19). The absorption of X-rays and γ-rays in air produces fast primary electrons; the secondary processes which ensue are given special attention in references 20 and 21.

Table I lists some of the absorption processes of the upper atmosphere together with remarks concerning their significance.

It is well known that the ionosphere reflects radio waves of wavelength greater than about 15 meters. However, the atmosphere ordinarily is practically transparent to radiation in the wavelength range from about 1 centimeter to 15 meters. The regular cutoff at about 1 centimeter marks the effective terminal wavelength for molecular absorption bands. The atmospheric window permits both radio communication between earth and space and the use of the techniques of radioastronomy in studying solar phenomena and the emissions of other celestial objects. Following certain disturbed solar conditions, however, the ionosphere may strongly absorb radiation in this range due to increased electron density in its lower regions, especially the D region. The absorption of radio waves in the ionosphere increases with increasing radio wavelength and increasing number of electron collisions (with air particles) per unit volume per second.

NONRADIATIVE ENERGY TRANSFER AT THE EARTH'S SURFACE

Processes Involving Water

A large segment of meteorology is concerned with evaporation, sublimation, and precipitation, and their primary role in providing means for heat exchange between the surface and the atmosphere. Closely related to these is the transfer of heat by ocean currents, rivers, and so forth. These processes are treated in references 3, 12, 13, and 15, for example, but do not warrant further consideration here.

Processes Involving Air

The flow of air at the earth's surface is generally turbulent and characterized by a boundary-layer thickness of the order of 1 kilometer. Accordingly, the transfer of heat and water vapor across the surface layer of air must be analyzed with due account taken of turbulence. (See, for example, ref. 13, pp. 492-509.)

Net Heating of the Atmosphere From Below

This must be equal in total (including radiative) energy to the percentage of the incident solar energy which is absorbed at the surface (that is, 47 percent) minus the energy radiated directly to space from the surface. As a result of the general circulation of the atmosphere and oceans, of course, the distribution of atmospheric heating from below bears little relation to the distribution of insolation absorbed at the surface.

TERRESTRIAL RADIATION

Terrestrial radiation is primarily confined to the wavelength range from 4 to 100 microns and proceeds mainly from the troposphere. A crude description of this radiation is afforded by considering a black surface at one-half of the altitude of the tropopause and at a temperature of approximately 250° K. This model satisfies the Stefan-Boltzmann law for the values of the earth's albedo and the solar constant mentioned previously; the assumption that the earth suffers no net gain or loss of heat is also made. The actual terrestrial radiation is much more complicated, of course, than the radiation from a black sphere at constant temperature.

Approximately 8 percent of the total terrestrial radiation is directly attributable to the earth's surface; this is radiation which escapes absorption in the atmosphere and may be called "window radiation," although the atmospheric spectral windows vary with water-vapor content, and so forth. The remainder of the terrestrial radiation proceeds from the atmosphere (chiefly from cloud tops, air, and dust); approximately 87 percent originates in the troposphere and 4 percent in the stratosphere. (See ref. 1, p. 71.) In addition, a small amount of radiation to space originates in the aurorae and the airglow layers of the upper atmosphere. (See refs. 2, 5, 6, and 22.)

The absorption and emission of longwave radiation in the atmosphere are mainly governed by the highly variable distribution of water vapor, which absorbs (and therefore emits) strongly in the wavelength ranges from 5.5 to 7 microns and from 20 to 100 microns and to a smaller extent elsewhere. Next in importance is carbon dioxide with strong absorption in the range from 12 to 18 microns. The troposphere is practically transparent in the range from 8.5 to 11 microns, which is sometimes called Simpson's window. However, ozone absorbs strongly in the range from 9 to 10 microns. The distribution of ozone in the atmosphere, although much more regular than that of water vapor, is far more complicated than that of carbon dioxide. Absorption by water vapor is partically limited to the troposphere, but carbon dioxide is very effective in absorption up to altitudes of the order of 20 to 30 kilometers. (Cf. refs. 1, 11, 13, 23, and 24.)

The radiation from earth to space is, therefore, generally characterized by absorption and reemission, with the net result that it gradually diffuses upward to atmospheric levels where the overlying gases are no longer effective in impeding the efflux. As in the case of black-body radiation, the emission intensities are dependent upon the local gas temperatures. Since the atmospheric temperatures concerned are, in general, considerably lower than the earth's surface temperatures, the blanketing effect of the atmosphere is rather large.

OTHER ENERGY TRANSFERS

Atmospheric heating due to auroral activity has been considered by Bates and was found, on a global basis, to be small compared with heating associated with photoionization; a heat source at great altitudes is needed to account for the rate at which temperature increases in the thermosphere (ref. 5, p. 343).

Chapman has developed a theoretical model of the solar corona which takes heat conduction into account and has concluded that heat must flow into the earth's upper atmosphere from the hot coronal gas (ref. 25 and ref. 5, p. 11). Some objections to this work have been raised by Bates, who has also discussed the thermal economy of the upper atmosphere (ref. 26).

It is well known that atmospheric tides, produced by the gravitational fields of the sun and the moon, cause large effects in the upper atmosphere. The regular dissipation of a part of the energy concerned yields an additional source of heat in the atmosphere which is presently difficult to assess. Discussions of atmospheric tides, the resulting equatorial electrojets, the magnetic field variations, and so forth, will be found in references 2, 3, 5, 6, 13, and 15. Discussions of the airglow will also be found in these references.

APPLICATIONS

General

The electromagnetic-radiation environment of a space vehicle would be completely known if the specific or monochromatic intensity (ref. 14, p. 287) were known for all wavelengths and directions at every point of space. The problem may be broken down according to the following list:

Solar radiation
- Variations with solar activity
- Shadow effects - umbrae and penumbrae of earth, moon, and so forth
- Reflection and scattering by planets and atmospheres
- Lens effects - refraction by atmospheres
- Special effects - zodiacal light, comets, and so forth

Planetary radiation
- Longwave radiation
- Aurorae and airglows

Radiation from outside the solar system

The outline is very broad and does not, for example, give due emphasis to particular wavelength ranges. Moreover, in the case of the earth, the distribution of clouds has a considerable effect in a number of the categories. However, the outline may serve as a starting point for listing the effects which require consideration in a particular engineering problem.

Appearance of the Earth

A problem of increasing importance is the appearance of the earth when it is observed from a space vehicle. For some purposes of orientation and navigation, it would be desirable to have the earth, including its atmosphere, appear as a bright, sharp-edged disk or ring whose angular size and shape bore a known relation to the position of the observer. In view of the earlier discussion of radiation in relation to the atmosphere, this goal is only approximately attainable. Furthermore, the utilization of terrestrial radiation in some manner which is not subject to overpowering effects of solar radiation seems to be necessary. Several possibilities will now be considered.

Since the window radiation from the earth's surface is subject to absorption by clouds, an apparent edge of the earth must be sought in the atmosphere. For an intensity-measuring instrument which admits and integrates overall wavelengths in the range from 4 to 100 microns, the variability of the cloud, water-vapor, and (to some extent) temperature distributions implies that the observed edge may lie anywhere in the troposphere or perhaps higher. It is conceivable that some advantage may be gained by using an instrument with sufficiently low threshold for the lower troposphere to appear bright in profile even in cases of low humidity. The accuracy would appear to be limited in any method of this type, however, to approximately the thickness of the troposphere.

The 15-micron band emitted by carbon dioxide, effectively in the stratosphere, is a particularly interesting atmospheric radiation in this connection. Although it is an order of magnitude less intense than the total tropospheric radiation considered in the preceding paragraph, the 14- to 16-micron radiation emerges essentially from layers which lie above practically all clouds and water vapor. (See ref. 23, fig. 8, p. 316.) In addition, the distribution of carbon dioxide in the atmosphere is far more regular than that of water vapor. The overlying ozone has an interfering band, but it appears unlikely that this will be strong enough to obscure the carbon dioxide emission seriously. (See ref. 24, fig. 1, p. 1452.) The variability of temperature, with latitude and time, at the effective level of emission for CO_2 does not seem to be great enough to cause significant difficulties. In view of the foregoing remarks, further study of the utilization of this radiation is warranted.

The 9.6-micron band of ozone is fairly strong, but the variability of the ozone distribution puts this radiation in an unfavorable position in the present application.

Nacreous and noctilucent clouds (see ref. 27, p. 88), which generally occur in the altitude ranges from 22 to 30 kilometers and from 80 to 90 kilometers, respectively, are not likely to be more than an occasional nuisance to the infrared systems discussed, provided their presence over limited areas of the earth is allowed for in the particular design. Volcanic dust may also fall into this class.

In the infrared ranges considered, the earth would appear as a disk with a somewhat fuzzy edge. On the other hand, the earth's upper atmosphere, viewed from outside in the wavelength of an airglow emission, should appear as a ring whose outer edge corresponds to the "top" of the particular airglow layer. The effective inner edge of the ring may be less well defined and, therefore, of less interest. Furthermore, reflected and scattered light from the earth's surface and lower atmosphere (and, sometimes, refracted light) complicate the ring's interior unless the space vehicle is sufficiently far inside the earth's umbra. The solar or lunar disk may, of course, appear behind an arc of the ring at times. In addition, auroral radiation may further complicate the picture. Global studies from rockets and satellites are needed before the usefulness of the airglow layers as "edge-of-the-earth markers" can be determined.

Radio Communication Between Earth and Space

The structure of the ionosphere is largely controlled by the high-energy solar electromagnetic and corpuscular radiations, both of which may vary over wide ranges in cases of disturbed solar conditions. As

a result, radio communications may be disrupted for considerable periods of time. Abnormal ionospheric conditions associated with disturbed solar conditions are summarized in table II. More detailed discussions are available in references 2, 5, 6, and 28.

NEEDS FOR FURTHER RESEARCH

Scarcely any aspects of radiation and its interaction with the earth's atmosphere are thoroughly understood. The need for further research in this broad field is very evident to the space-flight engineer, the aeronomist, the meteorologist, the radio engineer, and many others.

A few of the general questions which require additional attention are:

1. To what extent does atmospheric behavior indicate radiation-environment conditions in space beyond the sensible atmosphere?

2. What is the role of nitrogen in the radiative properties of the upper atmosphere?

3. How do variations in the absorption and emission of radiation affect the weather?

4. If good forecasts of solar disturbances were presently available, to what extent could abnormal ionospheric conditions be predicted?

The last of these raises the same basic question as the first, that is, the sun's effect on the earth's environment, but the partial duplication is clearly justified by the importance of these matters to successful space operations.

Large steps toward obtaining the answers to the second and third questions will undoubtedly result from rocket and satellite experiments within the next few years. (See, for example, ref. 29.) Early planning of an adequate program in theoretical research to keep pace with the wealth of experimental findings which are expected presently deserves careful consideration.

REFERENCES

1. London, Julius: A Study of the Atmospheric Heat Balance. AFCRC-TR-57-287, ASTIA no. 117227, College Eng., New York Univ., July 1957.

2. Massey, H. S. W., and Boyd, R. L. F.: The Upper Atmosphere. Phil. Lib. (New York), 1959.

3. Bates, D. R., ed.: The Earth and Its Atmosphere. Basic Books, Inc. (New York), 1957.

4. Murgatroyd, R. J., and Goody, R. M.: Sources and Sinks of Radiative Energy from 30 to 90 km. Quarterly Jour. Roy. Meteorological Soc., vol. 84, no. 361, July 1958, pp. 225-234.

5. Ratcliffe, J. A., ed.: Physics of the Upper Atmosphere. Academic Press, Inc. (New York), 1960.

6. Mitra, S. K.: The Upper Atmosphere. Second ed., The Asiatic Society (Calcutta, India), 1952. (Available from Hafner Pub. Co., New York.)

7. Adams, Leason H., ed.: United States National Report, 1957-1960 - Twelfth General Assembly, International Union of Geodesy and Geophysics. Trans., American Geophys. Union, vol. 41, no. 2, June 1960, pp. 129-318.

8. Johnson, F. S., Purcell, J. D., Tousey, R., and Wilson, N.: The Ultraviolet Spectrum of the Sun. Rocket Exploration of the Upper Atmosphere, R. L. F. Boyd and M. J. Seaton, eds., Pergamon Press Ltd. (London), 1954, pp. 279-288.

9. Roberts, Walter Orr, and Zirin, Harold: Recent Progress in Solar Physics. Jour. Geophys. Res., vol. 65, no. 6, June 1960, pp. 1645-1659.

10. Kuiper, Gerard P., ed.: The Sun. The Univ. of Chicago Press, c.1953.

11. Coulson, K. L.: Atmospheric Radiative Heating and Cooling. Sci. Rep. 1 (AFCRC-TN-60-273), Stanford Res. Inst. (Menlo Park, Calif.), Mar. 1960.

12. Humphreys, W. J.: Physics of the Air. Third ed., McGraw-Hill Book Co., Inc., 1940.

13. Malone, Thomas F., ed.: Compendium of Meteorology. American Meteorological Soc. (Boston), 1951.

14. Charney, J.: Radiation. Handbook of Meteorology. F. A. Berry, Jr., E. Bollay, and Norman R. Beers, eds., McGraw-Hill Book Co., New York, 1945, pp. 283-311.

15. Kuiper, Gerard P., ed.: The Earth as a Planet. The Univ. of Chicago Press, c.1954.

16. Watanabe, K.: Ultraviolet Absorption Processes in the Upper Atmosphere. Vol. 5 of Advances in Geophysics, H. E. Landsberg and J. van Mieghem, eds., Academic Press, Inc. (New York), 1958, pp. 153-221.

17. Zelikoff, M., ed.: The Threshold of Space. Pergamon Press (New York), c.1957.

18. Nicolet, Marcel: The Constitution and Composition of the Upper Atmosphere. Proc. IRE, vol. 47, no. 2, Feb. 1959, pp. 142-147.

19. Seddon, J. Carl: Summary of Rocket and Satellite Observations Related to the Ionosphere. NASA TN D-667, 1961.

20. Massey, H. S. W., and Burhop, E. H. S.: Electronic and Ionic Impact Phenomena. First ed., The Clarendon Press (Oxford), 1952. (Reprinted 1956.)

21. Meyerott, R. E., Landshoff, R. K. M., and Magee, John: Physics of the Ionization Processes in Air. LMSD-48361, Lockheed Aircraft Corp., Dec. 12, 1958.

22. Hunten, D. M., and Jones, A. Vallance: Basic Research on Aurora and Airglow. AFCRC-TR-60-257, Dept. Physics, Univ. of Saskatchewan, Apr. 30, 1960.

23. Plass, Gilbert N.: Infrared Radiation in the Atmosphere. American Jour. Phys., vol. 24, no. 5, May 1956, pp. 303-321.

24. Howard, J. N.: The Transmission of the Atmosphere in the Infrared. Proc. IRE, vol. 47, no. 9, Sept. 1959, pp. 1451-1457.

25. Chapman, S.: Interplanetary Space and the Earth's Outermost Atmosphere. Proc. Roy. Soc. (London), ser. A, vol. 253, no. 1275, Dec. 29, 1959, pp. 462-481.

26. Bates, D. R.: Some Problems Concerning the Terrestrial Atmosphere Above About the 100 km Level. Proc. Roy. Soc. (London), Ser. A, vol. 253, no. 1275, Dec. 29, 1959, pp. 451-462.

27. Perrie, D. W.: Cloud Physics. John Wiley & Sons, Inc., 1950.

28. Sherman, H., Enticknap, R. G., and Bailey, A. B.: High Frequency Propagation Predictions. Memo. 20-0011 (Contract NAS 1-229), Lincoln Lab., M.I.T., Sept. 4, 1959.

29. Bignell, K. J.: Heat Balance Measurements From an Earth Satellite - An Analysis of Some Possibilities. Quarterly Jour. Roy. Meteorological Soc., vol. 87, no. 372, Apr. 1961, pp. 231-244.

TABLE I.- SOME ABSORPTION PROCESSES OF THE UPPER ATMOSPHERE

Threshold, A	Species	Process	Significance
2,420	O_2	Dissociation (Herzberg)	Step in formation of ozonosphere
1,750	O_2	Dissociation (Schumann)	Produces atomic oxygen in thermosphere
1,345	NO	Ionization	Contributes to D-layer ionization largely by Lyman-alpha absorption
1,269	N_2	Dissociation	Probably negligible
1,027	O_2	Ionization	Contributes to E-layer ionization largely by absorption in Hopfield bands
910	O	Ionization	Contributes to ionization of F layers
852	N	Ionization	Unknown
796	N_2	Ionization	Step in formation of atomic nitrogen

TABLE II.- ABNORMAL IONOSPHERIC CONDITIONS

[Cause loss of signal strength, sometimes complete blackout]

Characteristic	Sudden ionospheric disturbances (SID, or Mogel-Dellinger fades)	Ionospheric storms	
		Sudden commencement	Gradual commencement
Cause	Ultraviolet or high-frequency radiation* from solar active region	Entry of charged particles from solar active region	
Solar active region	Solar flare	Solar flare	Solar M region
27-day-recurrence tendency	None	None	Pronounced
Most likely to occur	Around sunspot maximum	Around sunspot maximum	About 2 years after sunspot maximum
Onset	At visual appearance of solar flare	1 to 4 days after visual appearance of solar flare	Uncertain, due to indefinite information on M regions
Duration	Several hours	Several hours to several days	Average is 5 days
Global extent	Sunlit side*	Worldwide	Worldwide
Effect on D region	Increased total ionization and consequent increased absorption of radio waves		

*Accompanied by worldwide, cosmic-ray enhancement in the case of unusually intense solar flares. Increased D-region ionization, particularly in polar regions, may severely attenuate radio transmissions through the ionosphere.

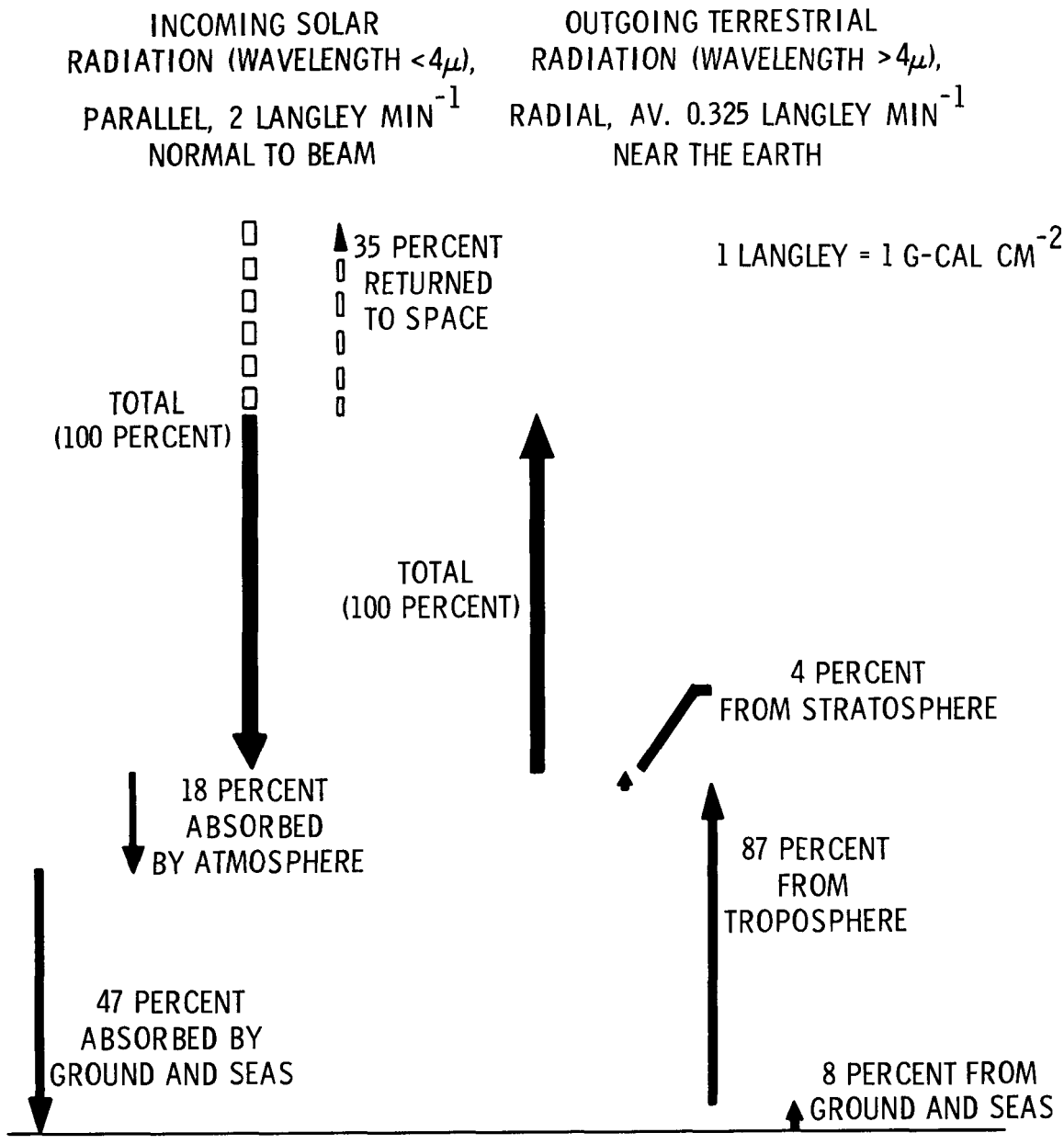

Figure 1.- Schematic diagram of overall radiation balance of earth and its atmosphere

III. WINDS AND MOTIONS IN THE ATMOSPHERE

By Harold B. Tolefson

INTRODUCTION

The dynamics of the atmosphere present a number of problems in regard to space vehicle operation and constitute an important element in the space environment. The large-scale circulation systems of the atmosphere, the smaller sized eddy or turbulent velocities at different altitudes, and the particle movements in the outer fringes of the atmosphere all react in varying degrees with the missile or satellite system so that their nature must be known and their effects on the operation recognized.

The manner in which the space vehicle reacts to the forcing functions represented by the atmospheric motions varies to a considerable extent depending on the altitudes under consideration, primarily because of air density, and on the vehicle configuration and flight speed. As examples, the winds, turbulence, or other characteristics of the flow fields encountered during the exiting flight phases through the lower altitudes are of considerable importance to the vehicle design and operation because of the severe dynamic loading conditions experienced by the missile system. At orbital altitudes, however, neither the motions of the atmospheric particles nor the satellite responses to these motions are clearly understood. In addition, aerodynamic loads as used in the usual sense are nonexistent at orbital altitudes because of the essential absence of an atmosphere at altitudes, say above 200 kilometers (about 125 statute miles). Nevertheless, estimates made by various workers in this area (for example, see ref. 1) have suggested that upward expansion of the earth's atmosphere through long solar exposure, particularly during the nearly continuous exposure of the arctic summer, could produce relatively large density increases at high altitudes and effect satellite drag. It is also pointed out in reference 2 that the large transfers of energy to the earth's atmosphere following solar outbursts cause similar expansions and have been observed to produce rather marked changes in the satellite period of revolution. Thus, the dynamic characteristics of the atmosphere enter into the varied problems of satellite operations regardless of the phase of the operation and constitute an important element in the development of space technology.

This part of the survey is concerned with the various dynamic processes of the atmosphere and the role that these processes play in defining the environment of a satellite. The approach to this problem is primarily that of assessing the pattern of atmospheric motions at

the different altitudes through the use of observational and theoretical results and of associating these atmospheric inputs with the vehicle reactions for the various phases of space operations. This approach requires a documentation or review of the various experimental measurements of atmospheric motions together with a consideration of theoretical deductions on the conditions existing at different altitudes. It also necessarily involves a consideration of the lower atmosphere as a starting point or "stepping stone" to space flight. In the overall sense, no particular altitude segment of the atmosphere can be considered entirely independently of others because of interactions between atmospheric motions at one altitude with those at adjoining altitudes. Insofar as possible, such crossties in energy exchange will be indicated, together with their significance to satellite operations.

In undertaking this part it is recognized that any discussion of such a rapidly growing field of investigation cannot be complete. Beyond the question of time and space limitations, some of the atmospheric measurements are preliminary in nature and are subject to revision when additional and more exact information becomes available. Also, no effort has been made to synthesize the information into a consistent pattern throughout the different altitudes as distributions of some of the wind components with altitude have already been developed by fitting together various observational data. (See refs. 3, 4, and 5.) It is also recognized that the following discussion reflects the thoughts and efforts of a great number of scientists and organizations within this country and abroad. It will be impossible to recognize individually the results which might be attributed to the many workers in this wide field of investigation.

SCOPE OF DATA

A wide variety of measurements is available from investigations during and prior to the International Geophysical Year for studying atmospheric dynamics. Some of the primary observational methods are listed in table I together with an indication of the approximate altitude coverage. A few remarks on the nature of the information obtained are also noted in the table. This table is intended only as a general listing of the various sources of information and cannot be exact because of the overlapping altitude ranges to which different observational methods apply and the quantity and quality of data represented by any case. The scope of these measurements will be mentioned only briefly here, but will be more fully described in subsequent sections which deal with the individual measurements.

For altitudes below 30 kilometers, measurements of the winds and other motion parameters are, of course, made daily by a large number of surface and upper air balloon stations and have established the climatology of the lower atmosphere. Direct measurements by means of rocket flights to the higher altitudes have been made only sporadically so that the available information decreases drastically with increasing altitudes. As noted in table I, the rocket probing methods used in obtaining information throughout the higher altitudes include the use of artificially generated trails such as sodium vapors ejected from vertically rising rockets and more indirect sounding methods as the rocket-grenade sound-propagation studies. By good fortune there are available several natural phenomena which also provide methods of exploring the dynamics of the upper atmosphere. Noctilucent clouds have provided a convenient natural system of tracers to indicate atmospheric winds at about 80 kilometers whereas optical tracking methods have been used for a number of years to measure the drift and distortion of long-enduring meteor trails from altitudes of about 70 kilometers to 150 kilometers. In quite a different manner, reflected radio waves have served to measure the local and temporal drift patterns of the ionized layers in the E and F regions and also of the highly ionized trains of meteors entering the atmosphere. Finally, very sensitive magnetic measurements furnish evidence of current and tidal systems in the ionosphere.

Although the various sources of information summarized in table I have begun to present a picture of the nature and state of motions of the atmosphere to the higher altitudes, many of the measurements (particularly the rocket data) have been obtained from only a few locations and only at selected times of the year. Nevertheless, sufficient data appear to be available to confirm many of the features of the circulation that have been derived by theoretical methods and to indicate that large variations in the circulation pattern occur, say as a function of season or time of day.

THE LOWER ATMOSPHERE

As a starting point, it seems quite natural to consider first some of the characteristics of the lower and denser portions of the atmosphere which are of concern to satellite operations. For this discussion, a division has been made at about 20 or 30 kilometers; although this division is rather loose, it still is quite logical for the following reasons.

First, as has been mentioned, the portions of the atmosphere up to 20 or 30 kilometers are comparatively accessible to observation and have been widely studied through use of a variety of measuring and sounding

methods. To reach altitudes above 30 kilometers (the usual sounding-balloon ceiling), entirely different methods must be used and the quantities of interest are frequently quite different. The nearly isothermal region of the stratosphere also ends at about 30 kilometers and is overlaid by regions which become rather tenuous with increasing altitude and which are characterized by high and low temperature peaks. Second, the ground handling and launch phases of satellite operations are strongly dependent on the complex circulation or "weather" systems of the troposphere and the important convective and surface effects leading to strong winds and turbulence. Many of the structural and guidance aspects of the vehicle are also defined by the strong winds and shears encountered in the vicinity of jet streams near tropopause levels and by strong stratospheric winds sometimes encountered at higher levels. Finally, many of the processes occur throughout the lower 20- to 30-kilometer altitude region which maintain the heat balance of the earth and its atmosphere, and by energy exchange solar radiation is utilized as the main driving force of the atmosphere.

In the following paragraphs the radiation balance of the lower atmosphere is reviewed briefly for background information on the general features of the circulation. Subsequent paragraphs then cover some particular characteristics of this portion of the atmosphere which are of major importance to the satellite launch and exiting flight phases.

Radiation Balance

The earth's atmosphere is generally considered to operate as an enormous heat engine in the sense that the energy in the form of heat from the sun is applied essentially in equatorial zones and the resulting temperature gradients cause the large-scale motions of the atmosphere and thus convert heat energy into kinetic energy. Some idea of the distribution of the net radiative energy absorbed by the earth and its atmosphere at different latitudes can be gained from figure 1 (adapted from ref. 6). In this figure the shaded area represents various estimates of the net absorbed radiation in gram-cal/cm^{2}min as a function of latitude for the Northern Hemisphere. Although considerable variation exists in the estimated radiation absorbed at any latitude, note that there is agreement in a net heating south of latitude about 35° N. and net cooling at more northerly latitudes.

The radiative energy which is available for driving the atmosphere is only a portion of the total incoming solar radiation but it still represents enormous values. Wexler in reference 7 has estimated that the resulting wind systems of the earth have a total kinetic energy equal to nearly 7×10^6 atomic bombs which must be replenished every

9 to 12 days due to frictional losses. Most of the ultraviolet radiation and charged particles coming from the sun do not penetrate very deeply into the atmosphere and only that portion in or near the visible range of wavelengths, from 3,800 to 7,800 A (angstrom units), is the dominant form of solar energy entering the lower atmosphere. Part of this light is reflected back into space chiefly by clouds, snow, and ice, and the balance is absorbed by the atmosphere and the earth from which it is then radiated in the infrared region to maintain the heat balance. The state of knowledge of the atmospheric radiation balance is reviewed in Part II of the present volume; of particular interest here is the paper by London. (See ref. 8.)

General Circulation

As the result of the differential solar heating processes outlined in the preceding paragraphs, together with the earth's rotational effects, complex circulation patterns develop within the lower atmosphere. If the earth did not rotate, polar air would move equatorward at the surface to replace the air lifted by the more intense heating and expansion in equatorial regions. A direct thermal circulation between the equator and the poles cannot develop, however, because of the effect of the earth's rotation (Coriolis effect). The Coriolis force is generally viewed as the conservation of angular momentum in that an element of the thermal circulation being carried from the pole toward the equator would have a deficit of west-to-east momentum with respect to the earth and the flow would curve to the west. Since the atmospheric flow of air is essentially horizontal, the accelerations of an air parcel and hence the wind velocties are mainly determined by the horizontal components of the pressure gradient due to heating and the Coriolis forces. In the absence of friction these two forces, that is, pressure-gradient force and Coriolis force, are equal and opposite.

The geostrophic flow conditions under which the horizontal pressure gradient and Coriolis forces are in balance are covered rather thoroughly in the literature (see, for example, refs. 9 and 10) and for straight-line flow these conditions are usually expressed in the form:

$$-\frac{1}{\rho}\frac{\partial p}{\partial y} = 2v_g\Omega \sin \phi$$

where, in the left-hand term, p, ρ, and y denote, respectively, pressure, density, and horizontal distance perpendicular to the isobars; and in the right-hand term v_g, Ω, and ϕ denote the horizontal wind component, the earth's angular speed of rotation, and the latitude angle. As an illustration, the conditions of geostrophic flow are sketched in the upper left-hand portion of figure 2. It is to be noted from this

sketch that the effect of the earth's rotation is to force the air to flow more or less parallel to the isobars rather than directly across them from high to low pressure.

Below the height of the geostrophic winds (about 1 or 2 kilometers), frictional effects between the winds and the earth's surface considerably influence the character of the flow fields. The flow in this altitude region is not only generally turbulent, but a further turning of the wind toward the low-pressure region also occurs because of viscous and frictional effects. These effects are indicated schematically by the sketch in the upper right-hand portion of figure 2. As can be noted from this sketch, the wind is directed toward the low-pressure region and makes an angle of about 30° with the isobars. In addition, its speed is reduced to about 60 percent of the corresponding frictionless geostrophic speed.

One of the more familiar models which shows the primary structure of the general circulation of the Northern Hemisphere and which takes into account the heating, frictional, and Coriolis effects is sketched in the lower half of figure 2. (See ref. 9, pp. 502-529.) In this sketch the meridional components of the cells are shown in vertical cross section and the surface flow pattern is shown in the map plan.

The three circulation cells (in each hemisphere) of the model in figure 2 postulate the breakdown of the north-south loop by retardation of the winds due to surface frictional stresses. The formation of these cells (the two most southerly which are named for Hadley and Ferrell who first suggested their existence) results in rather permanent flow patterns near the ground. The surface pattern associated with the Hadley cell is noted in figure 2 as the broad belt of easterlies (trade winds) between the equator and latitude 30° N. The flow in this region is usually weakest near the equator and near the northern boundary. Between latitudes 30° and 60° N., the westerlies correspond to the Ferrell cell, and, from latitudes 60° N. to the pole, easterlies again generally prevail as the result of the polar cell. This circulation system as depicted for the Northern Hemisphere varies somewhat with the season of the year and also with the distribution of land and sea masses throughout the globe.

At a height of 2 or 3 kilometers the average flow is more zonal than shown by the map plan in figure 2 so that the southwesterly surface winds between latitudes 30° N. and 60° N. actually become nearly westerlies. On the average, all the winds increase in velocity and become more nearly westerlies as altitude is increased within the troposphere. As has been well documented, the strongest winds are encountered near tropopause levels in the so-called jet streams which on occasion have velocities of 100 mps or more.

Within the stratosphere, the winds generally decrease and then again increase in velocity as altitude increases. Very definite seasonal reversals in direction are also dominant features of the upper stratospheric circulation. The day-to-day changes in tropospheric winds which are associated with the rapidly moving weather systems are reflected to some extent in the lower stratosphere, but their influence becomes smaller and smaller with increasing altitude. It has been considered that, in general, changes occur relatively slowly in the stratosphere as compared with the troposphere. Some exceptions to this general rule have been observed during late winter periods when rather sudden movements and temperature increases (which have been termed "explosive warmings") occur in the lower polar stratosphere. These occurrences are believed to be manifestations of processes occurring at even higher altitudes and result in rapid subsidence in polar regions.

As has been noted, only the persistent large-scale features or the global aspects of the motions of the atmosphere can be inferred from a model such as that of figure 2 and other factors such as land or sea effects or changes of atmospheric characteristics with changing longitude at any fixed latitude must be neglected entirely. In addition, the small-scale perturbations and turbulent fluctuations which are associated with the circulation patterns and which are of most significance to the missile launch and exiting flight phases cannot be described. Despite these shortcomings, the model still permits certain general features of the circulation to be abstracted and thereby placed in relief to gain an overall understanding of atmospheric dynamics.

In the following paragraphs, some of the more important smaller scale perturbations on the flow fields are briefly discussed from the viewpoint of their effect on missile operations.

Atmospheric Perturbations

Aside from the obvious restriction of launch operations to non-storm conditions, the effects of surface winds and turbulence while the missile is in an unsupported condition on the launch pad and the dynamic loading conditions resulting from the strong wind shears encountered up to stratospheric altitudes constitute major operational and design factors for satellite systems. Some aspects of these surface and higher altitude wind problems are considered next.

Surface winds.- Large missiles which are launched from a vertical position are frequently subject to significant structural deflections and bending moments as the result of loads induced by strong or gusty surface winds. In addition to the loads on the missile arising from direct drag forces caused by the wind, vortex shedding leads to sizable

crosswind forces which in turn induce oscillatory bending moments in the structure of the vehicle. This so-called "smokestack" problem has recently been studied in a number of wind-tunnel tests using scaled models of different missile types or in full-scale tests of actual operational missiles. The results (see ref. 11 as an example of wind-tunnel tests) have indicated that strong wind conditions may impose catastrophic loadings if the missile is not protected.

Surface wind measurements are available, of course, from standard anemometer data taken over many years at numerous stations throughout the world. From these results, estimates of average or maximum launch wind conditions have been derived for various locations. For more detailed studies, time-history-type measurements are required from fast-response wind-measuring equipment. Information of this type which defines the surface wind environment for specific locations and for various altitudes up to 150 meters above the surface is summarized in references 12 and 13. Figure 3 has been reproduced from reference 12 as a sample of some of these results. The curves of figure 3 describe the power spectra of the horizontal wind fluctuations for a number of measurement periods in which the mean winds varied from 4 to 15 mps. This figure indicates that over the range of wavelengths of 30 to about 3,000 feet (approximately 10 to 1,000 meters), there is a general similarity in the shape of the spectra, although as would be expected, the power spectral density for the samples taken on different days varies by more than an order of magnitude. Relationships between the form and intensity of the spectrum of the horizontal wind components and variables such as temperature, lapse rate, mean wind speed, and height above surface were also developed in reference 12. These relationships serve as a starting point in the determination of input values of surface winds in a form suitable for studying satellite launch environmental conditions. Work of this nature is being continued by a number of agencies.

Wind shear and turbulence through stratospheric levels.- The wind disturbances experienced by a missile during its exiting phase through the atmosphere have long represented one of the major dynamic loading sources for satellite systems in which every pound of structural weight is held at a premium and guidance and control requirements are extremely high for mission success. These atmospheric disturbances become of increased importance to the larger and more flexible booster systems because of excitation of the various structural modes by the resulting unsteady aerodynamic loading conditions. For many missile systems the critical period occurs near tropopause levels because of the combination of high dynamic pressures at these altitudes and the severe wind shears associated with jet-stream occurrences.

In the past 5 years or more a number of studies of available balloon wind measurements have been made to establish the wind-shear characteristics of the atmosphere for application to missile design

and operational problems. Perhaps some of the best known and most widely used data of this type are those of Sissenwine as given in references 14 and 15. As an example of these results, figure 4 has been reproduced from reference 14. The wind profile in this figure was derived from a synthesis of a number of wind soundings taken from the northeastern portion of the United States during the winter season and represents the conditions which would be exceeded only 1 percent of the time. In figure 4 the maximum wind speed is given as 300 fps (approximately 91 mps) at tropopause altitudes and wind-shear intensities of 0.45 sec^{-1} are specified immediately above and below the level of maximum wind speed.

Descriptions of the wind conditions as given in figure 4 have served a number of useful purposes but it is generally recognized that balloon-measured wind data are deficient in a number of respects. Briefly, the balloon data are of questionable accuracy, particularly under strong wind conditions at the higher altitudes, and at best provide only a highly smoothed definition of the wind structure in the vicinity of a given station. Thus, irrespective of the merits of various procedures for analyzing balloon data, the results are not completely adequate for all aspects of missile response studies.

A number of investigations have been under way in the past few years to develop measuring techniques which would provide a more detailed and accurate picture of the wind structure actually traversed by a missile during its near vertical flight through the atmosphere. In this regard, Reisig in references 16 and 17 has utilized measurements derived from angle-of-attack and attitude sensors installed on operational missiles together with surface tracking data to establish the detailed wind fluctuations encountered during flight. The measurement and data-reduction methods are described in detail in reference 16. A sample of the results showing the magnitude of the wind vector plotted against altitude is shown in figure 5 (taken from ref. 17). This figure also shows the nearly simultaneous balloon-measured winds.

A somewhat different technique for measuring the detailed structure of the vertical wind profile has recently been developed by the Langley Research Center of the National Aeronautics and Space Administration. In this method (which is described in ref. 18) photogrammetric techniques are used to measure the drifts and distortions of a visible trail left by a rocket. The trail consists of either an artificially generated filament produced by expelling a solution of sulphur trioxide in chlorosulfonic acid along the flight path or the natural exhaust trail of solid-propellant rockets. In either case, the microscopic particles forming the trail assume the ambient air motions very rapidly after ejection and take the form of a continuous tracer of the winds traversed by the rocket. The position of the complete trail in space and its displacements over short intervals of time is then determined by optical triangulation methods to deduce the wind velocities. Figure 6 (taken from ref. 18)

shows the west-to-east and north-to-south components of a wind profile obtained by this method.

Both figures 5 and 6 indicate that the actual wind structure along the near-vertical path of the missile during its exiting flight phase through the lower atmosphere is a continuous and random disturbance with small-scale velocity fluctuations superposed on the thicker shear layers. A comparison of the measured missile winds with the near simultaneous balloon-sounding results given in figure 5 indicates that the thicker shear layers, say those extending over an altitude range of several kilometers, are fairly well defined by the balloon soundings. The smaller wind fluctuations, of course, are completely masked in the balloon-sounding results.

It might be noted in figure 5 that the altitude interval at which the successive wind determinations were made varies from about 50 meters at the lower altitudes to 500 meters or so at the higher altitudes because of the equal time interval (0.5 second) used in evaluating the telemetered and tracking records. In figure 6 the winds are defined at equal altitude intervals of about 30 meters (100 feet) throughout the altitude range covered. Thus, figure 6 provides a rather consistent definition of the wind fluctuations to wavelengths as short as 100 meters. The technique of figure 6 also provides the opportunity for studying the time-space variations in the vertical wind structure.

As a brief comment on the implications of the fine-scale features of the wind profiles given in figures 5 and 6, it is only necessary to note that the predominant structural frequencies of the larger missile systems fall within a range of about 1 to 5 cps. The combination of the missile flight speed through the altitude range shown on the figures and the spatial distribution of the wind fluctuations (especially apparent in fig. 6) results in input frequencies which are also within the range of 1 to 5 cps. Obviously, this condition of resonance between the aerodynamic loading inputs and the natural frequencies of the missile structure can lead to large load amplifications and seriously affect its complete dynamic behavior. Work of the nature summarized in figures 5 and 6 is continuing so that the detailed wind structure of the lower atmosphere can be defined for use in the design and operation of satellite vehicles.

THE UPPER ATMOSPHERE

Because of the rapidly decreasing air densities at altitudes above 20 or 30 kilometers, the problems of satellite operations which are associated with atmospheric motions in the upper stratosphere and in the higher altitudes of the ionosphere differ somewhat in nature from those

at lower altitudes. In the stratosphere at 30 kilometers, the density is about one-seventieth of that at the surface, while in the ionosphere, at altitudes of about 100 kilometers, the density is of the order of one-millionth of surface values; that is, the density is of the same order as that in the so-called vacuum of ordinary light bulbs. The flight dynamic pressures drop off rather rapidly as a consequence of the low densities. Depending on the type of propulsion system, the staging sequences, and flight trajectory, maximum values of dynamic pressure usually seem to occur at altitudes between 7 and 15 kilometers, or near tropopause levels. Beyond this point, the pressures ordinarily decrease quite rapidly and become near zero in the ionosphere at 100 kilometers. Thus, aerodynamic loads as used in the usual sense seem to decrease in importance within the altitude interval of 30 kilometers to 80 kilometers and become essentially negligible at higher altitudes. Instead, while perhaps not causing a sizable change in the instantaneous pressure loading, strong winds or shears at altitudes from 30 to 100 kilometers may cause the deviations from a planned trajectory to be greater than those desired. In some cases, it might be that the deviations would exceed the values which could ordinarily be compensated for by the guidance system. Strong and variable winds within these altitudes may also affect staging operations and thus have a rather important bearing on the complete flight path of the vehicle.

At the still higher altitudes throughout the ionosphere, the winds or other motion effects such as upward expansions may produce oscillations about the glide path at injection of a boost-glide vehicle, extend or reduce the range, or otherwise affect the trajectory, and thus modify the reentry heating history. Finally, as has been mentioned previously, the atmospheric motions may perturb the orbit of satellites and compromise the success of the mission.

For altitudes above the stratosphere, the winds and atmospheric motions are influenced to a large degree by the effects of the sun's gravitational field. These tidal effects, in fact, predominate to such a degree at, say 100 kilometers that in some cases it has been difficult to extract a consistent or mean picture of the wind from the large tidal components. In view of the importance of tidal phenomena to high-altitude flows, tidal oscillations will be discussed next. Some pertinent results of the various measurements indicated in table I for these altitudes will then be covered.

Tidal Oscillations in the Atmosphere

Surface measurements of the variations in atmospheric pressure and in the earth's magnetic field have long suggested that the gravitational fields of the sun and the moon produce tidal motions in the atmosphere similar to those produced in the oceans. Direct effects of tidal

variations observable as surface barometric pressure changes are small, amounting to a pressure swing of about 0.1 inch Hg at the equator which repeats itself every 12 hours. Indirect effects are noted by similar cyclic swings in the magnetic fields on a quiet day.

The 12-hour period as noted previously, rather than either a 24-hour period as would be expected on the basis of purely solar heating or an almost $12\frac{1}{2}$-hour period expected from the moon's tidal effect, results from resonance because of direct coupling between the sun's gravitational field and the natural period of free oscillations in the upper atmosphere. These resonance effects lead to large amplifications of the ionospheric motions. Actually, depending on the source of the energy fed into the atmosphere, the lower or higher altitudes may be excited with somewhat different resonant frequencies. Observations of the intense sound waves produced by the Krakatau volcanic eruption in 1883 indicated that the pressure waves were propagated through the atmosphere with a speed that corresponded to a free period of $10\frac{1}{2}$ hours. Pekeris in reference 19 subsequently showed that because of the vertical temperature gradients, the earth's atmosphere has two modes of free oscillations, the one for the portion of the atmosphere from the surface to the temperature minimum at the tropopause being $10\frac{1}{2}$ hours, and the one for the atmosphere between the tropopause and the second temperature minimum at about 80 kilometers being 12 hours.

According to Pekeris' calculations for the semidiurnal free oscillation of the upper atmosphere, the nodal surface is located at about 30 kilometers with the regions above and below this level swinging in opposite directions and the pressure changes being of opposite sign. Since the mean energy in a parcel of air is related to dynamic pressure $\left(\frac{1}{2}\rho V^2\right.$, where ρ is density and V is velocity$\left.\right)$, the tidal speed in the upper layers can obviously become very great. Estimates based on tidal theory have indicated the amplitudes of the 12-hourly horizontal motions at 100 kilometers to be 200 times as great as those at the surface. Figure 7 (taken from data given in ref. 19) shows the amplification factors by which the 12-hourly tidal velocities increase at the higher altitudes for a temperature distribution with altitude that approximates the real atmosphere. The sign of the velocity ratio on the abscissa of figure 7 indicates the direction of the motion relative to the surface. The nodal surface and the large amplifications of the horizontal motions at high altitudes stand out clearly in the figure. The sharpness of the tuning of the atmosphere to this 12-hour period of oscillation becomes quite evident from the fact that the effect of the approximate $2\frac{1}{2}$ times greater gravitational attraction of the moon at its out-of-phase tidal period of almost $12\frac{1}{2}$-hours long escaped detection.

Measurements obtained from ionospheric sounding methods clearly show the 12-hourly oscillations in the drift rate in accordance with tidal theory. As will be discussed in subsequent sections, these measurements indicate semidiurnal components of 25 mps or more in both the zonal and meridional directions. Although lunar tidal effects must also be present at the high altitudes, the larger amplifications of the solar gravitational effects almost completely mask lunar influences.

Finally, it might be well to mention at this point that worldwide ionospheric current systems which are readily detected at the earth's surface are generated by tidal effects. For the so-called quiet-day S_q variations in the magnetic field, electromotive forces are generated as the conducting ionized regions cut the magnetic field of the earth, causing electric currents to flow in the upper atmosphere. Verification of this explanation by comparing observed magnetic variations with those predicted by dynamo theory has not been fully successful because of incomplete knowledge on atmospheric conductivity and other factors affecting the current flow. Upon reexamination of some of these factors, however, dynamo currents of about the correct strength have been indicated by Mitra and others (refs. 20 and 21). It might be noted that although tidal flows are largely semidiurnal in nature, the strongest S_q components are diurnal. This anomaly is ascribed to the overriding influence of the conductivity of the ionosphere which is expected to vary diurnally. Dynamo theory appears to be well established and might be expected to give important clues to the ionization drifts or winds in the upper atmosphere.

Ionospheric Soundings

The ionization densities which occur at altitudes above approximately 60 kilometers due to the action of solar ultraviolet rays permit the motions in the ionosphere to be studied by radio deflective and other methods. If the ionized region is quite extensive, as in the case of the E and F regions, radio waves may be totally absorbed or reflected, depending on the frequency of the radio pulses. Because of the rather distinctive features of these ionospheric probing methods, atmospheric motions deduced from their use will be covered separately in the following section.

Ionospheric wind measurements by radio reflective methods.- Several radio techniques have been developed in the past years for measuring the horizontal winds which occur within the ionosphere. In general, the methods make use of vertical incidence radio signals which are reflected to ground receiving equipment either by irregularities in the ionized layers of the atmosphere or by highly ionized meteor trails. The methods employed are discussed quite widely in the literature. (See, for example, refs. 22 and 23.) As pointed out by various workers in these areas, there

is some possibility that the movements or winds determined by the radio fading patterns from irregularities in the ionization are not true motions of the air molecules but may be due to electrodynamical effects. These uncertainties do not apply to the observations of radio echoes from ionized meteor trails as, in general, only well-defined echoing sources in which the electron density may be several orders of magnitude greater than that of the surrounding ionosphere are used.

The results obtained from the several radio reflective methods indicate quite large diurnal and seasonal variations in the wind velocities at altitudes of about 100 kilometers (the E region) and above 200 or 250 kilometers (the F region). Within both the E and F regions the measured values seem to range from about 25 mps to 200 mps with the most frequently observed velocities being about 80 or 90 mps. Occasionally, velocities greater than 300 mps are observed, especially during times of severe magnetic disturbances.

Some samples of the data from reference 22 for a number of ionospheric measurements taken by the method of closely spaced receivers are given in figure 8 to illustrate the mean velocities and some of the diurnal variation in the velocities within the E and F regions. These data represent results obtained at the Cavendish Laboratory, Cambridge, England, for a series of observations taken over the 1949-53 period. During this period the observations were made continuously for 3 days of every month. By using radio frequencies of 2 mc/sec and 4 mc/sec, reflections were obtained from both the E and F regions. The curves given in reference 22 were redrawn for figure 8 so that the directions from which the winds were blowing are shown in order to conform to the standard meteorological practices used in other figures of this paper.

The results in figure 8 indicate rather striking contrasts between the wind behavior in the E and F regions. In the E region the diurnal variation is characterized by a uniformly rotating velocity vector in the clockwise sense (see the lower part of fig. 8(a)). The same effect shows up in the upper part of figure 8(a) by the sinusoidal variation in the north-south and west-east components of the winds with about 2 cycles being completed in a 24-hour period. This semidiurnal wind variation is in general agreement with predictions based on atmospheric tidal theory which predicts that the wind should blow towards the north at 0700 local time at an altitude of 100 kilometers. Departures from this cyclic variation in the E region appear to occur mainly in the summer season when the drifts are predominantly from westerly directions during the day with tendencies for direction reversals during the night. Measurements taken at other locations in the Northern Hemisphere seem to agree with the results in figure 8 in rough outline but not in detail. In the Southern Hemisphere, the direction of the rotating velocity vector is reversed.

In contrast to the 12-hour period of the velocity vector in the E region, the velocity vector in the F region (fig. 8(b)) appears to have a predominant 24-hour period with the direction of the winds changing rather suddenly near sunrise and sunset. During all seasons the drifts in the F region are predominantly from the west during the day and from the east during the night. As an average over the entire year, figure 8(b) indicates that the north-south components of the drift velocity in the F region are small compared to the west-east components.

The results obtained from meteor-trail reflections in the lower ionosphere are in general agreement with the results just discussed for the ionized-layer reflective measurements in the E region. The results given in reference 23 clearly indicate that the principal periodic wind is semidiurnal in character and is approximately represented by a vector of 10 to 40 mps in amplitude which rotates in a clockwise direction, as is the case in figure 8(a). The phase of the rotating vector undergoes marked changes during autumn months, but for most of the year represents winds blowing towards the north near 0600 and 1800 local time, again in reasonable agreement with the theory of atmospheric oscillations. Prevailing winds of 5 to 25 mps blowing towards the east in summer are usually observed. The observations also indicate that the winds in the lower E region are extremely turbulent. Studies of long-duration meteor trails show that wind velocities at points separated by only 5 kilometers may differ by as much as 50 mps.

Some results which summarize the data presented in reference 23 from meteor-trail reflections in the lower E region are given in figure 9 (fig. 11 of reference 23). This figure shows the average variation of wind speed with height as obtained from measurements taken over a period of several days. Figure 9 indicates that the average speed increases almost linearly with height, the increase being from 14 mps at 78 kilometers to over 60 mps at 98 kilometers. For the altitude range from about 75 to 100 kilometers in figure 9, the 12-hourly oscillating wind component appears to advance in phase by about 10° to 12° per kilometer as altitude increases.

In addition to the averaged values for the drift velocity given in figures 8 and 9, large variations in the wind velocity have been reported and correlated with periods of strong magnetic activity. In this connection, figure 10 summarizes Chapman's results as given in reference 22. As can be noted from this figure, the velocities in the E region are independent of the magnetic K-figure up to values of 4. For the larger K-figures associated with periods of strong magnetic activity, however, the drift velocities in the E region increase rapidly and assume values as large as 500 mps. The results in figure 10 for the F region indicate a more steadily increasing drift velocity as the K-figure increases.

Although not shown in figure 10, drift velocities as great as 1,000 mps have been observed in the F region. The overall results from this and other investigations suggest pronounced velocity gradients with height within both the E and F regions during periods of strong magnetic activity.

Scintillation of radio stars.- Closely akin to the ionospheric sounding methods for deducing winds in the ionosphere are the methods based on the scintillation or fluctuations in signal strength of the radio emission from intense star sources. The fluctuations are believed to be caused by the passage of incoming radio waves through irregularities in the ionization of the upper F region at heights of possibly 400 to 500 kilometers. Appreciable fluctuations occur only at night. By taking observations of the fluctuations in signal strength on receiving equipment separated by a few kilometers, the resulting time displacements in the occurrence of individual fluctuations give a measure of the drift velocities at altitudes inaccessible to normal ionospheric sounding methods. Some results from these observations are given in reference 22; more complete results are given in reference 24.

The results of these investigations indicate systematic movements in the upper part of the F region and that these movements are similar over wide geographical areas. Figure 11 has been taken from reference 24 to indicate the distribution of the drift velocities derived from 400 observations made at Jodrell Bank, University of Manchester. Most of these observations were taken during the months of December to March. Figure 11 indicates that the drift velocities varied over the range from 30 to 1,200 mps; the largest of these values were associated with periods of strong magnetic activity. The mean value for the observations in figure 11 was found to be about 200 mps. The mean values for observations taken over auroral zones have been found to be somewhat larger, being about 350 mps.

The direction of the motions indicated in figure 11 has been measured to be nearly always along an east-west line. Usually the direction of movement was from the east during nighttime hours, but after midnight and during periods of strong magnetic activity the movement has been found to reverse to a west wind, with the reversal usually taking place about 1200 hours. Small components from the south have also appeared before midnight followed by small northerly components during morning hours. Tendencies for components from the south during summer months and from the north during fall months have also been observed but seasonal effects have, as yet, not been firmly established.

The apparent anomaly that the movements in the F region as detected by radio reflective methods were predominantly from the east at night (fig. 8(b)) as contrasted to the movements from the west after midnight as given by radio astronomical methods is attributed to the differences in altitude sensed by the two methods (the radio reflective methods

apply to a somewhat lower altitude). These differences suggest that the circulation in the upper part of the F region may be quite distinct from that of the lower levels.

Meteor-Train Photography

In addition to the application of radio reflective principles for obtaining wind measurements from meteor trails, visual and photographic observations of long-enduring meteor trains have also supplied information on the winds in the lower ionosphere. Because of the relative scarcity of visual meteoric phenomena, only a few photographic meteor-train measurements have been obtained as compared to literally thousands of meteor-trail radio reflective measurements. Several measurements from a systematic observational program of meteor-train photography are reported by Liller and Whipple in reference 25. Figure 12 has been prepared from data given in reference 25 to illustrate the nature of the results obtained from photographic studies of this type.

Figure 12 indicates a very irregular wind pattern over the altitude range from 82 to 113 kilometers with the maximum wind being somewhat greater than 100 mps. These velocities are in agreement with the radio reflective results presented earlier. Strong shears (up to 50 mps/km or more) are indicated in figure 12 as well as by other results given in reference 25. Consideration of a number of the relatively steep velocity gradients within shallow layers has suggested that an eddy or current structure might be embedded in horizontal planes in the lower ionosphere. The very stable temperature lapse rate from 80 to 100 kilometers would tend to restrict large vertical motions and favor the development of such horizontal circulation systems.

Wind Measurements Obtained From Artificial Tracer Elements

Considering other methods of measuring the winds and circulation patterns throughout the stratosphere and into the ionosphere, a number of rocket systems utilizing various artificial types of tracers have been under development for the last several years and have provided wind measurements to altitudes of 80 kilometers and beyond. The most commonly used tracers include chaff, metalized parachutes, or spheres which are ejected near apogee of rather small and inexpensive meteorological sounding rockets and tracked during their fall through the atmosphere by means of radar. The uses and accuracies of these systems are described rather fully in the literature (see refs. 26 to 29) and will not be repeated here.

As an example of the measured wind structure within the mesosphere, a sample of chaff-measured winds is given in figure 13. This figure

was prepared from data presented in reference 30 and represents the mean wind measurements taken during the winter and summer seasons at Tonopah Test Range, Nevada. Wind measurements throughout the altitude range shown in the figure were averaged over approximately 1.7 kilometers (5,000 feet) altitude intervals. Because of radar-tracking and wind-sensing limitations of chaff or similar types of targets, averages over rather large altitude intervals are used; in many cases the averaging intervals are 6 to 7 kilometers, thus yielding only indications of the gross flow characteristics. Wind directions for the chaff measurements in figure 13 were westerly during the winter season and predominantly easterly during the summer season.

The main features of the chaff data in figure 13 are the relatively strong westerly winds during the winter months as contrasted to the lighter easterlies during the summer months. These tendencies for a strong westerly wintertime flow and a weaker and more variable easterly summertime flow appear typical for the upper stratosphere and mesosphere at about 40° N. latitude. The measurements at Tonopah also indicated diurnal fluctuations in the wind speed of about 5 to 25 mps during both winter and summer seasons. Good correlation was also noted between the wind velocities and seasonal solar insolation values, thus implying strong thermal influences which possibly result from absorption of solar radiation by ozone throughout these altitudes.

A relatively large number of wind measurements from chaff, parachute, or inflatable-sphere systems are being obtained from other locations. The recent initiation of the Meteorological Rocket Network (under IRIG) is perhaps the first effort to obtain these measurements within the mesosphere on a systematic basis and from a number of widely spaced locations within the North American continent. The results from a 1-year sample of these measurements are summarized in reference 31. Further effort along these lines should contribute considerably to an understanding of the circulation throughout the upper stratosphere and the mesosphere.

Sound-Propagation Studies

Perhaps some of the earliest probing methods for obtaining wind (and temperature) measurements within the upper stratosphere were based on the so-called anomalous sound-propagation method. The initial work of this type utilized measurements of the time required for acoustic waves from surface or relatively low-altitude explosions to be refracted upwards to 40 or 50 kilometers and then back to the earth's surface. Some of the results from this work are described in reference 32. The results of these anomalous sound-propagation studies served to establish the average seasonal and latitudinal trends of the higher altitude winds.

More recently, acoustical methods have been developed for determining winds at altitudes from 30 to about 90 kilometers through the use of the rocket-grenade technique. This now classic experiment utilizes a cluster of grenades which is ejected from a rocket and exploded at preselected altitudes on the upward leg of the rocket trajectory. The locations of the explosions in space are accurately determined by combinations of ballistic camera and radio doppler tracking methods. The times of arrival at the ground of the acoustic waves from each grenade explosion are recorded by an array of sound ranging microphones. The average winds (and temperatures) in atmospheric layers bounded by the successive explosions are then determined from the times and angles of the sound arrivals at the ground. The upper altitude limit for the grenade method is about 95 kilometers. Experience has indicated that sufficient energy cannot be coupled into the atmosphere at higher altitudes to generate a sound wave that will reach the ground. The rocket-grenade method, together with estimates of the accuracies of the wind determinations, is covered in complete detail in reference 33.

Wind measurements have been obtained in the past several years through the use of the rocket-grenade technique from tests made at various typical areas of the Northern Hemisphere. These areas include subtropical and midlatitude regions (White Sands, New Mexico, and Wallops Island, Virginia), subarctic regions (Fort Churchill, Canada), and Pacific equatorial regions (the island of Guam). The White Sands and Fort Churchill measurements are given in references 34 and 35, respectively. The measurements from Wallops Island and Guam have not as yet been completely evaluated.

The averaged wind measurements from the White Sands rocket-grenade experiments (ref. 34) are plotted in figure 13 for comparison with the chaff measurements which were taken near the same location. It is to be noted that the rocket-grenade measured wind speeds are in general agreement with those from the chaff measurements for both the winter and summer seasons, particularly at altitudes above about 60 kilometers. At altitudes below 60 kilometers the grenade data indicate somewhat stronger winds, the averages reaching about 80 mps in the winter season. The expected reversal from westerly winds in winter to easterly winds in summer is indicated by the grenade data as was the case for the chaff measurements.

In order to compare the wind pattern of the mesosphere for arctic regions with that of the more southerly latitudes as given in figure 13, the rocket-grenade data from the Fort Churchill firings of reference 35 were averaged and are summarized in figure 14. Figures 13 and 14 indicate that the winter and summer wind patterns are quite similar for both locations for altitudes up to the mesopeak at 50 kilometers. At higher altitudes, the wintertime winds, in particular, are much stronger at Fort Churchill with average values reaching 95 mps. These strong

wintertime winds indicate very active and disturbed regions in the arctic mesosphere during winter seasons as compared with a more consistent or less variable summer atmosphere.

Detailed studies of the individual sounding data from Fort Churchill indicate other interesting features of the dynamics of the arctic mesosphere and possible interactions between the mesosphere and the upper stratosphere. In one clear example of "explosive" stratospheric warming, the rocket-grenade wind data in reference 35 indicated that the breakdown of the stratospheric flow was preceded by a reversal to southerly winds of the mesosphere circulation to altitudes of 75 kilometers or beyond. From this sequence of events, it appears that the circulation breakdown first occurred in the mesosphere and was then propagated to the lower altitudes, resulting in the explosive stratospheric warming noted. Thus, the dynamic processes occurring in the mesosphere may trigger many of the phenomena observed at lower altitudes.

Noctilucent Clouds

Luminous clouds at altitudes of about 82 kilometers have occasionally been observed during summer twilight hours from high-latitude stations in the Northern Hemisphere. The clouds are of a very tenuous structure and are visible only by scattered sunlight when the sun lies 10° to 15° or so below the horizon and only occasionally are seen higher than 10° above the horizon. The measured heights of a large number of such noctilucent cloud formations have varied from 79 to 90 kilometers with the mean at about 82 kilometers. The cause and composition of noctilucent clouds are not known for certain, and it has been suggested that they may be composed of ice crystals or of dust from either volcanic or meteoric origin. Ludlam in a rather complete study in reference 36 concludes that they are most likely composed of small solid particles which are produced by condensation of gases in the wakes of meteors or of particles which enter the higher atmosphere from below during major volcanic eruptions.

Observations of the altitudes and drifts of noctilucent clouds through the use of visual or photographic triangulation methods have yielded a number of measurements of the wind velocities within the upper mesosphere. From the drift measurements given in reference 36 the measured winds seem to be predominantly from the east, although occasionally north and south components have been observed. Observations of an apparent nighttime clockwise rotation of the wind vector from the north through the east has suggested that a semidiurnal component may be superposed on the main easterly flow at these altitudes. These directional characteristics of the flow determined from noctilucent cloud studies are noted as agreeing with the results from the radio reflective studies of the lower E region at about the same altitude.

The mean wind speed obtained from the noctilucent cloud studies seems to be about 50 mps with the majority of the observations covering a range of about 15 to 90 mps. Even higher speeds are reported, up to 200 mps or more. These extreme cases, however, might have resulted from optical effects and some questions exist as to whether they represent true wind velocity measurements. Ludlam and other workers in this field have also reported wavelike motions and eddies in the cloud shapes which would indicate the presence of rather large areas of turbulence at the 80-kilometer altitude level.

In addition to the wind measurements afforded by tracking noctilucent-cloud movements, their presence also serves as an indication of other dynamic processes in the upper stratosphere and mesosphere. As outlined in reference 36, the dust particles distributed throughout this altitude region may act as heat absorbing and radiating bodies during the hours that adjacent belts of the atmosphere remain in sunlight or shadowed areas. Conceivably, then, there may be a tendency for a circulation to develop in the vicinity of the shadow at 50 to 80 kilometers as the result of ascending motions in the sunlight (or heating) region and descending motions in the shadowed (or cooling) region. Such a circulation would involve a motion at the 80-kilometer level which would be directed away from the sun and thus agree with the observed wind directions noted previously.

Photochemical Experiments

The use of artificially produced airglows at high altitudes for studying atmospheric motions stems from studies of the sources of natural airglows in the upper regions. Based on suggestions as early as 1950 that an artificial glow at an altitude of 80 kilometers could be produced by releasing evaporated sodium into the atmosphere, the first successful photochemical experiment was carried out at White Sands Proving Ground, New Mexico, in 1955 (ref. 37). In this initial experiment, enhanced sodium emission was observed during twilight hours with the emission fading gradually as the cloud was obscured by the earth's shadow, an indication that the emission was a resonance effect due to solar radiation. Other sodium releases carried out since that time by Bedinger, Manring, and others (refs. 38 and 39) have provided a measure of the upper atmospheric winds. In similar experiments, nitric oxide or ethylene gas have also been released into the atmosphere to obtain a visible cloud through resonance radiation or chemiluminescence processes. (See ref. 40, for example.) At present, however, no wind measurements have been published as the result of the latter types of experiments.

As a general description of the techniques employed in these measurements of upper air winds, a vertical filament is produced in the

sodium experiment through the use of several sodium vaporizers in the rocket. Each vaporizer carries about 1 kilogram of metallic sodium pellets in a thermite mixture. At the appropriate altitude the thermite is ignited by an electrical squib. The sodium is vaporized by the heat of the burning thermite and released through a vent tube into the atmosphere. Scattering of the solar radiation at the resonant frequency of sodium emission at 5,890 A then produces a visible yellow trail which acts as a tracer of the atmospheric motions. Application of photogrammetric triangulation methods to define the drifts and distortions of the vertical trails provides the necessary data to deduce the wind velocities at the altitudes in question.

In the initial experiment in 1955 the fluorescing sodium cloud extended from an altitude of about 85 kilometers to 113 kilometers, the peak altitude obtained by the rocket. In subsequent experiments sodium trails were obtained over altitudes of 77 to 200 kilometers. The wind velocity measurements obtained from the different experiments at White Sands, New Mexico, are given in reference 39. These measurements are summarized in the following table:

Date	Time, m.s.t.	Altitude above sea level, km	Wind speed, mps	Wind direction, deg
Oct. 12, 1955	1800	85	80	320
		110	45	120
Apr. 11, 1956	1905	77	43	118
		84	175	82
		92.5	107	47
		93	125	48
		102	100	287
		102.3	91	290
		105	179	276
Nov. 26, 1957	0556	104	125	250
		106	115	280
		108	43	360
		109	153	350
		110	75	30
		114	63	50
		119	36	60
		122	20	120
		126	28	155
		132	33	240
		142	40	270
		152	30	245
		162	20	230
		172	40	200
		182	41	210
		192	42	220
		202	38	240

Some of the main features of the data summarized in the table are the very strong winds (generally greater than 100 mps) and severe shear layers up to about 110 kilometers and the consistently weaker winds (less than 50 mps) from there to the top of the measurements at about 200 kilometers. This is particularly evident from the measurements made on November 26, 1957. A rather marked change in wind direction also accompanies the abrupt change in wind speed, the winds being mostly from the west and northwest up to 110 kilometers and then veering through east to the southwest in the region of the weaker winds.

The Solar Wind

For satellites orbiting at great distances from the earth, say at distances of several earth's radii, the earth's atmosphere has merged with the highly ionized gas of interplanetary space and the environment of the satellite is defined primarily by the fast-moving corpuscules which originate in the sun's corona. Only a few brief remarks will be made on these high-velocity particle streams inasmuch as it might be considered that the atmosphere ends when its density dwindles to that of the interplanetary gas.

Evidence obtained by Biermann (ref. 41) from observations that the tails of comets are displaced away from the sun suggests that corpuscular streams more or less continuously issue from the sun and, at the orbit of the earth, move with velocities of 500 to 1,500 km/sec. Parker (ref. 42) subsequently arrived at similar velocities by considering a continuously expanding spherical corona and termed the stream the solar wind. The implications of the solar wind to satellite vehicles are not clearly understood, although various investigators (see ref. 43) have called attention to the possibilities of sputtering and radiation damage to various structures in space. Bergstralh, Blifford, and Kieffer in reference 43 note that in applications such as thin plastic or metallic coatings used in the construction of balloons, solar sails, or windows and filters, damage may result due to ejection of surface atoms from the impact of the solar wind particles. Uncertainties on the erosion rates due to sputtering seem to extend over several orders of magnitude for different materials, but, as noted in reference 43, there appears to be little doubt that certain materials may be damaged under long-period exposure to the solar wind.

CONCLUDING REMARKS

The preceding discussion is an attempt at highlighting some of the dynamic characteristics of the atmosphere which are of particular

significance to satellite operations. As indicated, it is impossible in a short discussion of this sort to summarize all the information which relates to the various motions of the atmosphere. Also, as indicated, no effort has been made to synthesize the information into a consistent pattern throughout the different altitudes as distributions of some of the wind components with altitude have already been developed by fitting together various observational data.

As a general conclusion, it appears that for satellite operations the motions of the atmosphere are not satisfactorily described by the movements of large wind layers as may be the case for other purposes. For the lower atmosphere in particular, the superposed fluctuations in the wind velocities strongly affect the basic response of satellite vehicles. The consequences of a sequence of different forces arising from strong and sudden wind reversals at high altitudes depend to a large extent on the nature of the vehicle and the programing of its mission.

General circulations with strong repetitive daily and seasonal variations appear in the upper as well as in the lower atmosphere with considerable evidence of short-period wind variations. The main driving forces in the ionosphere are often assumed to be tidal influences, although large effects have also been ascribed to atmospheric heating. At heights above 400 kilometers the motions probably become predominantly hydromagnetic with the earth's magnetic field exercising a strong control over the fluid motions.

Langley Research Center,
National Aeronautics and Space Administration,
Langley Station, Hampton, Va., June 12, 1962.

REFERENCES

1. LaGow, H. E., Horowitz, R., and Ainsworth, J.: Arctic Atmospheric Structure to 250 km. Experimental Results of the U.S. Rocket Program for the International Geophysical Year to 1 July 1958. IGY Rocket Rep. Ser. No. 1, Nat. Acad. Sci., July 30, 1958, pp. 38-46.

2. Jastrow, R.: Geophysical Effects of the Trapped Particle Layer. Space Research, Hilde Kallmann Bijl, ed., Interscience Publ., Inc. (New York), 1960, pp. 1009-1018.

3. Kellogg, William W., and Schilling, Gerhard F.: A Proposed Model of the Circulation in the Upper Stratosphere. Jour. Meteorology, vol. 8, no. 4, Aug. 1951, pp. 222-230.

4. Murgatroyd, R. J.: Winds and Temperatures Between 20 km and 100 km - A Review. Quarterly Jour. Roy. Meteorological Soc., vol. 83, no. 358, Oct. 1957, pp. 417-458.

5. Kellogg, William W.: Review of I.G.Y. Upper Air Results. [Paper] P-1717, the RAND Corp., June 5, 1959.

6. Fritz, Sigmund: U.S. Special Meteorological Studies for the IGY. Geophysics and the IGY, Hugh Odishaw and Stanley Ruttenberg, eds. Geophys. Monograph No. 2, American Geophys. Union, 1958, pp. 161-168.

7. Wexler, Harry: The Circulation of the Atmosphere. Scientific American, vol. 193, no. 3, Sept. 1955, pp. 114-124.

8. London, Julius: A Study of the Atmospheric Heat Balance. AFCRC-TR-57-287, ASTIA No. 117227, College Eng. New York Univ., July 1957.

9. Berry, F. A., Jr., Bollay, E., and Beers, Norman R., eds.: Handbook of Meteorology. McGraw-Hill Book Co., Inc., 1945.

10. Brunt, David: Physical and Dynamical Meteorology. Second ed., Cambridge Univ. Press, 1941.

11. Fung, Y. C.: Fluctuating Lift and Drag Acting on a Cylinder in a Flow at Supercritical Reynolds Numbers. GM-TR-0165-00343, Space Tech. Labs., The Ramo-Wooldridge Corp., May 7, 1958.

12. Henry, Robert M.: A Study of the Effects of Wind Speed, Lapse Rate, and Altitude on the Spectrum of Atmospheric Turbulence at Low Altitude. Rep. No. 59-43, Inst. Aero. Sci., Inc., Jan. 1959.

13. Panofsky, Hans A., and Deland, Raymond J.: One-Dimensional Spectra of Atmospheric Turbulence in the Lowest 100 Metres. Vol. 6 of Advances in Geophysics, F. N. Frenkiel and P. A. Sheppard, eds., Academic Press, Inc. (New York), 1959, pp. 41-64.

14. Sissenwine, Norman: Windspeed Profile, Windshear, and Gusts for Design of Guidance Systems for Vertical Rising Air Vehicles. Air Force Surveys in Geophysics No. 57 (AFCRC-TN-54-22), Air Force Cambridge Res. Center, Nov. 1954.

15. Sissenwine, Norman: Development of Missile Design Wind Profiles for Patrick AFB. Air Force Surveys in Geophysics No. 96 (AFCRC-TN-58-216, ASTIA Doc. No. AD.146870), Air Force Cambridge Res. Center, Mar. 1958.

16. Reisig, Gerhard H. R.: Instantaneous and Continuous Wind Measurements up to the Higher Stratosphere. Jour. Meteorology, vol. 13, no. 5, Oct. 1956, pp. 448-455.

17. Reisig, Gerhard: Resumé of Missile Measured Winds at Cape Canaveral, Florida. Rep. No. DA-TR-3-59, Dev. Operations Div., Army Ballistic Missile Agency (Redstone Arsenal, Ala.), Jan. 22, 1959.

18. Henry, Robert M., Brandon, George W., Tolefson, Harold B., and Lanford, Wade E.: The Smoke-Trail Method for Obtaining Detailed Measurements of the Vertical Wind Profile for Application to Missile-Dynamic-Response Problems. NASA TN D-976, 1961.

19. Pekeris, C. L.: Atmospheric Oscillations. Proc. Roy. Soc. (London), ser. A, vol. 158, no. 895, Feb. 3, 1937, pp. 650-671.

20. Mitra, S. K.: The Upper Atmosphere. Second ed., The Asiatic Society (Calcutta, India), 1952, p. 382. (Available from Hafner Pub. Co., New York.)

21. Hirono, M., Maeda, H., and Kato, S.: Wind Systems and Drift Motions in the Ionosphere Deduced From the Dynamo Theory. Jour. Atmospheric and Terrestrial Phys. vol. 15, no. 1/2, Sept. 1959, pp. 146-150.

22. Briggs, B. H., and Spencer, M.: Horizontal Movements in the Ionosphere. Vol. XVII of Reports on Progress in Physics, A.C. Strickland, ed., The Phys. Soc. (London), 1954, pp. 245-280.

23. Greenhow, J. S.: Systematic Wind Measurements at Altitudes of 80-100 km Using Radio Echoes From Meteor Trails. Phil. Mag., ser. 7, vol. 45, no. 364, May 1954, pp. 471-490.

24. Maxwell, A., and Dagg, M.: A Radio Astronomical Investigation of Drift Movements in the Upper Atmosphere. Phil. Mag., ser. 7, vol. 45, no. 365, June 1954, pp. 551-569.

25. Liller, William, and Whipple, Fred L.: High-Altitude Winds by Meteor-Train Photography. Rocket Exploration of the Upper Atmosphere, R. L. F. Boyd and M. J. Seaton, eds., Pergamon Press Ltd. (London), 1954, pp. 112-130.

26. Jenkins, Kenneth R., and Webb, Willis L.: Rocket Wind Measurements. Tech. Memo. 531, Missile Geophys. Div., U.S. Army White Sands Signal Agency, June 1958.

27. Cline, Dudley E.: Rocket-Beacon Wind-Sensing System. Eng. Rep. No. E-1205, U.S. Army Signal Eng. Labs. (Fort Monmouth, N. J.), June 14, 1957.

28. Leviton, Robert, and Palmquist, William E.: A Rocket Balloon Instrument. Presented at the Nat. Conf. on Stratospheric Meteorology (Minneapolis, Minn.), Sept. 1959.

29. Lally, Vincent E., and Leviton, Robert: Accuracy of Wind Determinations From the Track of a Falling Object. Air Force Surveys in Geophysics No. 93, (AFCRC-TN-58-213, ASTIA Doc. No. AD 146858), Air Force Cambridge Res. Center, Mar. 1958.

30. Smith, Lawrence B.: Monthly Observations of Winds Between 150,000 and 300,000 Feet Over a One-Year Period. Presented at the Forty-First Annual Meeting, American Geophys. Union (Washington, D.C.), Apr. 27-30, 1960. (Abstract in Jour. Geophys. Res., vol. 65, no. 8, Aug. 1960, p. 2524.)

31. Joint Sci. Advisory Group: The Meteorological Rocket Network - An Analysis of the First Year in Operation. Jour. Geophys. Res., vol. 66, no. 9, Sept. 1961, pp. 2821-2842.

32. Crary, A. P.: Stratosphere Winds and Temperatures in Low Latitudes From Acoustical Propagation Studies. Jour. Meteorology, vol. 9, no. 2, Apr. 1952, pp. 93-109.

33. Bandeen, William R.: The Recording of Acoustic Waves From High-Altitude Explosions in the Rocket-Grenade Experiment and Certain Other Related Topics. Tech. Rep. 2056, U.S. Army Signal Res. and Dev. Lab. (Fort Monmouth, N. J.), July 1, 1959.

34. Stroud, W. G., Nordberg, W., and Walsh, J. R.: Atmospheric Temperatures and Winds Between 30 and 80 km. Jour. Geophys. Res., vol. 61, no. 1, Mar. 1956, pp. 45-56.

35. Stroud, W. G., Nordberg, W., et al: Rocket Grenade Measurements of Temperatures and Winds in the Mesosphere Over Churchill, Canada. Space Research, Hilde Kallmann Bijl, ed., Interscience Publ., Inc. (New York), 1960, pp. 117-143.

36. Ludlam, F. H.: Noctilucent Clouds. Tellus, vol. IX, nr. 3, Sept. 1957, pp. 341-364.

37. Edwards, Howard D., Bedinger, John F., Manring, Edward R., and Cooper, C. W.: Emission From a Sodium Cloud Artificially Produced by Means of a Rocket. The Airglow and the Aurorae, E. B. Armstrong and A. Dalgarno, eds., Pergamon Press (New York), 1955, pp. 122-134.

38. Bedinger, J. F., Ghosh, S. N., and Manring, E. R.: Emission From Sodium Ejected From Rockets. The Threshold of Space, M. Zelikoff, ed., Pergamon Press (New York), c.1957, pp. 225-231.

39. Manring, Edward, Bedinger, J. F., Pettit, H. B., and Moore, C. B.: Some Wind Determinations in the Upper Atmosphere Using Artificially Generated Sodium Clouds. Jour. Geophys. Res., vol. 64, no. 6, June 1959, pp. 587-591.

40. Pressman, Jerome, Aschenbrand, Leonard M., Marmo, Frederick F., Jursa, Adolph, and Zelikoff, Murray: A Synthetic Atmospheric Chemiluminescence Caused by the Release of NO at 106 km. The Threshold of Space, M. Zelikoff, ed., Pergamon Press (New York), c.1957, pp. 235-240.

41. Biermann, L.: Kometenschweife und solare Korpuskularstrahlung. Z. Astrophys., Bd. 29, Nr. 3, 1951, pp. 274-286.

42. Parker, E. N.: The Interplanetary Gas and Magnetic Fields. Physics of Fields and Energetic Particles in Space. Ch. VII of Science in Space, J. A. Simpson, ed., Nat. Acad. Sci., 1960, pp. 6-12.

43. Bergstralh, Thor A., Blifford, Irving H., Jr., and Kieffer, Lee J.: The Solar Wind as a Hyper-Environmental Parameter. 1960 Proc. Inst. Environmental Sci., Apr. 1960, pp. 105-108.

TABLE I.- SUMMARY OF OBSERVATIONS

Method	Altitudes, km	Nature of results
Anemometers, sounding balloons or other artificial tracers, missile recordings.	0 to 30	Surface winds and turbulence, strong jet stream winds (150 mps) and shear.
Acoustical studies, artificial tracers, noctilucent clouds.	30 to 90	Strong winter westerlies (80 mps), weaker summer easterlies, active winter arctic regions, possible cellular convection.
Meteoric photography, chemical releases.	50 to 200	Irregular wind pattern and possibly horizontal eddy structure below 100 km, strong westerly winds to 100 km (100 mps), weaker southwest winds to 200 km.
Ionospheric and meteor-trail radio reflections, barometric fluctuations, terrestrial magnetic variations.	100 to 250	Semidiurnal components in E region, tidal oscillations, strong magnetic effects (velocities greater than 300 mps), predominate west-east components in F region with possibly 1,000 mps velocities.
Radio star scintillation.	Above 250	Mean velocities 200 mps; east winds at night, west winds after midnight; velocities to 1,200 mps during periods of strong magnetic activity.

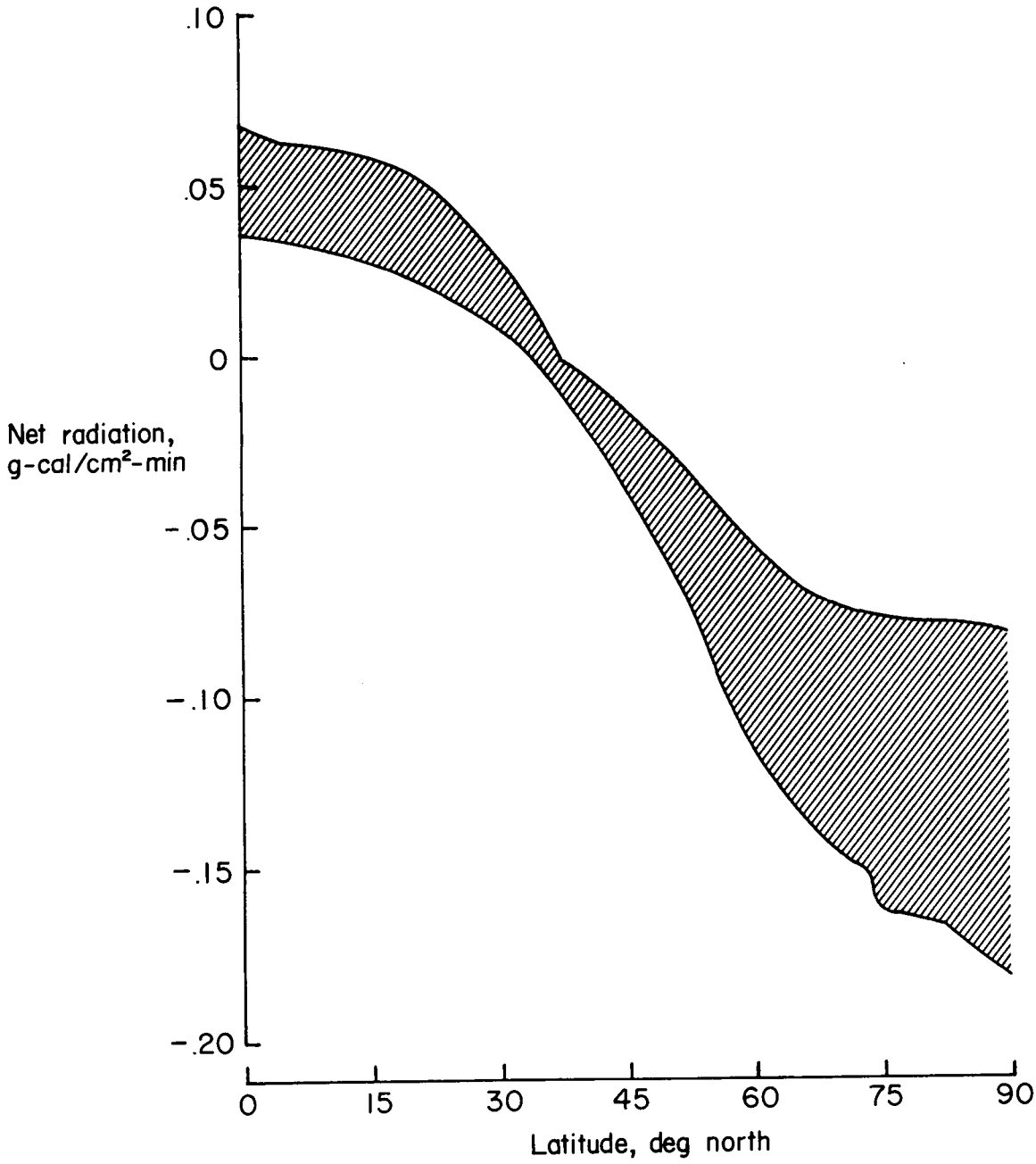

Figure 1.- Annual average absorbed radiation for different latitudes of Northern Hemisphere (adapted from ref. 6).

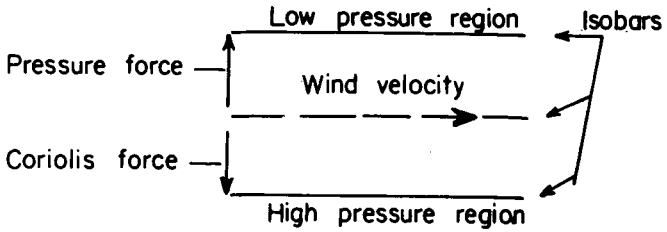

(a) Geostrophic wind.

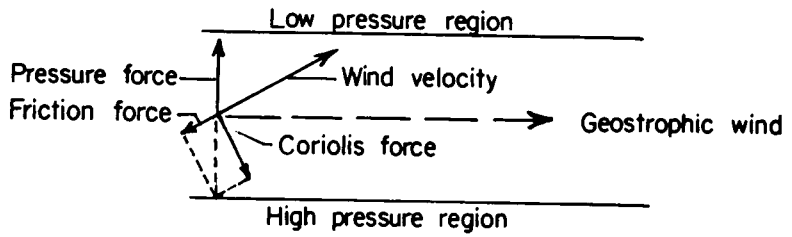

(b) Surface frictional effects.

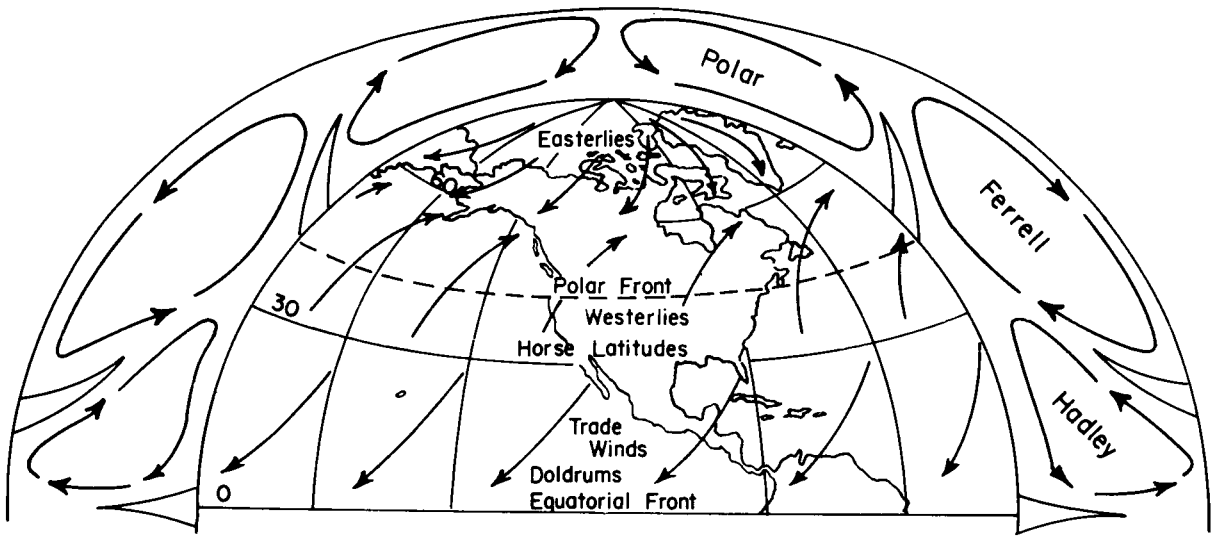

(c) Northern Hemisphere.

Figure 2.- The general circulation (based on discussion in ref. 9).

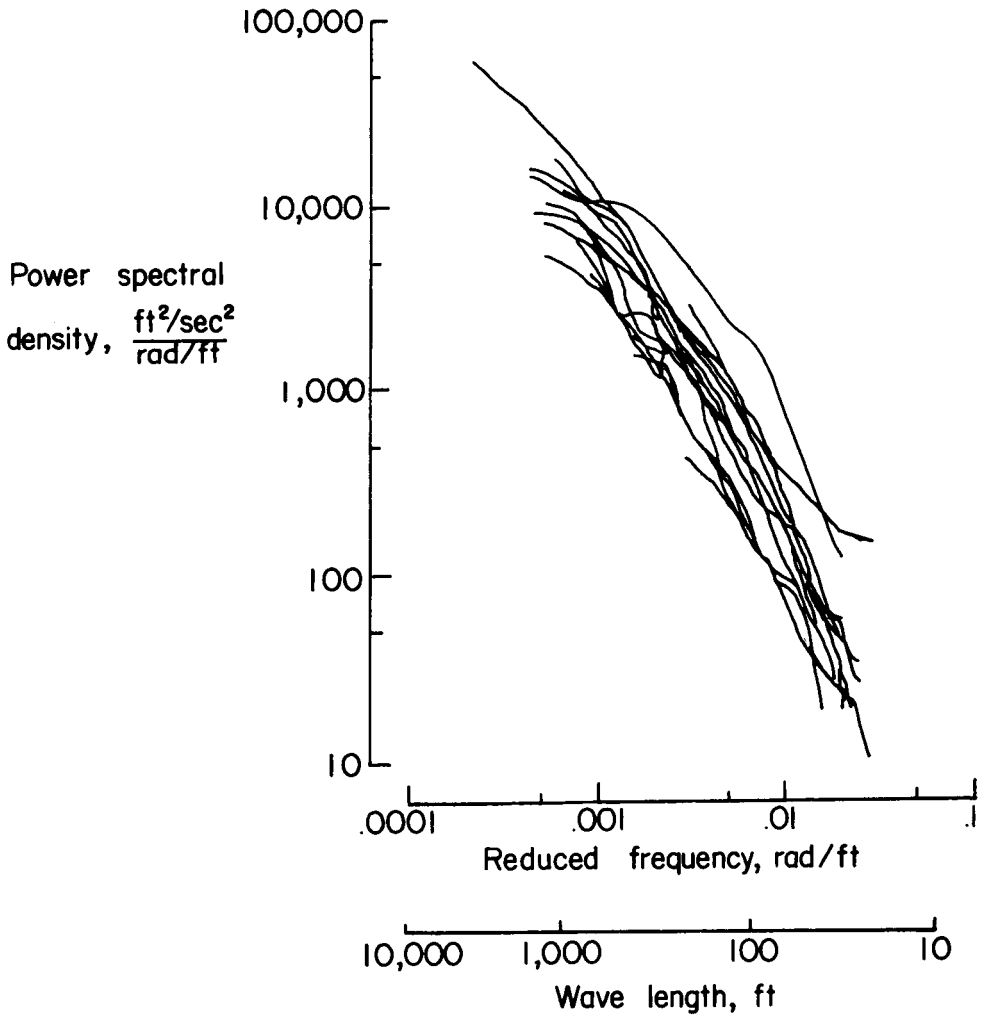

Figure 3.- Power spectra of the horizontal component of turbulence in the direction of the mean wind (from ref. 12).

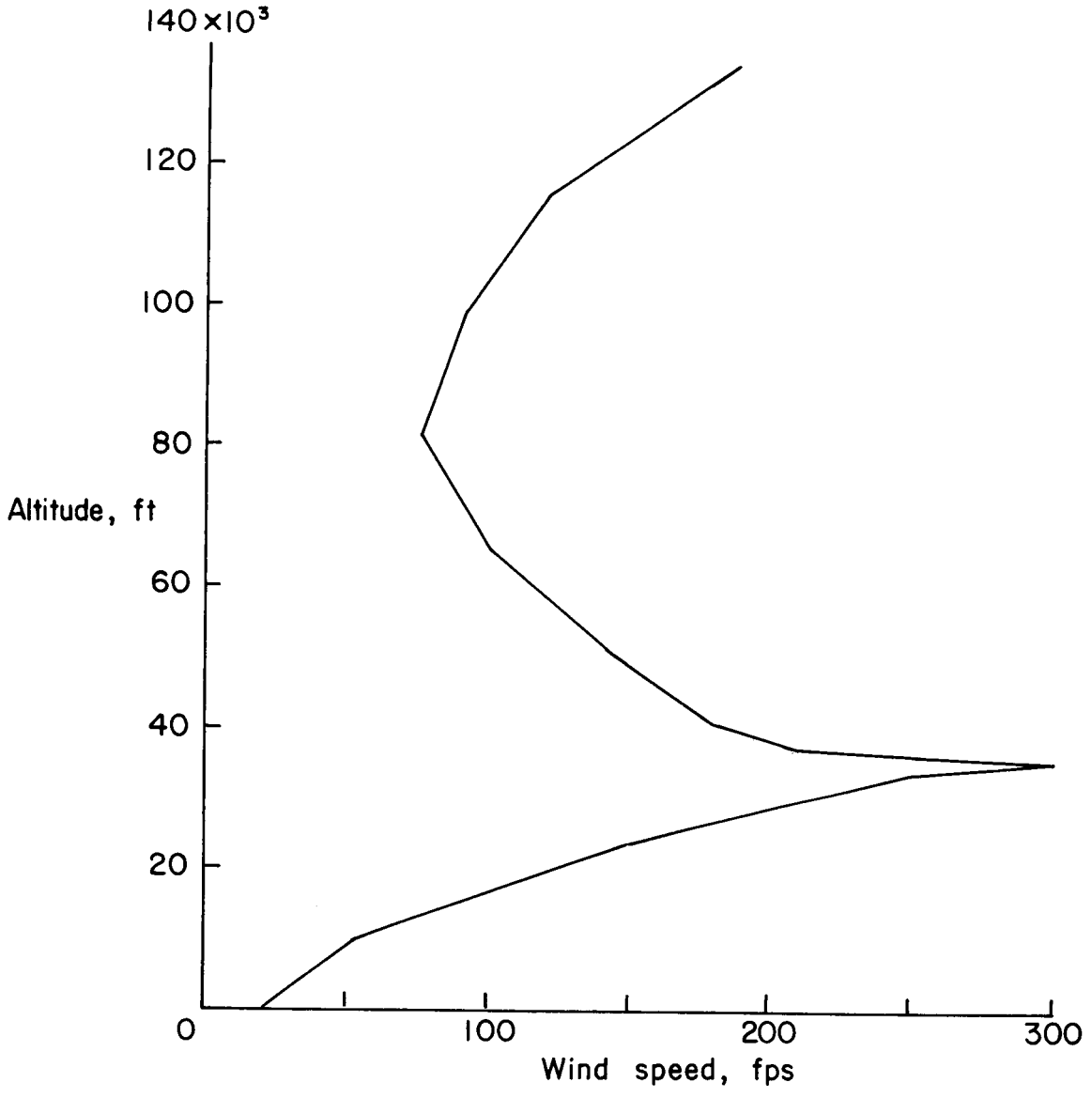

Figure 4.- Design wind profile (taken from fig. 5, ref. 14).

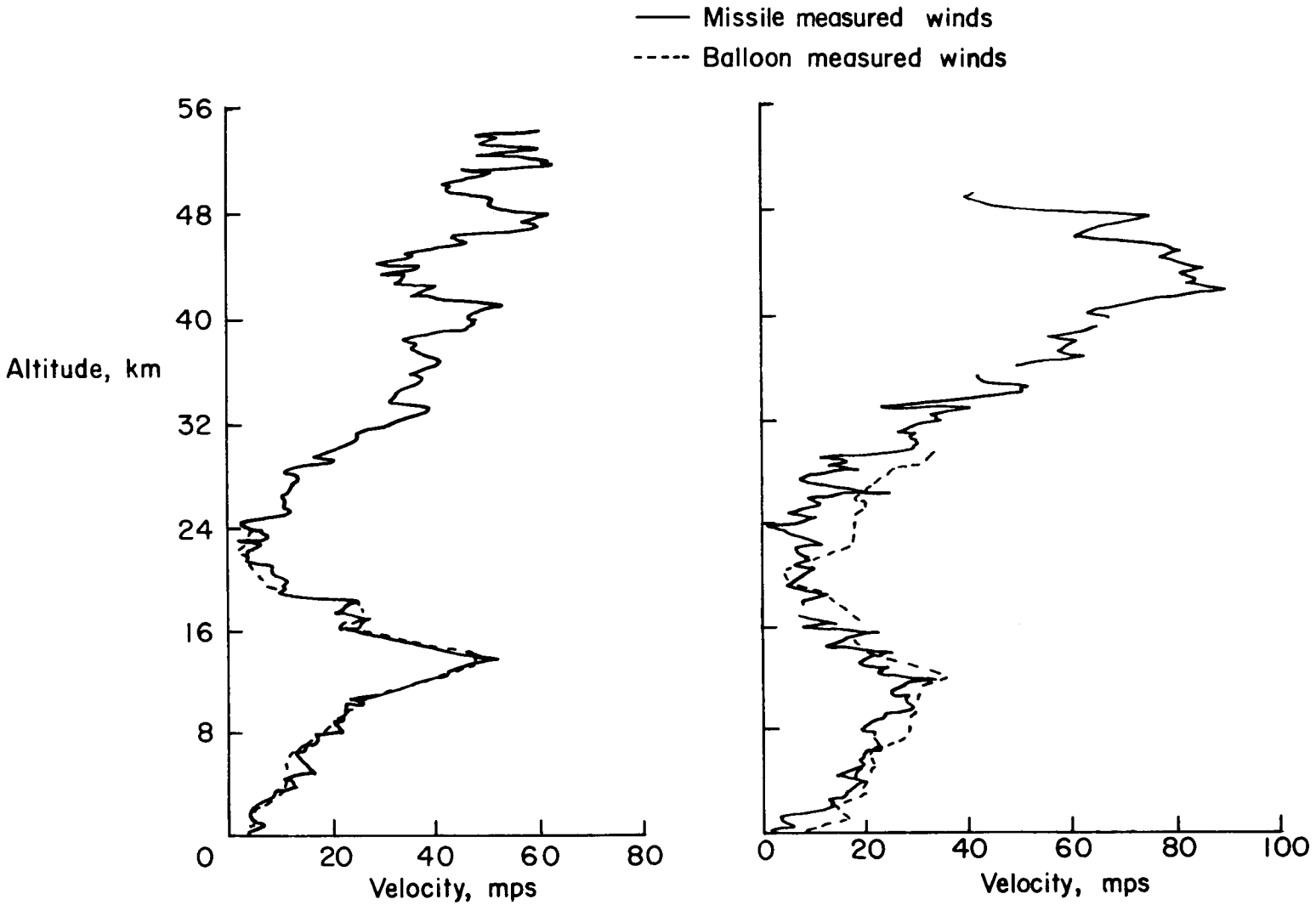

Figure 5.- Wind profiles determined from missile measurements (from ref. 17).

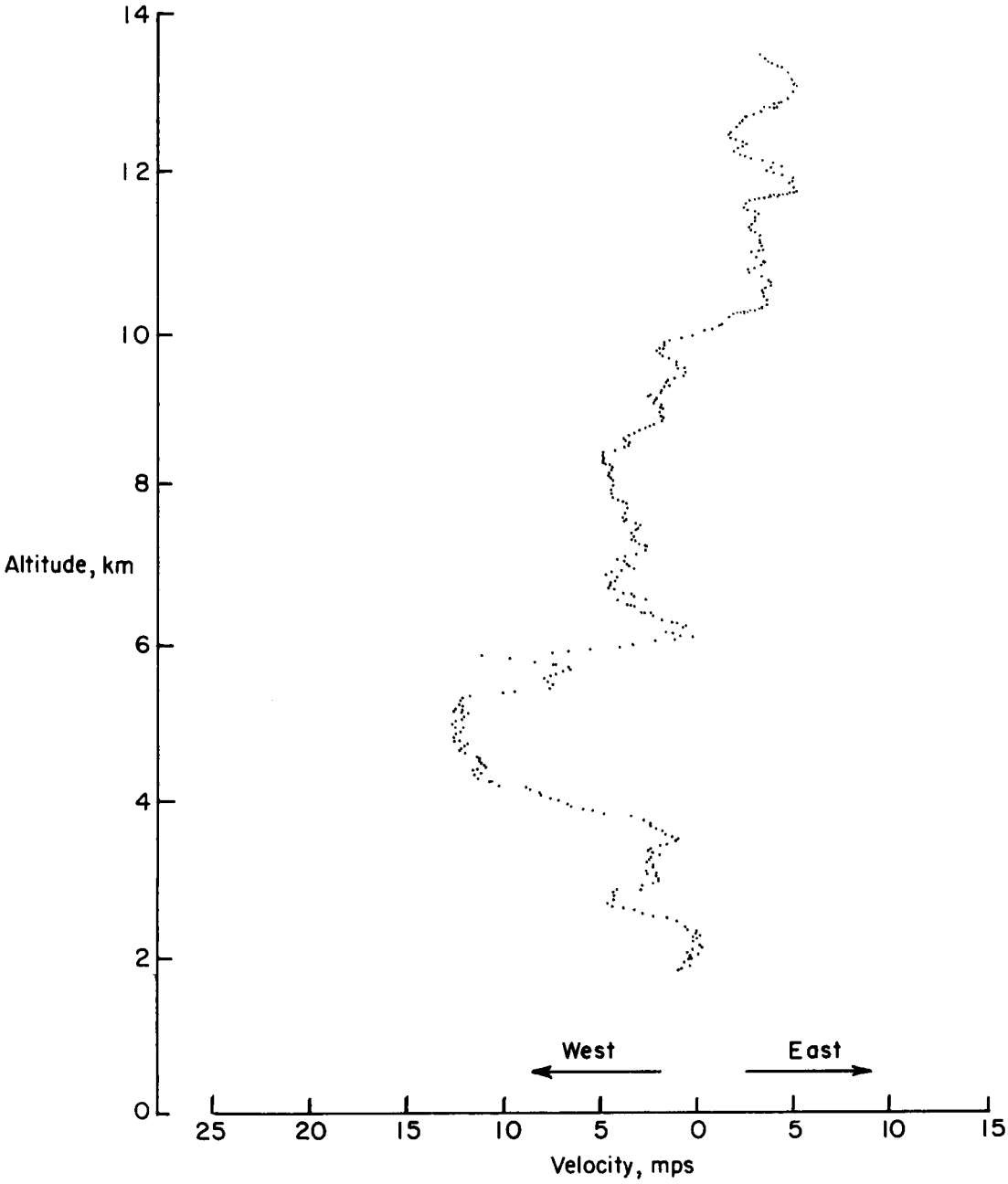

(a) West-to-east velocity component.

Figure 6.- Detailed wind profile determined through use of smoke-trail technique (from ref. 18).

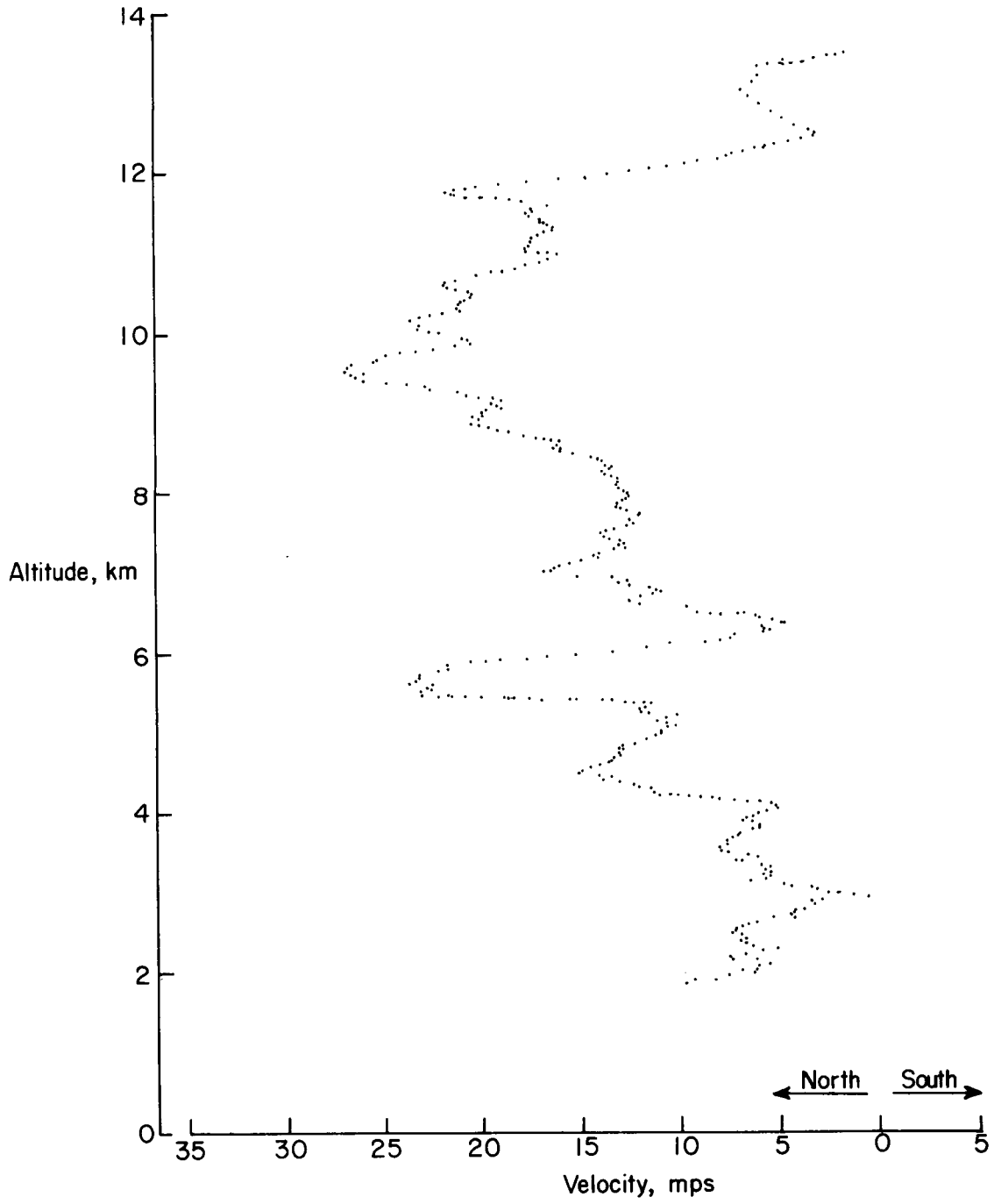

(b) North-to-south velocity component.

Figure 6.- Concluded.

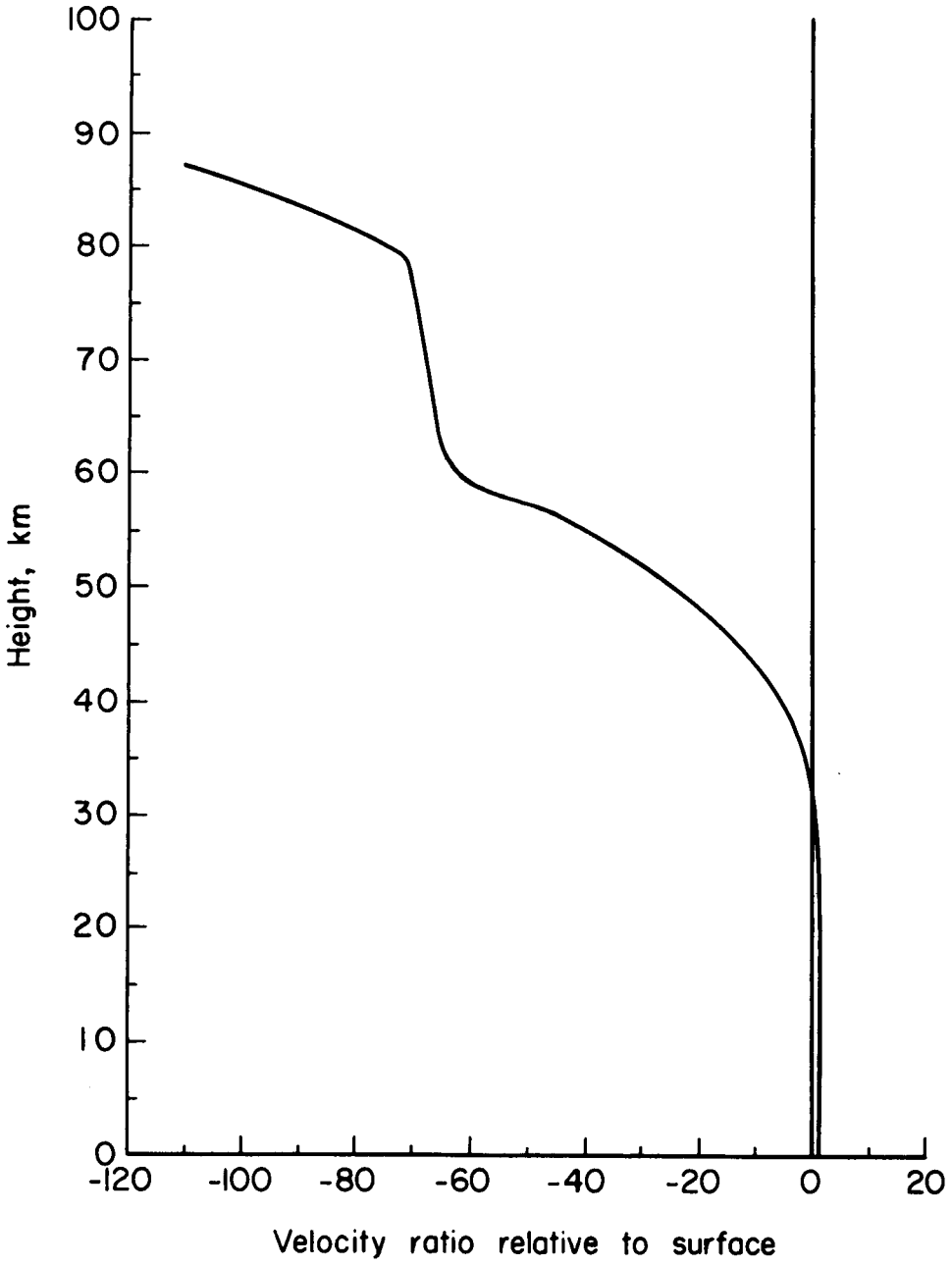

Figure 7.- Amplification with height of tidal velocities due to 12-hourly atmospheric mode (taken from ref. 19).

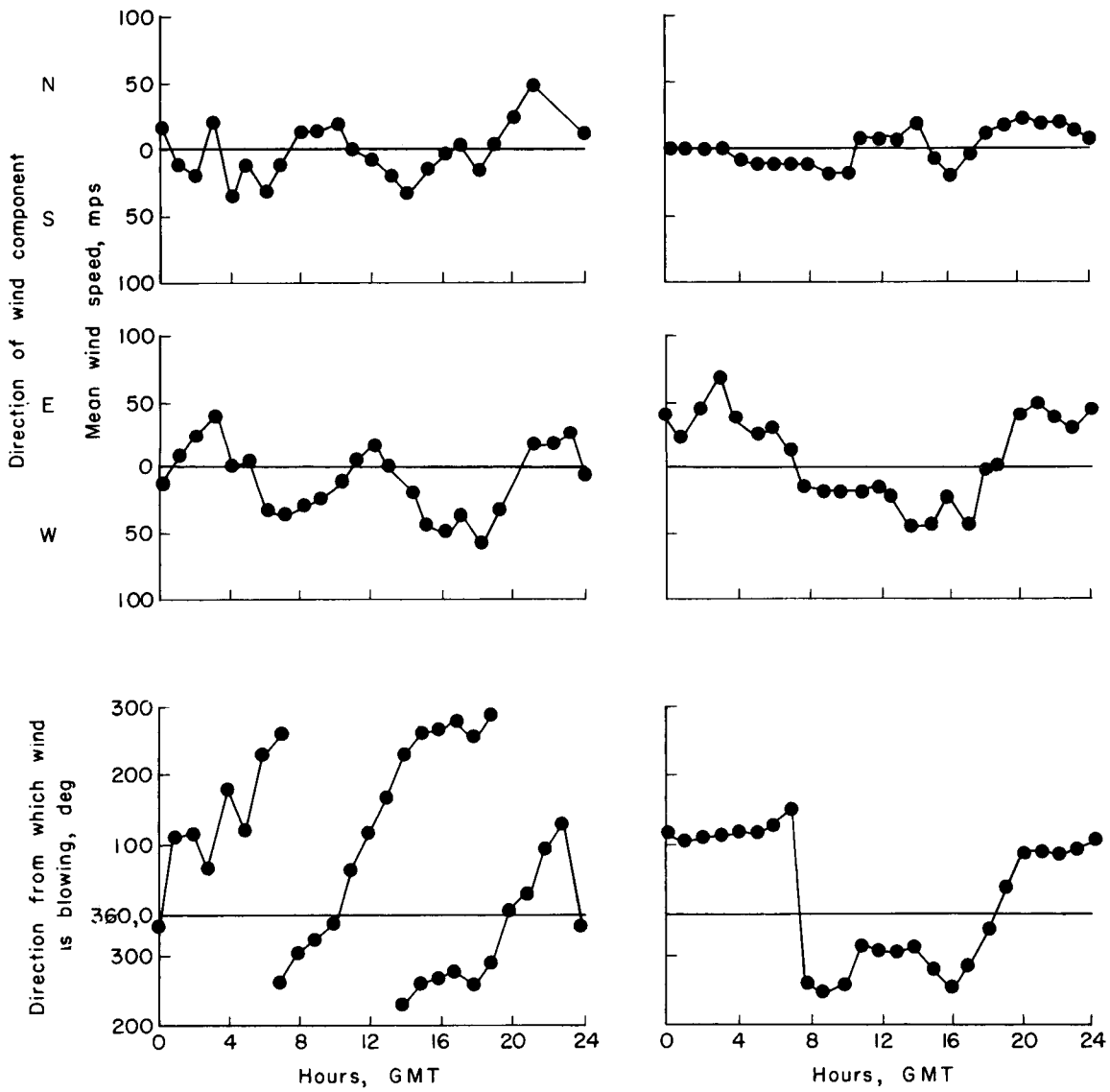

(a) E region. (b) F region.

Figure 8.- Overall mean and diurnal variations in wind velocities determined by ionospheric reflections from E and F regions (from ref. 22).

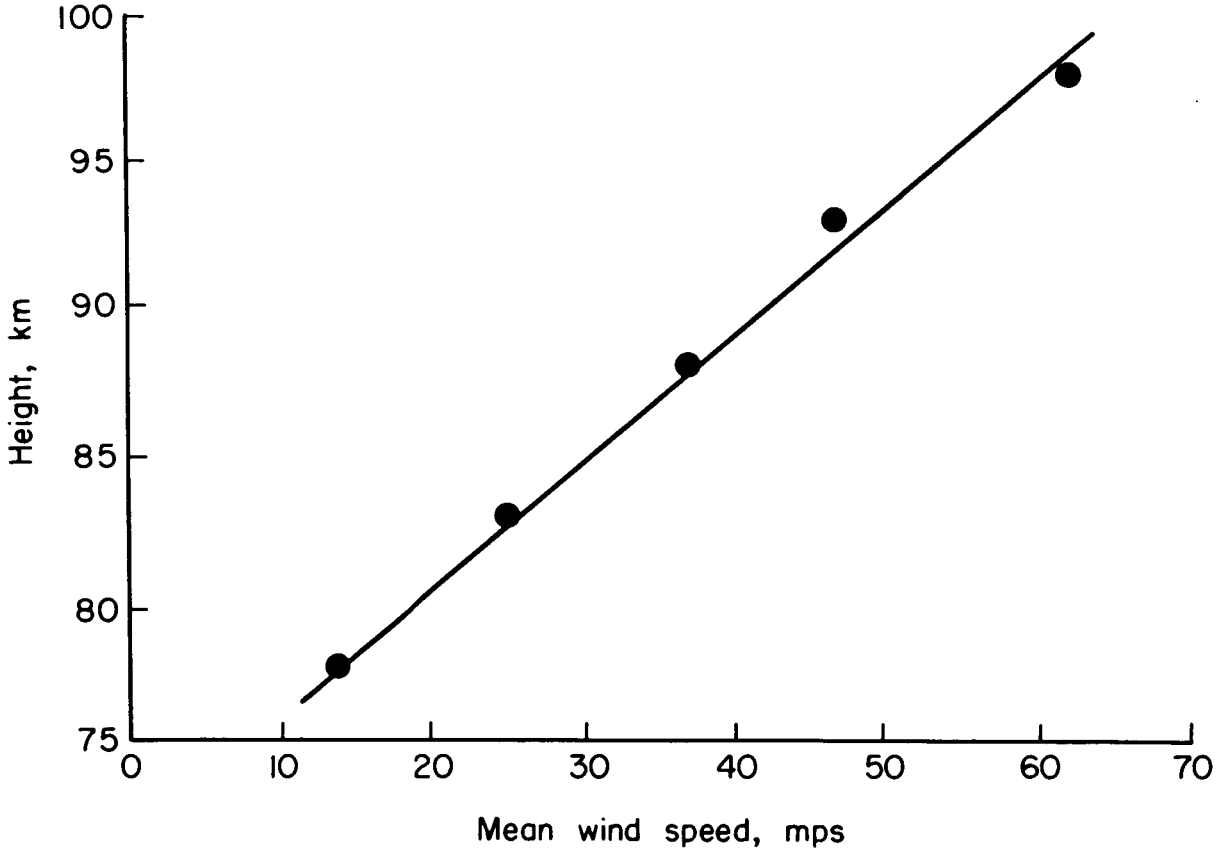

Figure 9.- Variation of mean wind speed with height (from meteor-trail echoes of ref. 23).

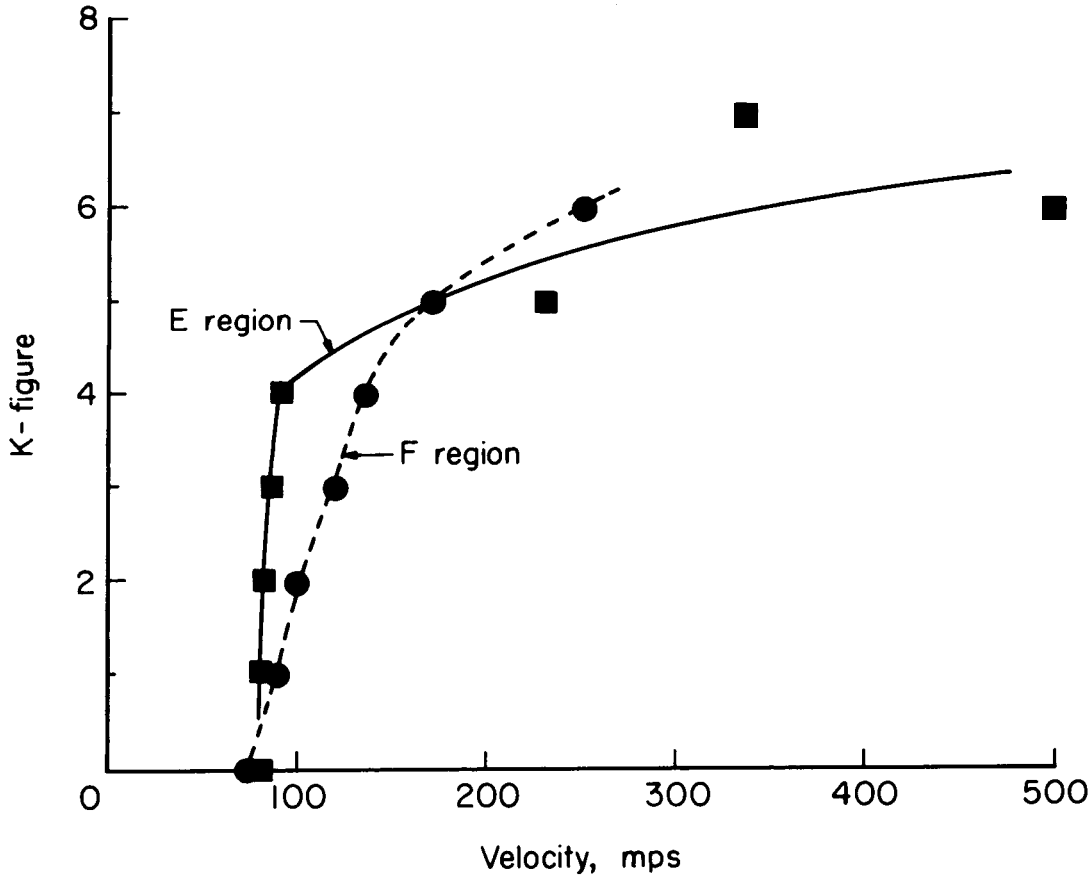

Figure 10.- Relation between magnetic K-figure and drift velocity in E and F regions (taken from fig. 14 of ref. 22).

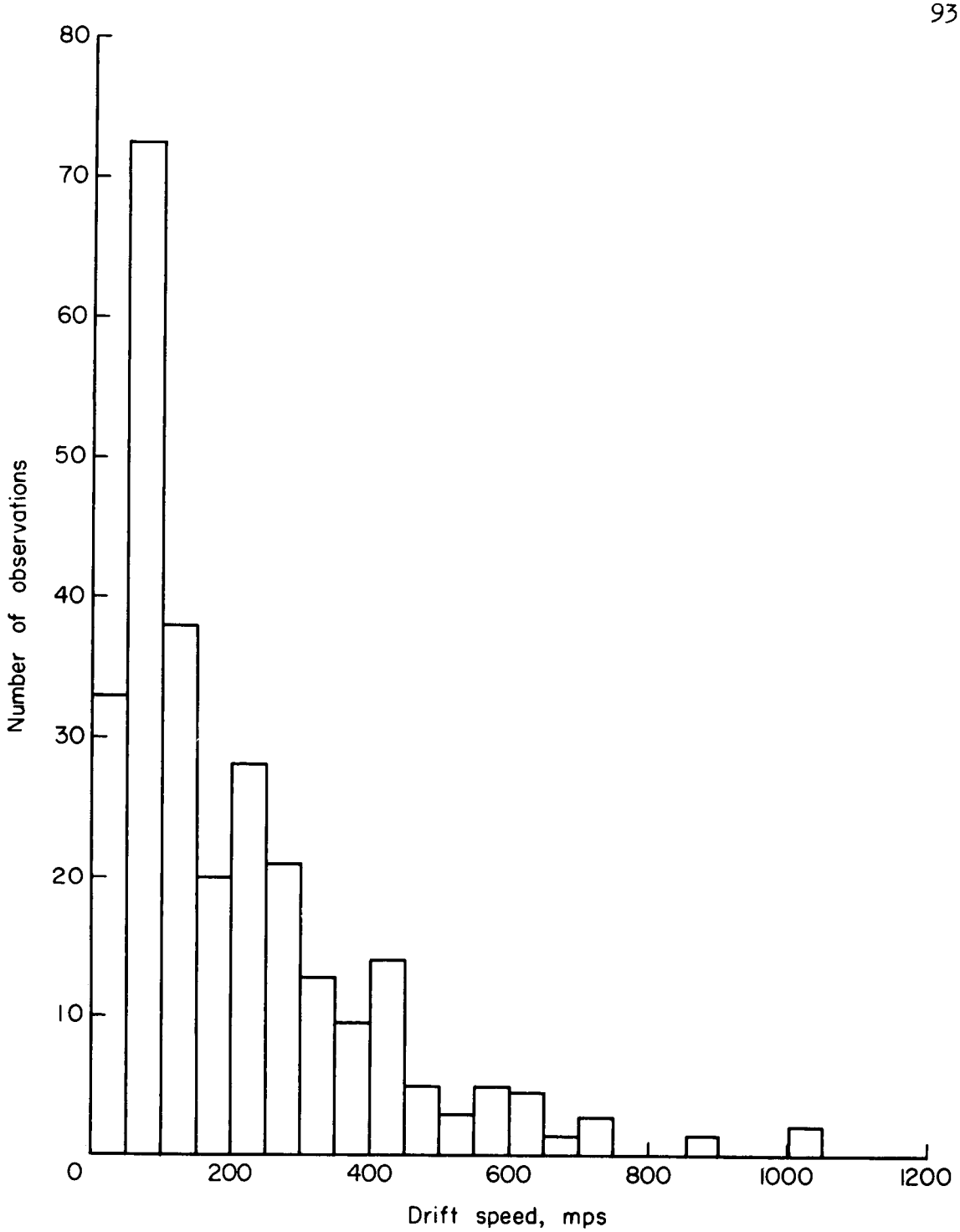

Figure 11.- Distribution of drift velocities in upper F region as derived from radio star scintillation measurements (taken from ref. 24).

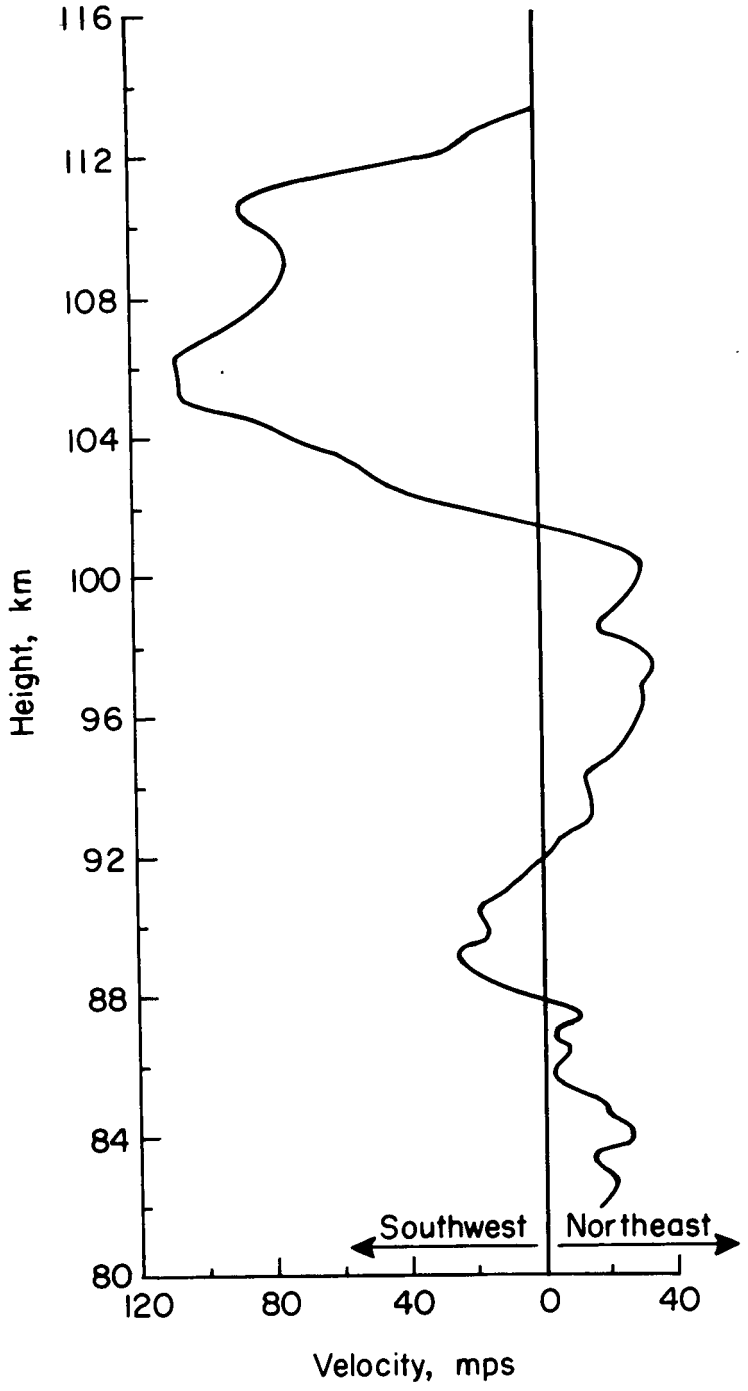

Figure 12.- Wind measurements obtained from photographic observations of meteor train (from ref. 25).

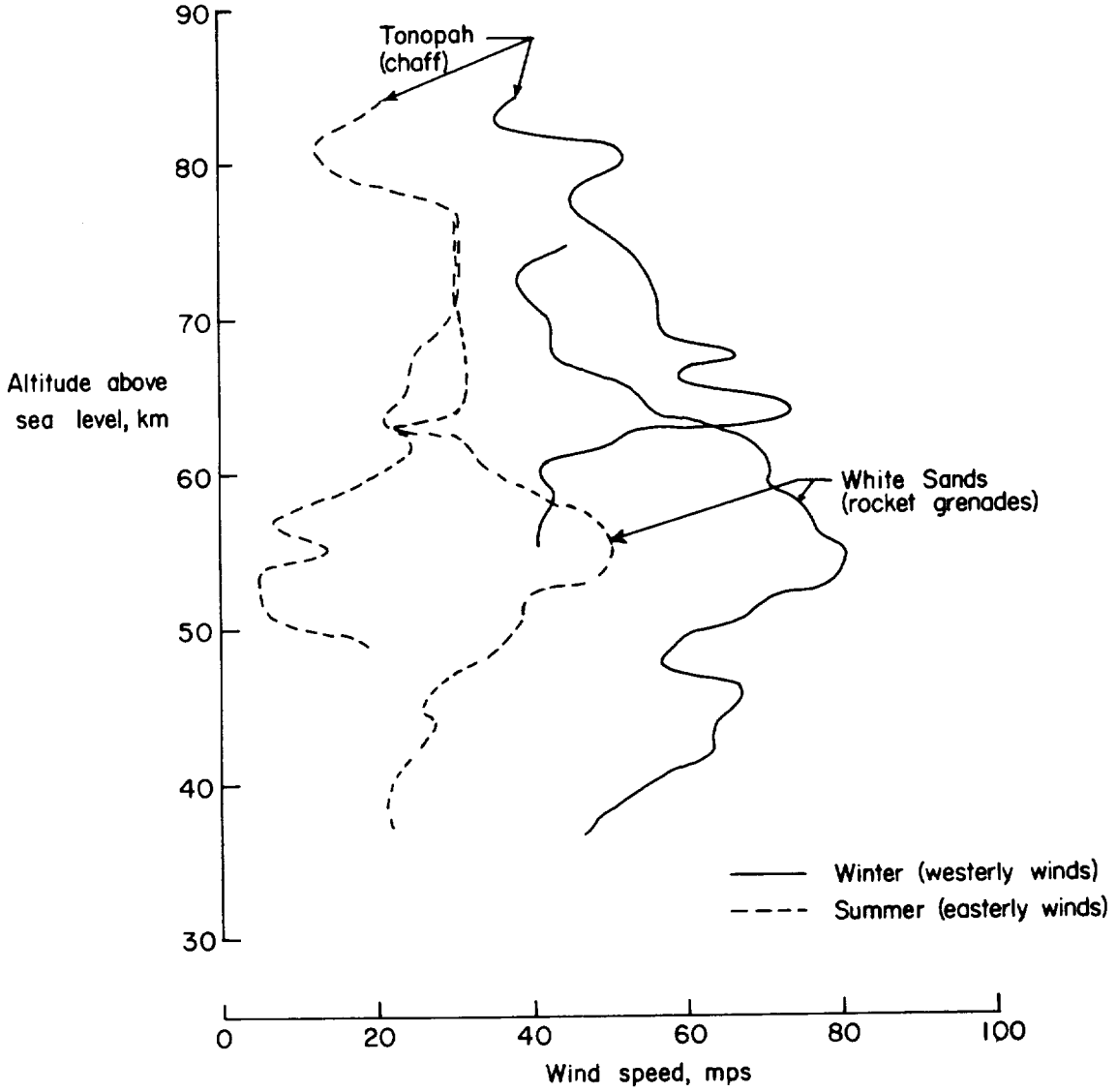

Figure 13.- Average wind speeds over Tonopah, Nevada, and White Sands, New Mexico, for winter and summer seasons (data from refs. 30 and 34).

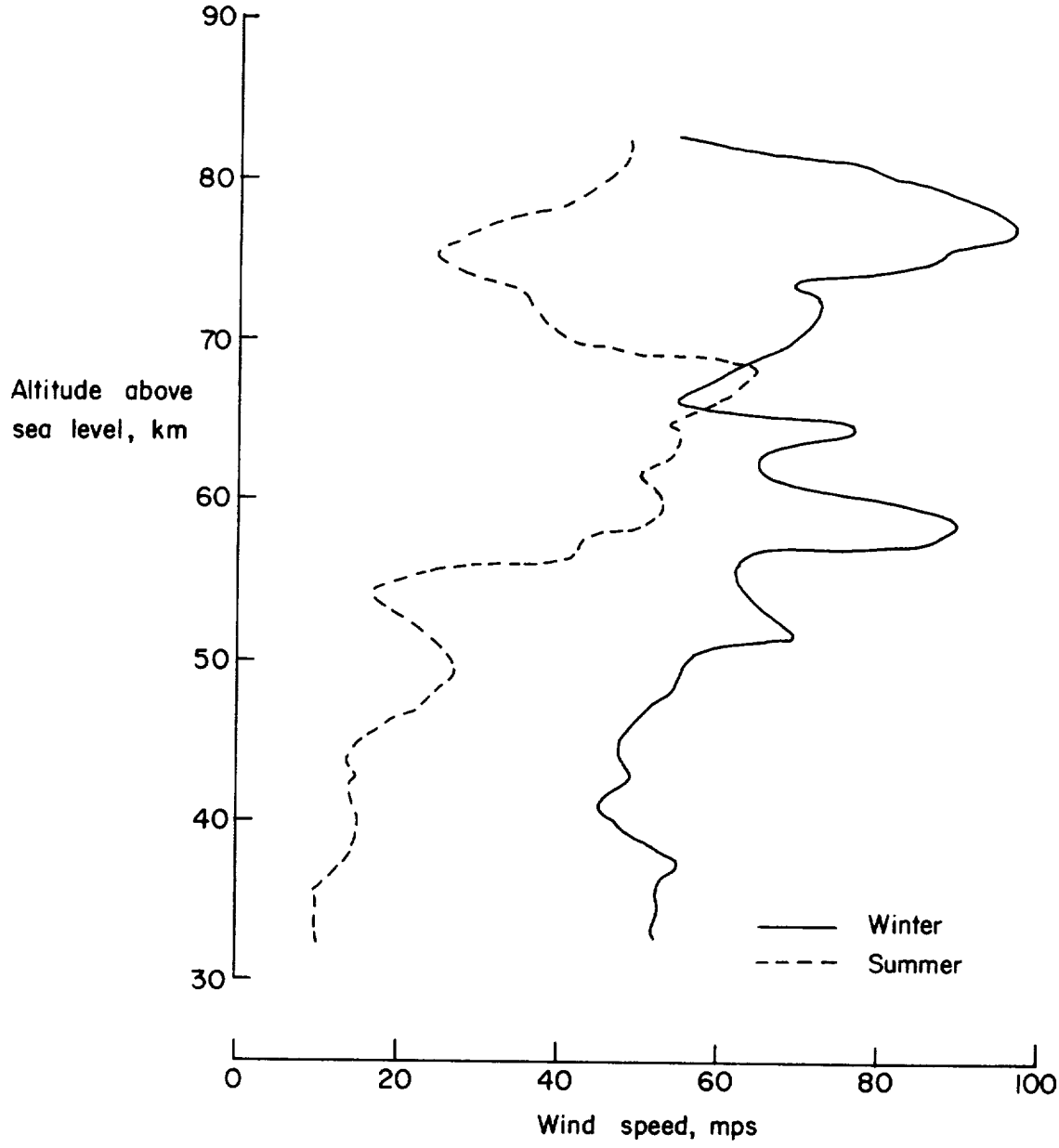

Figure 14.- Average wind speeds over Fort Churchill, Canada, for winter and summer seasons (data from rocket-grenade experiments of ref. 35).